

THE UNIVERSITY OF HULL

Selectivity and Enantioselectivity in the Palladium Catalysed Hydrogenation of
Pyrazine and some Substituted Pyrazines

being a Thesis submitted for the Degree of Doctor of Philosophy
in the University of Hull

by

John Robert Carroll B.Sc. (Hons)

September 2000

Acknowledgements

First and foremost, my utmost appreciation and thanks must go to my academic supervisor Prof. Peter Wells for his support, encouragement and friendship. Thanks must also go to my industrial supervisors Dr. Stuart Korn and Mr. Mike Howarth.

I would like to acknowledge the support of the EPSRC for funding this project and the additional support and assistance from my industrial sponsors Zeneca.

An important mention must go to the technical staff of the chemistry department in particular Alan Roberts (for mass spectra, teaching and his appreciation of the female form) and Brenda Worthington for the nmr work.

Thanks has to go to all the members of the Heterogeneous Catalysis Group for the fun, support, friendship and laughter. I certainly look back at those times with fond memories and a story or two to tell.

I could never go without giving a mention to my mum, dad and sister for their tireless support, encouragement and love over the years (I told you I'd get it done).

Last but not least I thank Amanda for her love, support and for being so understanding those many days and evenings when I was working instead of going out to play.

Summary

The palladium catalysed hydrogenation of pyrazine and some substituted pyrazines has been investigated over a range of reaction conditions.

This thesis reports and discusses work in three areas. The first being the hydrogenation of pyrazine over Pd/C, second the hydrogenation of some monosubstituted pyrazines also over Pd/C and finally, the enantioselective hydrogenation of methyl pyrazine-2-carboxylate over different chirally modified catalysts.

The hydrogenation of pyrazine over Pd/C and some other platinum group metal (PGM) catalysts has given an insight into its reactivity and selectivity. The interaction of pyrazine with the catalyst surface has been examined by use of deuterium-exchange which indicates pyrazine adsorbs in a co-planar manner to the surface. This has been verified experimentally by interpreting results obtained from the rates of hydrogenation for a range of aromatic N-heterocycles.

The hydrogenation of methyl pyrazine-2-carboxylate and 2-pyrazinecarbonitrile (2-PCN) over Pd/C has given an insight into the effects of substituents on the reactivity of the aromatic heterocyclic ring. In the case of methyl pyrazine-2-carboxylate, hydrogenation occurs in two distinct stages. The first stage is the rapid uptake of two moles hydrogen, followed by no further hydrogenation. Investigation of the compound formed after this two-mole uptake has shown 1, 4, 5, 6-tetrahydro methyl pyrazine-2-carboxylate as the product. On an electronic level, this compound is very stable and resists further reaction due to its conjugation and is in fact an α , β -unsaturated ester having a carbamate-like structure.

The unmodified hydrogenation of 2-PCN gave different results. It became evident that this compound, like methyl pyrazine-2-carboxylate before, is only partially

hydrogenated because reaction stops after a two-mole hydrogen uptake. Further investigation showed the cyano substituent is being partially hydrogenated as well as the ring. However, the degree of ring/substituent hydrogenation is affected by the pH of the reaction solvent, and the mechanism of hydrogenation is not complying with traditional observations.

The major aim of this project i.e. achieving the enantioselective hydrogenation of methyl pyrazine-2-carboxylate, has been fulfilled. An enantioselective outcome has been achieved over several differently modified catalysts. This is of particular importance to the industrial collaborator in this project, Zeneca Specialities.

The action of an adsorbed chiral modifier onto Pd/C is to induce the preferential formation of methyl piperazine-2-carboxylate in a typical enantiomeric excess of 2-25%; the highest value being obtained using a cinchonidine-modified catalyst.

The presented results indicate the first ever example of direct enantioselective hydrogenation of an aromatic N-heterocycle.

Mechanisms for the reaction predicting the experimental observations are given.

Contents

	Number
Chapter One	
Introduction	
1.1 Catalysis	1
1.2 Catalytic hydrogenation of N-containing aromatic heterocycles	2
1.2.1 Pyrrole	2
1.2.2 Pyridine	3
1.2.3 Pyrazine	4
1.2.4 Pyridazine	5
1.2.5 Pyrimidine	5
1.3 Chirality	6
1.3.1 History	6
1.3.2 Concepts	7
1.3.3 Nomenclature	7
1.3.4 Chirality and Bioactivity	9
1.4 Heterogeneous Enantioselective Catalysis	11
1.4.1 Background	11
1.4.2 The Orito Reaction	13
1.4.2.1 Mechanism	16
1.4.3 Palladium in Heterogeneous Enantioselective Catalysis	17
1.4.3.1 C = O Hydrogenation	17
1.4.3.2 C = C Hydrogenation	18
1.4.3.3 C = N Hydrogenation	20
References	22
Chapter Two	
Experimental	
2.1 Materials	27
2.1.1 Catalysts	27
2.1.2 Reactants	27
2.1.3 Solvents	28
2.1.4 Alkaloid modifiers	29
2.1.5 Synthetic Modifiers	30
2.1.6 Other materials	30

2.2 Apparatus	
2.2.1 Vacuum Apparatus	32
2.2.2 Static Reduction	32
2.2.3 Catalyst Modification	32
2.2.4 Büchi Autoclave	34
2.2.5 Baskerville Autoclave	37
2.2.6 Other reactor vessels	37
2.2.7 Product Separation	40
2.2.8 Gas Chromatography	40
2.2.9 Chiral Gas Chromatography	40
2.2.10 Polarimetry	41
2.2.11 Mass Spectrometry and GCMS	41
2.2.12 ¹ H NMR and FTIR	41
2.2.13 Catalyst Characterisation	42
2.2.14 Molecular Modelling	42
2.3 Procedures	43
2.3.1 Catalyst Activation	43
2.3.1.1 Pd/C	43
2.3.1.2 Other PGM catalysts	43
2.3.1.3 Raney Ni	43
2.3.2 Catalyst Modification	44
2.3.2.1 PGM catalysts	44
2.3.2.2 Raney Ni	44
2.3.3 Büchi Autoclave	45
2.3.4 Baskerville Autoclave	46
2.3.5 Product Separation and Analysis	46
2.3.6 Intermediate Investigation	47
2.3.7 Catalyst Characterisation	47
2.3.8 Competitive Reactions	48
2.3.9 Deuterium Tracer/Exchange investigation	49
2.3.9.1 Reaction of pyrazine with deuterium	49
2.3.9.2 Reaction of pyrazine-h ₄ with pyrazine-d ₄	49
2.3.9.3 Mass spectrometric analysis of deuteriated pyrazine	50
2.3.9.4 Mass spectrometric analysis of deuteriated piperazine	50
References	54

3.1 Introduction	55
3.2 Results	55
3.2.1 Hydrogen Uptake Curve	55
3.2.2 Orders of Reaction	56
3.2.3 Apparent Activation Energy	59
3.2.4 Deuterium Tracer Studies	59
3.2.4.1 Reaction of Perdeuteriopyrazine ($C_4N_2D_4$) with Hydrogen	59
3.2.4.2 Isotope Exchange between Pyrazine ($C_4N_2H_4$) and Perdeuteriopyrazine ($C_4N_2D_4$).	66
3.2.4.3 Isotope Exchange Reaction between Pyrazine ($C_4N_2H_4$) and Perdeuteriopyrazine ($C_4N_2D_4$) in the presence of hydrogen (H_2).	67
3.2.4.4 Isotope Exchange between Pyrazine ($C_4N_2H_4$) and Perdeuteriopyrazine ($C_4N_2D_4$) in the presence of deuterium (D_2).	70
3.2.5 Comparative Reactivities of five N-Heterocycles	72
3.3 Discussion	75
3.3.1 Kinetics of Reaction	75
3.3.2 Mechanisms of Pyrazine Exchange and Hydrogenation	86
3.3.3 Comparative Reactions of N-Heterocycles	82
References	84

4.1 Introduction	85
4.2 Results	85
4.2.1 Pyrazine-2-carboxylic acid	85
4.2.1.1 Reactant solubility	85
4.2.1.2 Hydrogen uptake curve	86
4.2.1.3 Variation of catalyst	88
4.2.2 Pyrazine-2-carboxylic acid methyl ester	89
4.2.2.1 Hydrogen uptake curve	89
4.2.2.2 Orders of reaction	89
4.2.2.3 Apparent Activation Energy	93
4.2.2.4 Product Distributions	93

4.2.2.5 Investigation of Reaction Intermediates	97
4.2.3 Pyrazine-2-carbonitrile	102
4.3 Discussion	103
4.3.1 Pyrazine-2-carboxylic acid	103
4.3.1.1 Reactant Solubility	103
4.3.1.2 Catalytic Hydrogenation	104
4.3.2 Pyrazine-2-carboxylic acid methyl ester	104
4.3.2.1 Variation of reaction variables	104
4.3.2.2 Analysis of Product Distributions	105
4.3.2.3 Investigation of Reaction Intermediates	105
4.3.3 Pyrazine-2-carbonitrile (PCN)	107
References	118
Chapter Five	Enantioselective Hydrogenation of Pyrazine-2-Carboxylic Acid Methyl Ester
5.1 Introduction	119
5.2 Results: Catalysis by Pd	119
5.2.1 Pyrazine-2-carboxylic acid	119
5.2.1.1 Hydrogen uptake curve	119
5.2.2 Pyrazine-2-carboxylic acid methyl ester	120
5.2.2.1 Hydrogen uptake curve	120
5.2.2.2 Orders of reaction	124
5.2.2.3 Dependence of reaction rate on temperature	124
5.2.2.4 Variation of rate and enantiomeric excess with modifier concentration	128
5.2.2.5 Product compositions	130
5.2.2.6 Variation of modifier	1335
5.2.2.7 Variation of catalyst support	137
5.2 Results: Catalysis by Ni	138
5.3 Discussion: Catalysis by Pd	140
5.3.1 Pyrazine-2-carboxylic acid (PCA)	140
5.3.2 Pyrazine-2-carboxylic acid methyl ester (PCME)	141
5.3.2.1 Proposed mechanism for enantioselective hydrogenation of PCME over cinchonidine modified Pd/C	142

5.3.2.1.1 Adsorption of cinchonidine on palladium	142
5.3.2.1.2 Adsorption of PCME on palladium	148
5.3.2.1.3 Proposed mechanism of reaction	151
5.3.2.2 Comparison between modified and unmodified reaction	155
5.3.2.3 Variation of reaction variables	155
5.3.2.4 Analysis of Product compositions	157
5.3.2.4.1 Unmodified hydrogenation	157
5.3.2.4.2 Hydrogenation over cinchonidine modified Pd/C	158
5.3.2.5 Other catalyst modifiers	159
5.3.2.5.1 Modification by quinine	159
5.3.2.5.2 Modification by ephedrine	160
5.3.2.5.3 Other modifiers	164
5.4 Discussion: Catalysis by Ni	164
5.4.1 Mode of enantioselection	165
References	167
Chapter Six	Conclusions
	169

Chapter One Introduction

1.1 Catalysis

A catalyst is a substance that increases the rate of a chemical reaction but is not consumed in the process. Catalysts have an important role in industry, the laboratory, and in nature. It is actually estimated that they contribute to one-sixth of the income of all manufactured goods in industrialised countries.

Generally catalysts can be classified as one of two types. If a catalyst is in the same phase as one or more of the reactants i.e. present as a solute in a liquid reaction mixture, it would be termed a homogeneous catalyst. If on the other hand the presence of a catalyst increases the number of phases present in the reaction mixture, it would be termed a heterogeneous catalyst.

This thesis is only concerned with heterogeneous catalysts, and the catalysts discussed are solids, which, by virtue of their surface properties, accelerate liquid phase reactions.

The stated definition for a catalyst has three key features:

- (i) the rate of reaction is increased by reducing the activation energy between reactants and products.
- (ii) catalyst concentrations do not appear in equilibrium constants, therefore not influencing the position of equilibrium.
- (iii) after a reaction a catalyst should be regenerated and able to effect an infinite number of further conversions.

Two important implications apply. In a typical reaction, if the activation energy is reduced and the equilibrium position unaltered, the reverse reaction must be catalysed to the same degree as the forward reaction. Second, the catalyst surface is regenerated after

each turnover, effectively giving the catalyst an infinite lifetime. This however, is often compromised in practice, leading to catalyst deactivation.

In practical terms, a useful heterogeneous catalyst is one for which the degenerative processes are slow enough to allow extensive conversion before deactivation becomes significant.

As the reaction path facilitated by a catalyst is conditioned by its own surface chemistry, products from reaction are catalyst dependent. This is the origin of catalyst selectivity. For example, under appropriate conditions, CO hydrogenation gives almost entirely CH₄ over Ni, methanol over promoted Cu, and high hydrocarbons over Ru, each process being operated on an industrial scale.

In each case, the unique chemical reactivity of the surface guides reaction along an energetically favoured pathway to the specific product.

1.2 Catalytic hydrogenation of N-containing aromatic heterocycles

1.2.1 Pyrrole

There have been extensive studies reporting the hydrogenation of substituted pyrroles to pyrrolidine derivatives using a range of catalysts (1-4). As the ring is electron-rich and difficult to reduce, complete hydrogenation is most easily achieved at higher temperatures and pressures (5). However, with certain substituents (e.g. electron withdrawing groups) hydrogenation occurs under very mild conditions, such as room temperature and atmospheric pressure (6).

Pt is more active and selective than Pd for the hydrogenation of substituted pyrroles to the corresponding pyrrolidine (7). However, in general hydrogenation studies, pyrrole has been shown to poison Pt, Pd and Ni (8). In pyrrole hydrogenation the product is

more strongly adsorbed, and exerts a stronger poisoning action than the reactant, self-poisoning can occur and conversion fails to reach 100%. The hydrogenation of pyrrole in ethanol over a Raney Ni catalyst at 150-200°C and 70-350 atm pressure gives high yields of pyrrolidine (9). Indeed, because poisoning behaviour is related to basicity, pyrrole is a stronger poison for all grades of Ni catalysts than is pyridine (10).

Pyrrole and substituted pyrroles behave differently. Pd is not active for pyrrole-2-carboxylic acid hydrogenation, and Pt only produces very small yields of pyrrolidine-2-carboxylic acid (11). However, the presence of an electron-withdrawing group (e.g. COOH) at the 2-position of the pyrrole ring facilitates hydrogenation over Ni where temperature can be lowered to 70°C without lowering rate or yield (12).

Pyrroles and their derivatives are regarded as the most catalytically poisonous of the N-heterocycles. However, research has shown that the addition of a protic acid to the reaction mixture eliminates this catalyst poisoning (13).

Newly developed routes using a Pd catalyst in non-acidic media have provided high conversion and selectivity (14). Non-acidic conditions are of importance when the pyrrole derivatives are acid sensitive. Lately, hydrogenation has also been achieved using Rh and Ru catalysts in non-acidic media under mild conditions (15). The success of these methods are such that they have been scaled up for industrial use.

1.2.2 Pyridine

Much work on the catalytic hydrogenation of various pyridines to their piperidine derivatives has been investigated over the years (16)

The earliest work on pyridine hydrogenation made use of a Pt catalyst under acidic conditions (17). When no acid was present the rate was negligible as the Pt catalyst was

poisoned. The use of Raney Ni in an acid free medium required severe conditions and gave an 83% yield of the piperidine (18).

Work by Skita with colloidal Pt led the way towards low-pressure hydrogenation of the pyridine ring (19). Also, Walker in 1962 utilised Pd/C under the relatively mild conditions of 70°C and 3 atm pressure (20). When using this catalyst to hydrogenate pyridine with either an aldehyde or ester substituent, only the ring was reduced. If this was carried out using a Pt catalyst the ring and the substituents were both reduced.

Rosenblatt achieved success with Rh/alumina and achieved modest yields of piperidine and substituted pyridines (21). Further work showed Rh/C to be effective when the loading of metal was sufficiently high (22).

As with pyrrole, various substituents affect the catalytic chemistry. Pyridines generally poison catalysts, but pyridine hydrochloride is readily hydrogenated. This is interpreted as being due to the reduced participation of the ring nitrogen atom in the adsorption.

There are advantages and disadvantages with each catalyst, for example, Ni often requires conditions that lead to side reactions, and Pt is only effective under acid conditions. Rh, which seems to be the best catalyst at low pressures, is adversely affected by strong nitrogen bases.

1.2.3 Pyrazine

The hydrogenation of pyrazine and substituted pyrazines has received less attention than the hydrogenation of pyridines or pyrroles. This report is concerned primarily with pyrazine and its substituted derivatives.

Pyrazines are readily hydrogenated under mild conditions to either their fully or partially reduced derivatives. The reaction has also been studied under more vigorous

conditions, Scigliano having reduced pyrazine to piperazine over supported Rh and Pd at high pressure and temperature (23).

The substituted pyrazines are of particular interest. Felder fully reduced pyrazine-2-carboxylic acid over Pd/C to the corresponding piperazine acid (24) and Behun reduced 2-alkylpyrazines over the same catalyst (25).

1.2.4 Pyridazine

There appears to be no references to the catalytic hydrogenation of pyridazine over Pt group metals. The aromatic ring appears to be more resistant to hydrogenation than pyrimidine or pyrazine. However, certain pyridazines are prepared by hydrogenation. For example, the pyridazine nucleus remained unchanged when 4-methyl-3,6-dichloropyridazine was dehydrohalogenated over 5% Pd/C to give 4-methylpyridazine in 91% yield (26).

1.2.5 Pyrimidine

The catalytic hydrogenation of pyrimidine is complex and depending on the conditions and substrate, fully and partially saturated products are obtained (27). Pt, Pd, and Rh catalysts have been used in these reductions with varying success. As the reactivity of pyrimidine is similar to pyridine, it would be anticipated that Rh and Ru would be effective metals for reduction. However, Rh, although effective has not been extensively used.

1.3 Chirality

1.3.1 History

The history of chirality dates back to 1812 when the French scientist, J. B. Biot discovered the ability of certain substances to rotate plane polarised light (28). Three years later, he extended this observation to organic substances, for example, turpentine and solutions of sucrose and tartaric acid (29).

Thirty years later, Louis Pasteur, a student of Biot, proposed that the optical activity was the result of molecular asymmetry (30). Pasteur was intrigued by the crystal shapes of argol formed on the side of wine barrels. It was found that the major component, (+) tartaric acid rotated plane polarised light clockwise, whereas the minor component, although chemically identical showed no optical activity and was referred to as the racemic acid. The sodium ammonium double salt of this mixture crystallised into two different forms. After Pasteur had separated these crystals by hand, he discovered that the different crystals rotated plane polarised light in opposite directions.

The principles of a molecular asymmetry were proposed by Van't Hoff and Le Bel in 1874 (31 and 32). Van't Hoff extended Kekule's ideas of the tetravalency of carbon and suggested a substance of the type Cabcd, (the four substituents (abcd) being tetrahedrally arranged around the central carbon atom) would generate two molecules, each being the mirror image of each other. In contrast, Le Bel's paper concentrated on a general theory for stereoisomerism, referring to the asymmetry of the entire molecule not the individual carbon atom.

1.3.2 Concepts

A molecule that is not superimposable upon itself is said to be chiral. The most common type of chiral molecule contains a tetravalent carbon atom that is attached to 4 different atoms or groups. Such a molecule is said to have a stereogenic centre. (In addition to C, P and S can also provide stereogenic centres).

This molecule will exist as two different compounds known as stereoisomers or enantiomers. The physical properties of the enantiomers are mostly identical, the exception being their ability to rotate plane polarised light in equal, but opposite directions. This phenomenon is the result of the interaction of the electric and magnetic field of the plane polarised light with the molecules that it encounters.

In a racemic mixture, where both enantiomers are present in equal amounts, every encounter with one molecule of a certain orientation is compensated by an encounter with the mirror-image molecular orientation, resulting in a net rotation of zero. When there is an enantiomeric excess (ee) of one enantiomer over the other, this cancelling effect does not occur and a rotation is observed. The degree of the rotation is dependent on the enantiomeric excess, concentration, temperature, wavelength, solvent and length of polarimeter tube.

1.3.3 Nomenclature

The nomenclature for distinguishing the configuration of enantiomers is based on the Cahn-Ingold-Prelog convention (33). This system allows the unambiguous designation of configuration of 4 different substituents around any stereogenic centre.

The substituents are designated $a > b > c > d$ in order of priority and the configuration is determined on whether the sequence of decreasing priority proceeds in a clockwise or anticlockwise manner (Figure 1.1).



Figure 1.1 Cahn-Ingold-Prelog convention for assigning enantiomer configuration

If the path of $a \rightarrow b \rightarrow c$ is clockwise, the configuration at the stereocentre is named (R) from the Latin for right, *rectus*. If however, the path of $a \rightarrow b \rightarrow c$ is counterclockwise the stereocentre is named (S) (*sinister*). A racemic mixture is therefore designated as (R, S).

A great majority of chiral molecules contain stereogenic centres however other molecules without this condition can still be chiral. In a molecule where rotation about a single bond is hindered, asymmetry of the molecule can occur. An example being in 1, 1-bi-2-naphthol (Figure 1.2)

The increasing awareness that racemic compounds are only 50% pure and that pharmacological studies of racemates may lead to unsound or misleading data has resulted in more stringent guidelines for registration of chiral drugs.

The United States Food and Drug Administration (FDA) has stated that sales of racemic compounds will only be approved when the bioactivity of both enantiomers are known (35). This could encourage companies to produce pure enantiomers rather than go to the expense of conducting trials and studies on unwanted enantiomers.

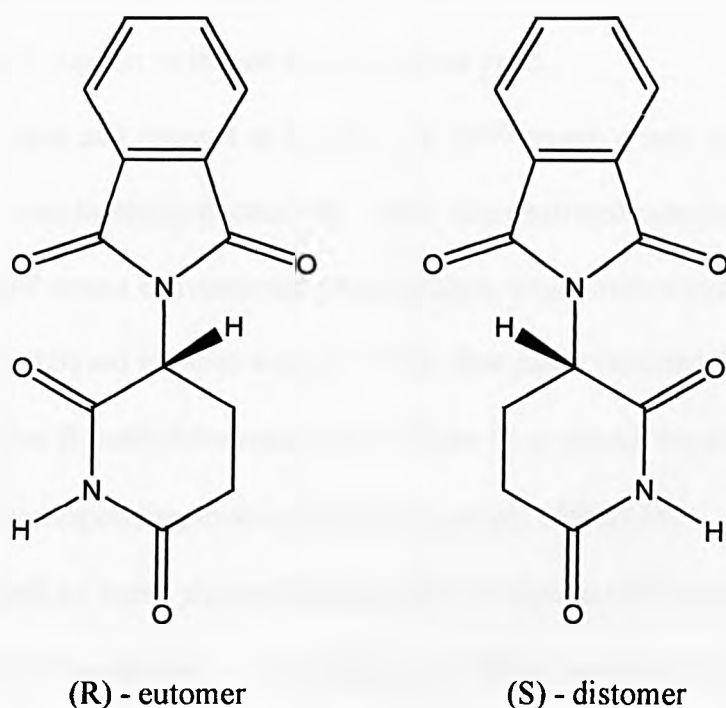


Figure 1.3. Thalidomide

1.4 Heterogeneous Enantioselective Catalysis

1.4.1 Background

The earliest heterogeneously catalysed enantioselective reaction, was reported by Schwab in 1932. Copper, nickel and platinum particles were supported on quartz for the dehydrogenation of racemic 2-butanol to 2-butanone (36, 37). The optical yields were very low and this approach was not developed any further.

Supported metal catalysts possess no inherent chiral quality and therefore a chiral environment must be created. Schwab's work made use of the dextro- and levo- rotatory faces of the quartz support to induce a small optical yield.

The work of Lipkin and Stewart at Berkeley in 1939 began a new era in the field of heterogeneous enantioselective catalysis. They demonstrated adsorption of a chiral organic compound onto a conventional metal catalyst, could induce enantioselectivity in hydrogenations catalysed at those surfaces. Their first paper reported the hydrogenation of hydrocinchonine β -methylcinnamate over Adams Pt to phenyl butyric acid giving an optical rotation corresponding to an enantiomeric excess of 8% (38).

In the 1950's, work by Izumi showed optical yields as high as 66% could be achieved. It was reported that Pd supported on silk fibroin was highly enantioselective for C = N or C = C hydrogenation (39). It was debated whether the catalysts were actually heterogeneous, based on the model of Lipkin and Schwab or a homogeneous mononuclear Pd/amino acid complex. Nevertheless, this work demonstrated that highly selective catalysed reactions were achievable.

Following this success, Izumi diversified into another area of selective catalysis. This work examined the effect of adsorbing a chiral organic acid, such as tartaric acid, onto

Raney Ni for the hydrogenation of β -ketoesters. Several groups have continued to develop this system, and the extensive literature has been reviewed (40-42).

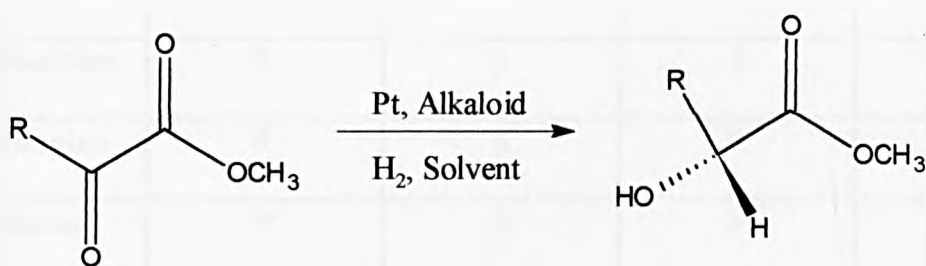
The system comprises of several features:

- i. Tartaric acid modifies both Ni/SiO₂ and Raney Ni catalysts providing modest values of the enantiomeric excess.
- ii. In the preparation of Raney Ni, the Ni:Al ratio in the pre-digested alloy is important. In the USA and Europe the 50:50 alloy is solely available, whereas in Japan they have access to a 58:42 alloy that is reported to be more enantioselective.
- iii. The presence of an alkali halide promotes enantioselectivity. The most effective promoter is NaBr, which is claimed to preferentially poison sites where racemic hydrogenation occurs.
- iv. The pH and temperature of the solution used in the modification step has a critical effect on enantioselectivity.

It must be said that catalyst reproduction in this system is very difficult due to the number of variables in a standard preparation. Recently, Harada and Tai reported the addition of pivalic acid (trimethylacetic acid) as a further promoter to the Raney Ni system. This has given a catalyst capable of enantioselectively hydrogenating isolated ketones, such as 2-octanone to 2-octanol (43). Additionally, the Hull group has used this catalyst to enantioselectively hydrogenate a substituted pyridine to its corresponding piperazine (44).

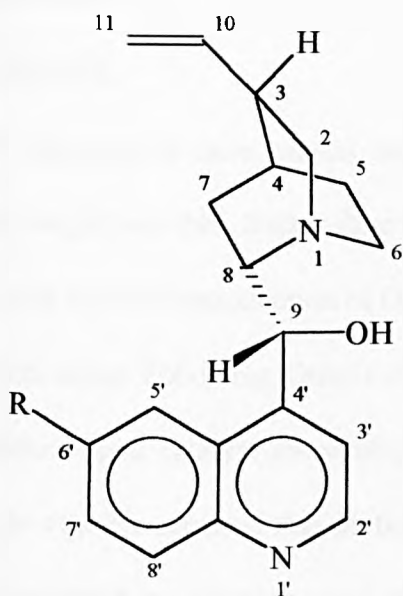
1.4.2 The Orito Reaction

The use of PGM catalysts for enantioselective hydrogenation received renewed attention in 1978 when a series of papers were produced by the group of Orito at the University of Tokyo (45-49). This work reported the enantioselective hydrogenation of α -ketoesters, particularly methyl pyruvate and methyl benzyl formate to methyl lactate and methyl mandelate respectively (Figure 1.4). It was found that preadsorption of a cinchona alkaloid onto a Pt/C catalyst provided a suitable environment for enantioselective reaction. If the catalyst was modified with cinchonidine (CD) or quinine, the S enantiomer was formed in excess, whereas if cinchonine (CN) or quinidine were used, the R enantiomer was preferentially produced. The structures of the cinchona alkaloids are given in Figure 1.5.



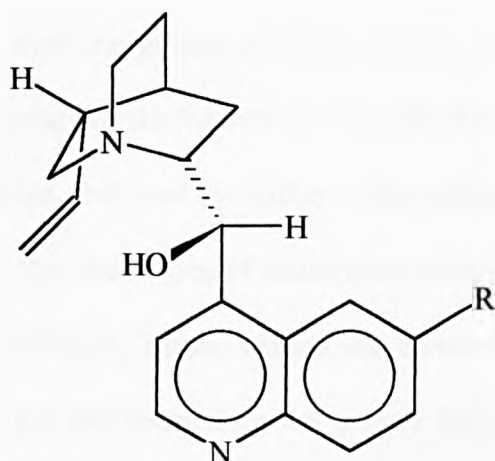
R = Me for methyl pyruvate, R = Ph for methyl benzyl formate

Figure 1. 4 The Orito reaction



Cinchonidine (R = H)

Quinine (R = OMe)



Cinchonine (R = H)

Quinidine (R = OMe)

Atom	C4	C5	C8	C9
Cinchonidine	R	S	S	R
Cinchonine	R	S	R	S
Quinine	R	S	S	R
Quinidine	R	S	R	S

Figure 1. 5 Structures and configurations of the cinchona alkaloids

This work also reported the effects of various catalyst pre-treatments. It was found that the optical yield could be increased by simply heating the catalyst in hydrogen at about 573 K. The choice of reaction solvent was also shown to be important. A range of

alcohols, esters and aromatic solvents were tested and the highest enantiomeric excess found to be 82 % when methyl benzyl formate was hydrogenated in methyl propionate. Enantioselectivity could also be increased by the addition of a base such as triethylamine.

Work appeared to have ceased until 1986, when the groups of Wells (Hull), Blaser (Ciba Geigy) and then Baiker (Zurich, ETH) renewed the interest in this area. Initially this work was the reproduction of Orito's findings, followed by system optimisation and diversification. Following Orito's observation that the degree of enantioselectivity was dependent upon catalyst morphology and preparation, Blaser studied the effect of Pt particle size. He reported that particles of 3-4 nm and dispersions not greater than 0.1-0.2, supported on alumina gave the greatest enantioselectivities (50-52). However, Wells and co-workers performed the majority of their studies using EUROPT-1, a 6.3 % Pt/SiO₂ catalyst. This was manufactured by Johnson Matthey in 1976 and characterised by the Council of Europe Research Group on Catalysis over the period 1976 to 1985. This characterisation programme was co-ordinated from Hull and the results published in a series of five papers (53-57). This catalyst has a mean metal particle size of 2 nm, and a dispersion of 60% (58). Using this catalyst, the highest optical yield obtained was 77% and this could be reduced using catalysts with smaller Pt particles (59).

The effect of solvent variation has been studied in detail. Blaser et al. produced their best results using acetic acid, whereas Well et al. predominantly used ethanol. Work reported by Vermeer, also working in Hull, discussed the separate effects of the choice of solvent for catalyst modification and reaction (60).

The most remarkable aspect of this reaction system is the rate enhancement accompanying the enantioselective reaction. In the absence of a modifier i.e. racemic hydrogenation, the typical rate of reaction is around 50-100 mmol h⁻¹ g⁻¹, whereas in

the presence of a cinchona modifier i.e. enantioselective hydrogenation, the typical rate is about $1500 \text{ mmol h}^{-1} \text{ g}^{-1}$ (61).

1.4.2.1 Mechanism

The work published by Orito and co-workers presented no mechanistic discussion as to the origin of the enantioselectivity. The first model was developed by the Hull group and reported in 1990 (62). The Template Model, as it has commonly become known, gave a molecular view of the mechanism and interpreted the observed sense of enantioselectivity. The model paid particular attention to the observation that successful catalyst modification required conditioning in air, leaving CD and oxygen adsorbed onto the Pt surface as a non-close packed monolayer. When the catalyst had been exposed to hydrogen, the oxygen would be removed as water, exposing groups of Pt atoms available for pyruvate adsorption and hydrogenation. These Pt atoms would be bounded by a number of adsorbed CD molecules possibly leaving a template at which pyruvate ester might undergo selective enantioface adsorption (SEA). The proposal that a number of alkaloid molecules, say three, form the enantioselective site was experimentally tested. Simons argued that the known variation of optical yield with alkaloid loading indicated a 1:1 interaction between CD and pyruvate. It was found that CD and CN can induce enantioselectivity even at very low loadings, where the likelihood of finding three alkaloid molecules adsorbed in close proximity would be unlikely (63).

This revised model took into account the proposal the quinuclidine-N of the modifier was responsible for stabilising the half-hydrogenated state (hhs) of the reactant, leading to the enhanced rate of reaction (64, Figure 1.6).

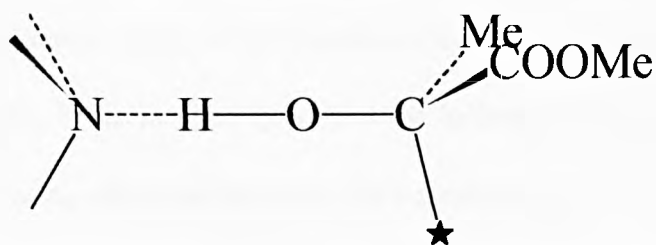


Figure 1.6 Origin of enhanced rate by hbs stabilisation

1.4.3 Palladium in Heterogeneous Enantioselective Catalysis

1.4.3.1 C = O Hydrogenation

It is well documented that the mechanisms of heterogeneous reactions catalysed by Pd differ to those of Pt. In the case of pyruvate hydrogenation over CD modified Pd, Blaser reported a low enantioselectivity of 4% in favour of the S-enantiomer (65). The sense of enantioselectivity was therefore reversed from that observed with CD modified Pt. Work by Wells et al. confirmed this inverse in enantioselectivity and reported that reaction over Pd differed in almost every particular to that over Pt (66). That is, in the fact no rate enhancement was observed, values of the enantiomeric excess are low, an excess of modifier is required, and the reaction is half order in hydrogen. Hall using isotope tracer studies investigated the mechanism of this reaction (67). It appears that hydrogenation is preceded by enolisation, so that reaction is not hydrogenation of the carbonyl group but of the carbon-carbon double bond.

1.4.3.2 C = C Hydrogenation

In 1956, Akabori et al. used Pd supported on silk fibroin to hydrogenate various alkenic substrates and claimed values of the enantiomeric excess up to 70% (39).

Work reported by Perez in 1985 described the hydrogenation of α - and β - substituted cinnamic acids using cinchona modified 5% Pd/carbon (68). The hydrogenation of E- α -phenylcinnamic acid over a CD modified catalyst gave the highest enantiomeric excess of 31% (S).

Bartók et al. reported the hydrogenation of the same α - substituted cinnamic acid over tartaric acid modified Raney Ni; virtually no enantiomeric excess was observed (69). However, when the alkali metal salt of the acid was produced, enantioselective hydrogenation was possible. Their best result was given as 17% in favour of (R)-2, 3-diphenylpropionic acid.

Work published by the group of Nitta et al. built on Bartók's work. The first paper explained how a series of supported 5% Pd catalysts were tested for activity and selectivity in the enantioselective hydrogenation of E- α -phenylcinnamic acid (70).

The highest enantiomeric excess was obtained using a 5% Pd/titania catalyst and an aqueous solvent mixture. Catalysts prepared by a precipitation method had higher activities than those prepared by impregnation, possibly due to a detrimental effect of chlorine remaining in the impregnated catalyst.

Further work on the system showed an amount of solvent specificity. A solvent with a higher dielectric constant resulted in higher enantioselectivities (71).

The enantioselectivity of the cinchonidine modified Pd/Titania catalyst varied with the extent of reactant conversion, a maximum being reached at an early stage in the reaction (72, 73).

The effect of modifier structure on enantioselectivity and activity was found to be important (74). Cinchonidine was the most successful modifier, but in contrast to α -ketoester hydrogenation over Pt, a catalyst modified by quarternised cinchonidine was moderately enantioselective.

Work reported by Watson et al. concentrated on the enantioselective hydrogenation of unsaturated esters and acids, particularly methyl tiglate and tiglic acid over cinchona modified Pd (75) however, only tiglic acid was hydrogenated enantioselectively. Hall extended the scope of this project and the preliminary results were presented at the 11th ICC (66). In the case of tiglic acid, it is thought a pre-cursor state formed by H-bonding between the acidic proton and the quinuclidine-N of the adsorbed alkaloid may precede selective enantioface adsorption and hydrogenation to chiral product. Unlike pyruvate hydrogenation, the bond being reduced is remote from the quinuclidine-N and therefore cannot influence the rate-determining step, hence no rate enhancement is observed. The highest value of the enantiomeric excess (~26%) was obtained in THF solvent using a cinchonine modified catalyst. In contrast to the work of Nitta, enantioselectivity was lost when the quinuclidine-N was quarternised.

Following this work, Borszky et al. (76) and Smith et al (77) independently reported the enantioselective hydrogenation of 2-methyl-2-pentenoic acid over modified Pd catalysts. Values of the enantiomeric excess were modest at 15 to 52%, and both groups discovered enantioselectivity increased with increasing hydrogen pressure.

Departing from unsaturated acids, the enantioselective hydrogenation of α , β -unsaturated ketones over Pd has also been reported. Tungler et al. have investigated the hydrogenation of isophorone over L-proline and dihydrovinpocetine modified Pd giving enantioselectivities of up to 80% and 50% respectively (78, 79).

Recently work by Thorey et al. discussed the hydrogenation of a range of α , β -unsaturated ketones using ephedrine modified palladium (80). Values of the enantiomeric excess were about 36% using acetonitrile as the solvent at atmospheric pressures of hydrogen.

1.4.3.3 C = N Hydrogenation

Enantioselective hydrogenation of the C = N function has been achieved almost exclusively over Pd of which there are very few examples.

In 1971, Yoshida and Harada reported the hydrogenation of pyruvic acid oxime over ephedrine-modified Pd/C to obtain modest yields of alanine having an enantiomeric excess of 10% (81).

Baiker et al. have recently examined the enantioselective hydrogenation of the same reactant over Pd/alumina modified by ephedrine, CD and CN (82). In the presence of small quantities of these modifiers, the rate was substantially reduced, giving alanine in an enantiomeric excess varying from 4 to 26%.

The enantioselective hydrogenation of substituted heterocyclic compounds is of major importance, especially to the pharmaceutical industry. Much work has been published on the general hydrogenation of various heterocycles over a heterogeneous catalyst, but the enantioselective hydrogenation remains to be an unattained goal.

A route developed by Fuchs and Roduit involved the production of a chiral piperazine from its corresponding pyrazine (83). This involved hydrogenation of the pyrazine over a palladium heterogeneous catalyst to its tetrahydro derivative (i.e. a two mole hydrogen uptake), followed by the addition of the final mole (and chiral induction) over a homogeneous Rh catalyst.

Recently, Blaser adopted this two-step approach for the enantioselective hydrogenation of ethylnicotinate to ethylnipecotinate (84), the first stage involving a two-mole hydrogen addition over Pd/C to produce the 1, 4, 5, 6-tetrahydro derivative. This was followed by an investigation into the enantioselective hydrogenation of the intermediate over a cinchona-modified catalyst. The highest enantiomeric excess was obtained at a low conversion (24 % ee, 10 % cnvsn) over a dihydrocinchonidine modified Pd/TiO₂. No mechanistic interpretation was given.

Here in Hull, the author has recently achieved the direct enantioselective hydrogenation of an aromatic N-heterocycle catalysed by alkaloid modified Pd/C (85). To the best of the authors' knowledge, this is the first reported example of direct heterogeneous enantioselective hydrogenation of an aromatic heterocycle (see Chapter Five).

Two notable inclusions are given. Bond and co-workers have recently achieved the enantioselective hydrogenation of MeC(=NH)COOMe, the imine analogue of methyl pyruvate, over cinchona modified Pt (86). This reaction, like pyruvate hydrogenation, was accompanied with a rate enhancement.

Wilkinson, working in Hull, has enantioselectively hydrogenated methylnicotinate to its fully saturated analogue over pivalic/tartaric acid modified Raney Ni (87), using the catalyst preparation method described by Tai and Sugimura (88).

REFERENCES

1. Andrews, L. H., and McElvain., *J. Amer. Chem. Soc.* **51**, 887 (1929)
2. Renshaw, R. R., and Cross., W. E., *J. Amer. Chem. Soc.* **61**, 1195 (1939)
3. Adkins, H., and Coonradt, H. L., *J. Amer. Chem. Soc.* **63**, 1563 (1941)
4. Landa, S. , Kafta, Z., Galik, V., and Safar, M., *Coll. Czech. Chem. Comm.* **34**, 3588 (1969)
5. Gilchrist, T. L., *Heterocyclic Chemistry*, 2nd ed. Longman Group, London 1992
6. Kaiser, H P., and Muchowski, J. M., *J. Org. Chem.* **49**, 4203 (1984)
7. Craig, L. C., and Hixen, R. M., *J. Amer. Chem. Soc.* **58**, 187 (1931)
8. Chang, Y. C., and Kalechits, I. V., *K'o Hseu T'ung Pao*, **15**, 478 (1958)
9. Balandin, A. A., and Khidekel. M. L., *Docklady Akat, Navk S. S. S. R.* **123**, 83 (1958)
10. Badger, G. M., and Jackson, G. D. F., *J. Chem. Soc.* 4438 (1960)
11. Putokhin, N., *J. Russ. Phys. Chem.* **62**, 2216 (1930)
12. Signaigo, F. K., and Adkins, H., *J. Amer. Chem. Soc.* **58**, 709 (1936)
13. Rainey, J.L., and Adkins, H., *J., Amer. Chem. Soc.* **61**, 104 (1939)
14. Hegedús, L., Máthé, T and Tungler, A., *App. Catal A.* **143**, 309 (1996)
15. Hegedús, L., Máthé, T and Tungler, A., *App. Catal A.* **147**, 407 (1996)
16. Freifelder, M., *Advances in Catalysis.* **14**, 203 (1963)
17. Skita, A., *Chem Ber.* **48**, 1486 (1915)
18. Skomoroski., and Shriesheim., *J. Phys. Chem.* **65**, 1340 (1961)
19. Skita, A., and Brunner, W., *Chem. Ber.* **49**, 1597 (1916)
20. Walker, S., *J. Org. Chem.* **27**, 2962 (1962)
21. Gilman, G., *Advances in Catalysis.* **9**, 733 (1957)
22. Freifelder, M., *J. Org. Chem.* **27**, 4046 (1962)

23. Scigliano, J. J., *US Patent*. 2,843,598 (1958)
24. Felder, E., Maffei, S., Pietra, S., and Pitré, D., *Helv. Chim. Acta.* **43**, 888 (1960)
25. Behun, J. D., and Levine, R., *J. Org. Chem.* **26**, 3379, (1961)
26. Mizzoni, R. H., and Spoerri, P. E., *J. Amer. Chem. Soc* **67**, 2201, (1954).
27. Henze, H. R., and Winthrop, S. O., *J. Amer. Chem. Soc* **79**, 2230 (1957)
28. Biot, J.B., *Mem. Cl. Sci. Math. Phys. Inst. Imp. Fr.* **13**, 1 (1812)
29. Biot, J.B., *Bull. Soc. Philomath, Paris* **190** (1815)
30. Pasteur, L., *C. R. Acad. Sci.* **26**, 535 (1848)
31. Le Bel, J. A., *Soc. Chim. Fr.* **22**, 337, (1874)
32. Van't Hoff, J. H., *Arch. Neerl. Sci. Exacts. Nat.*, **9**, 445
33. Cahn, R. S., Ingold, C. K., and Prelog, V., *Angew. Chem. Int. Ed. Engl.*, **5**, 385, (1966)
34. von Blaschke, G., Kraft, H. P., Finkenstcher, K., and Kohler, F., *Arzneim. Forsch./Drug Res.* **29**, 1640 (1979)
35. FDA policy statement, *Chirality*, **4**, 338 (1992)
36. Schwab, G. M., Rudolph, L., *Naturwiss*, **20**, 362 (1932)
37. Schwab, G. M., Rost, F., and Rudolph, L., *Kolloid-Zeitschrift*, **68**, 157 (1934)
38. Lipkin, D., and Stewart, T. D., *J. Amer. Chem. Soc* **61**, 3295 (1939)
39. Akabori, S., Izumi, Y., Fuji, Y., and Sakurai, S., *Nature*, **178**, 323 (1956)
40. Izumi, Y., *Advan. Catal.*, **32**, 215 (1983)
41. Brunner, H., Muschiol, M., Wishert, T., and Wiehl, J., *Tetrahedron Assym.*, **1**, 159 (1980)
42. Webb, G., and Wells, P. B., *Catal. Today*, **12**, 319 (1992)
43. Osawa, T., Harada, T., and Tai, A., *J. Catal.*, **121**, 7 (1990)
44. Wilkinson, A. G., and Wells, P. B., Unpublished work.

45. Orito, Y., Imai, S., and Niwa, S., *Nippon Kagaku Kaishi*, **30** (1978)
46. Orito, Y., Imai, S., Niwa, S., and Ngoyen, G-H., *J. Synth. Org. Chem. Japan*, **37**, 173 (1979)
47. Orito, Y., Imai, S., and Niwa, S., *Nippon Kagaku Kaishi*, 1118 (1979)
48. Orito, Y., Imai, S., and Niwa, S., *Nippon Kagaku Kaishi*, 670 (1980)
49. Orito, Y., Imai, S., and Niwa, S., *Nippon Kagaku Kaishi*, 137 (1982)
50. Blaser, H. U., Jallet, H. P., Monti, D. M., Reber, J. F., and Wehrli, J. T., *Stud. Surf. Sci. Catal.*, **41**, 153 (1988)
51. Wehrli, J. T., Baiker, A., Monti, D. M., and Blaser, H. U., *J. Mol. Catal.* **49**, 195 (1989)
52. Wehrli, J. T., Baiker, A., Monti, D. M., and Blaser, H. U., *J. Mol. Catal.* **61**, 207 (1990)
53. Bond, G. C., and Wells, P. B., *Appl. Catal.* **18**, 221 (1985)
54. Bond, G. C., and Wells, P. B., *Appl. Catal.* **18**, 225 (1985)
55. Geus, J. W., and Wells, P. B., *Appl. Catal.* **18**, 231 (1985)
56. Freuner, A., and Wells, P. B., *Appl. Catal.* **18**, 234 (1985)
57. Wells, P. B., *Appl. Catal.* **18**, 259 (1985)
58. Sutherland, I. M., Ibbotson, A., Moyes, R. B., and Wells, P. B., *J. Catal.* **125**, 77 (1990)
59. Jackson, S. D., Keegan, M. B. T., McLellan, G. D., Meheux, P. A., Moyes, R. B., Webb, G., Wells, P. B., Whyman, R., and Willis, J., *Prep. of Catalysts V*, (Poncelet, G., Jacobs, P. A., Grange, P., and Delmon, P., (Eds.), pp. 134-144, Elsevier, Amsterdam, 1991.
60. Wermeer, W. A. H., Ph.D Thesis, University of Hull (1995).
61. Sutherland, I. M., Ph.D Thesis, University of Hull (1989)

62. Sutherland, I. M., Ibbotson, A., Moyes, R. B., and Wells, P. B., *J. Catal.*, **125**, 77 (1990)
63. Bond, G., Simons, K. E., Meheux, P. A., Ibbotson, A., Wells, P. B., and Whan, D. A., *Catal. Today*, **12**, 421 (1992)
64. Bond, G., Meheux, P. A., Ibbotson, A., Wells, P. B., *Catal. Today*, **10**, 371 (1991)
65. Blaser, H. U., Jalett, H. P., Monti, D. M., Rebert, J. F., and Wehrli, J. T., *Stud. Surf. Sci. Catal.*, **41**, 153 (1988)
66. Hall, T. J., Johnstone, P., Vermeer, W. A. H., Watson, S. R., and Wells, P. B., *Surf. Sci. Catal.*, **101**, 221 (1996)
67. Hall, T. J., Ph.D Thesis, University of Hull (1997)
68. Perez, J. R. G., Malthete, J., and Jacques, J., *CR Acad. Sc. Paris*, **169**, 300 (1985)
69. Bartok, M., Wittman, G., Bartok, G. B., and Gondus, G., *J. Organomet. Chem.*, **384**, 385 (1990)
70. Nitta, Y., Ueda, Y., and Imanaks, T., *Chem. Lett.*, 1095 (1994)
71. Nitta, Y., and Kobiro, K., *Chem. Lett.*, 165 (1995)
72. Nitta, Y., and Kobiro, K., *Chem. Lett.*, 897 (1996)
73. Niita, Y., Kobiro, K., and Okamoto, Y., *Stud. Surf. Sci. Catal.*, **108**, 191 (1997)
74. Nitta, Y., and Shibata, A., *Chem. Lett.*, 161 (1998)
75. Watson, S. R., Ph. D Thesis, University of Hull (1995)
76. Borszky, K., Mallat, T., and Baiker, A., *Cat. Lett.*, **41**, 199 (1996)
77. Smith, G. V., Cheng, J., and Song, R., *Cat. Lett.*, **45**, 73 (1997)
78. Tungler, A., Mathe, T., Petro, J., and Tarnai, T., *J. Mol. Catal.*, **61**, 259 (1990)
79. Tungler, A., Fodor, K., Mathe, T., and Sheldon, R. A., *Stud. Surf. Sci. Catal.*, **108**, 157 (1997)
80. Thorey, C., Henin, F., and Muzart, J., *Tet. Asymm.*, **7**(4), 975 (1996)

81. Yoshida, T., and Harada, K., *Bull. Chim. Soc. Japan*, **44**, 1062 (1971)
82. Borszky, K., Mallat, T., Aeschmann, R., Schweizer, W. B., and Baiker, A., *J. Catal.*, **161**, 451 (1996)
83. Fuchs, R., and Roduit, J-P., EP 0744401A2961127, assigned to Lonza.
84. Blaser, H. U., Honig, H., Studer, M., and Wedemeyer-Exl, C., *J. Mol. Catal.* **139**, 253 (1999)
85. Carroll, J. R., and Wells, P. B., Submitted to Chem. Comm. (2000)
86. Bond, G., May, V. A., and Parks, G. M. B, Personal Comm.
87. Wilkinson, A. G., and Wells, P. B., Unpublished work
88. Sugimura, T., Osawa, T., Nakagawa, S., Harada, T., and Tai, A., *Stud. Surf. Sci. Catal.*, **101**, 231 (1996)

Chapter Two

Experimental

2.1 Materials

2.1.1 Catalysts

The catalyst most extensively used in this study was a 5% Pd/C paste, type 5R 87L, manufactured by Johnson Matthey. The total surface area of the catalyst, as measured by the BET method was $1000 \text{ m}^2 \text{ g}^{-1}$ with a metal surface area of $17.8 \text{ m}^2 \text{ g}$.

Other catalysts have been used.

Table 2.1.1 Catalysts used

Catalyst	Supplier
5% Pd/C	Johnson Matthey
EUROPT-1 ^a	Johnson Matthey
5% Pt/C	Johnson Matthey
5% Ru/C	Johnson Matthey
5% Rh/C	Johnson Matthey
5% Pd/TiO ₂	^b

^a. 6.3% Pt/SiO₂

^b. Sample provided by Prof. Tungler (Budapest)

2.1.2 Reactants

Reactants used in this study are listed in Table 2.1.2; all were used as received unless otherwise stated.

Table 2.1.2 Reactants used in this study

Reactant	Supplier	Stated Purity/%
Pyrazine	Lancaster	>99
Pyrazine-d ₄	Aldrich	>98
Pyrazine-2-carboxylic acid	Aldrich	99
Methylpyrazine-2-carboxylate	Lancaster	>98
Pyrazine-2,3-dicarboxylic acid	Lancaster	98
Pyrazine-2-carbonitrile	Aldrich	99
2-methylpyrazine	Lancaster	>99

2.1.3 Solvents

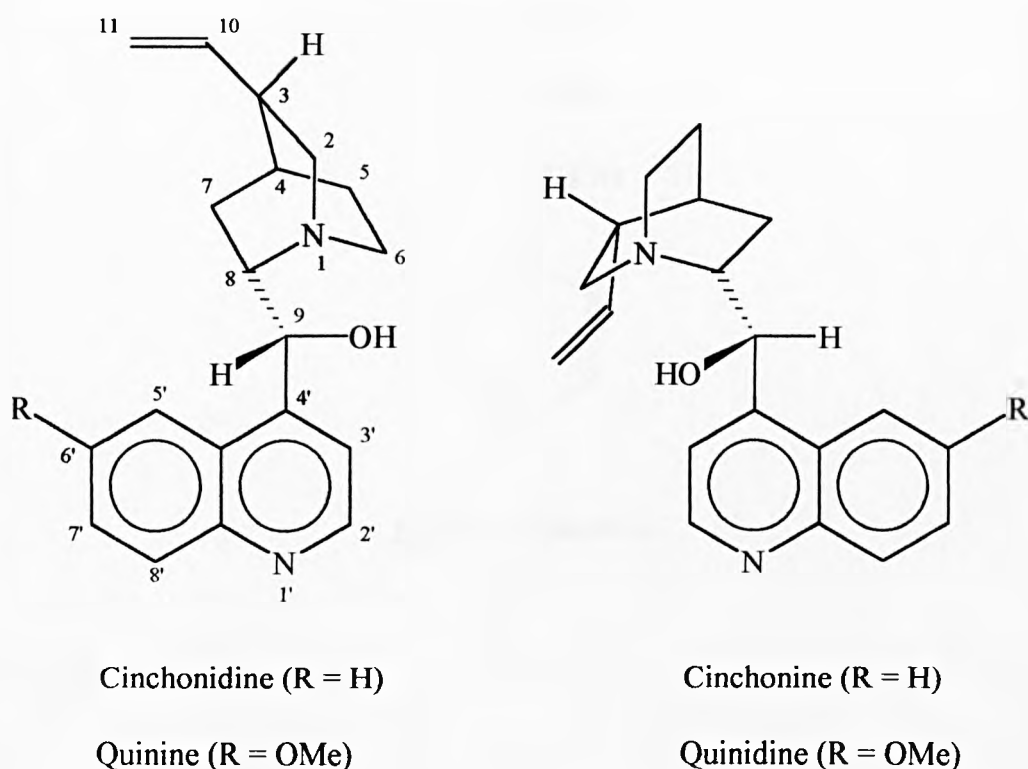
Solvents used in this study are listed in Table 2.1.3; all were used as received except where indicated.

Table 2.1.3 Solvents used in this study

Solvent	Supplier	Stated Purity/%
Methanol	AnalaR	-
Ethanol	AnalaR	-
Propan-2-ol	Prolabo	99
Butan-1-ol	Sigma-Aldrich	99
Glacial acetic acid	Pronalys AR	>99
Acetone	Fisher	>99
Dimethylformamide	Aldrich	99
Dichloromethane	Fisher	>99
Toluene	Fisher	99
Tetrahydrofuran	Fisher	>99

2.1.4 Alkaloid modifiers

Four cinchona alkaloids were used: cinchonidine (96%, Aldrich), cinchonine (Hopkins and Williams), quinine, and quinidine (both ACF Chemie). Their structures are given in Figure 2.1.1.



Atom	C4	C5	C8	C9
Cinchonidine	R	S	S	R
Cinchonine	R	S	R	S
Quinine	R	S	S	R
Quinidine	R	S	R	S

Fig. 2.1.1 Structures and configurations of the cinchona alkaloids

The four diastereoisomers of ephedrine (Figure 2.1.2) were investigated: -1R, 2R (Sigma), -1R, 2S (99%, Aldrich), -1S, 2S (Sigma), and -1S, 2R (98%, Aldrich). Their general structure is given in Figure 2.1.2.

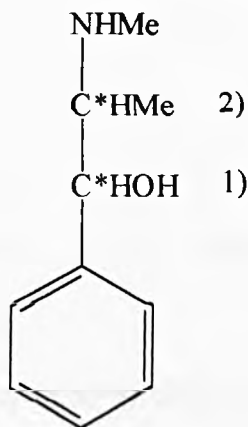


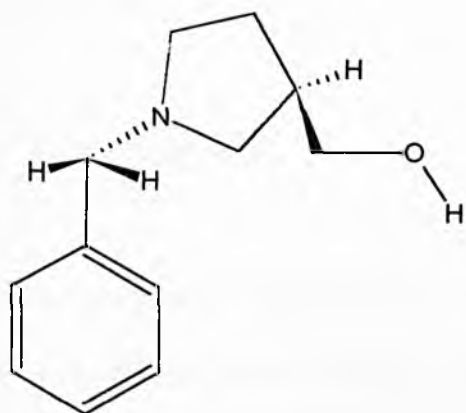
Fig. 2.1.2 Ephedrine

2.1.5 Synthetic Modifiers

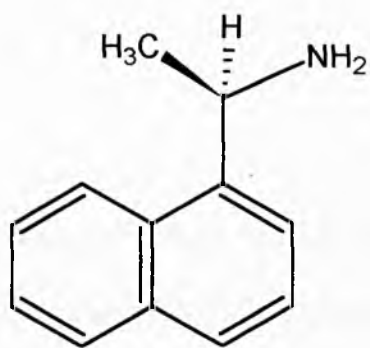
(R)-1-(1-naphthyl)ethylamine and (S)-(-)-1-benzyl-2-pyrrolidine methanol were investigated as modifiers; both have been used successfully as modifiers for the enantioselective hydrogenation of ethyl pyruvate over Pt (1,2). Their structures are given in Figure 2.1.3.

2.1.6 Other materials

Other materials used are listed in Table 2.1.4. All were used as received unless otherwise stated.



(S)-(-)-1-benzyl-2-pyrrolidine methanol



(R)-1-(1-naphthyl)ethylamine

Fig. 2.1.3 Structures of Synthetic Modifiers

Table 2.1.4 Other materials

Material	Supplier
Trifluoroacetic anhydride	Aldrich
Ethanol-OD	Aldrich
Hydrogen	Energas
Nitrogen	Energas
N-Benzylcinchonidium chloride	Aldrich
Deuterium	BOC
30% Nitrogen in helium	Linde
Amberlite mesh IR 45-OH	BDH
Pivalic acid	Aldrich
R, R-Tartaric acid	BDH
S, S-Tartaric acid	Aldrich
NaBr	Fisher

2.2 Apparatus

2.2.1 Vacuum Apparatus

Catalyst activation was achieved by use of a general-purpose glass vacuum apparatus fitted with greaseless taps (Young). A vacuum of approximately 10^{-4} Torr was achieved using an Edwards Speedivac rotary pump in conjunction with an Edwards oil diffusion pump. Pressures were measured using a mercury manometer and a Penning 8 gauge.

2.2.2 Static Reduction

Samples of catalyst (normally 0.1g) were placed into a 17 ml glass vessel equipped with a Youngs Tap and a No. 17 Suba-Seal as shown in Figure 2.2.1. This reduction vessel was attached to the vacuum line by a B14 cone, using a Viton O-ring. If the reduction required elevated temperatures, an Amalgams tubular furnace, controlled by a Eurotherm (822) programmable temperature controller was used to heat the lower part of the vessel.

2.2.3 Catalyst Modification

When a reaction involved a modified catalyst, the modifier solution was injected into the static reduction vessel described above, using a 10 ml disposable syringe fitted with a 1.5" LeurLock needle. If modification in air was required, the catalyst-modifier slurry was transferred to a 100 ml glass beaker and placed on a stirrer hotplate and its contents stirred using a 1" Teflon coated stirrer bar for the required amount of time.

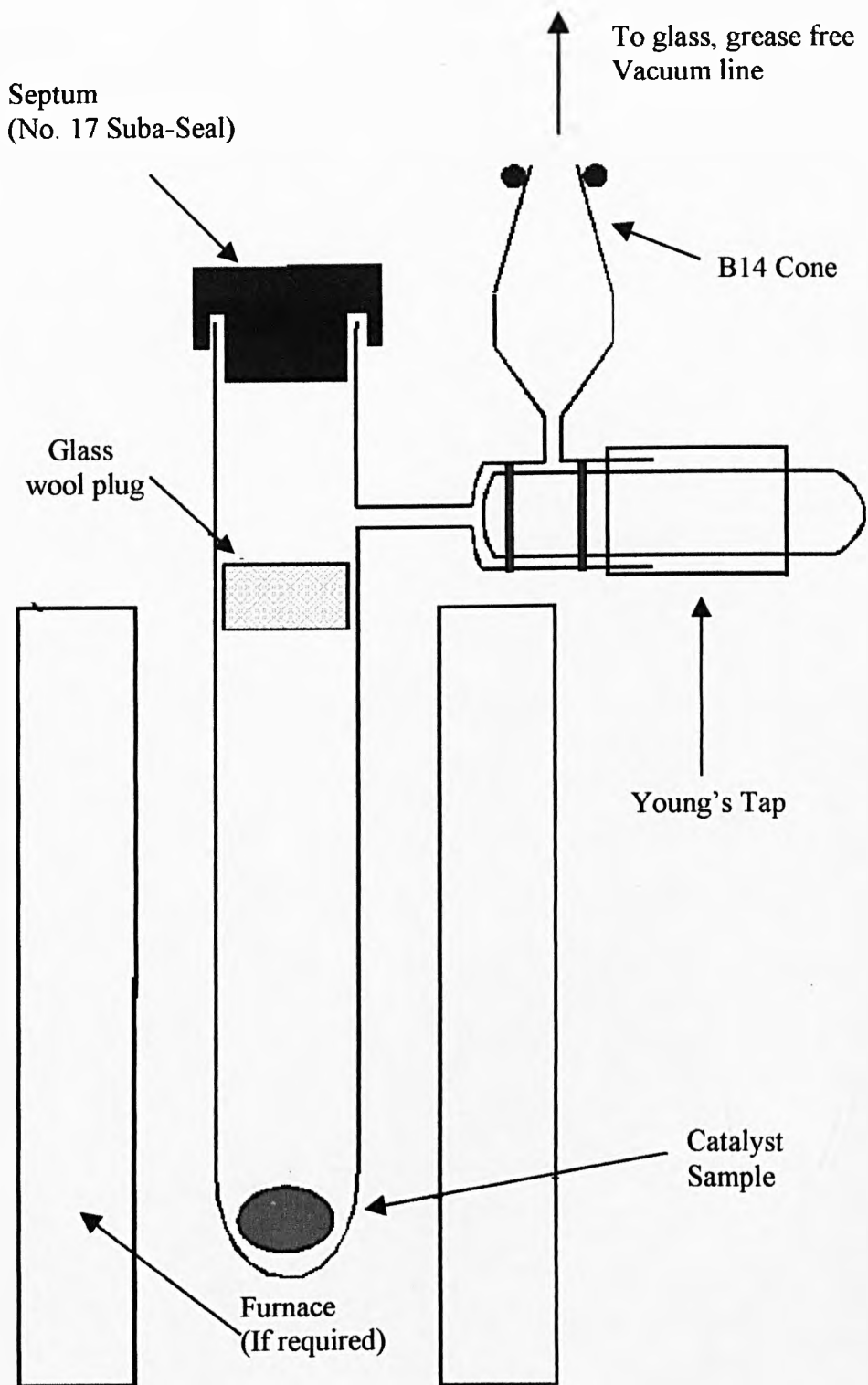


Figure 2.2.1 Static reduction vessel

2.2.4 Büchi Autoclave

Hydrogenation at pressures up to 10 bar pressure were achieved in the Büchi glass autoclave which was pressure tested to 20 bar at 473 K. A schematic representation of the system is shown in Fig. 2.2.2.

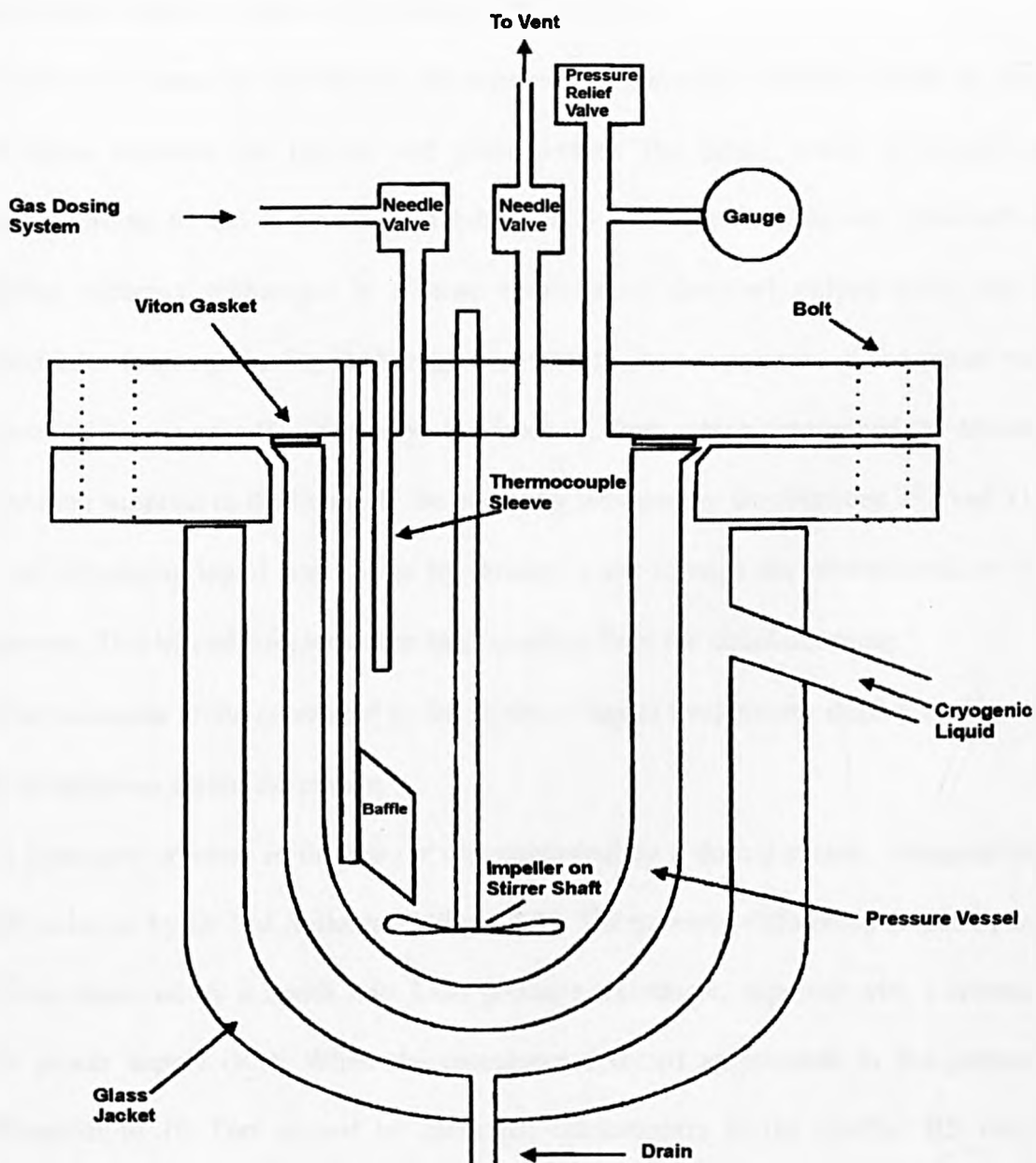


Figure 2.2.2 Büchi Autoclave

The 250 ml round bottomed glass reaction vessel was housed in a 1000 ml glass jacket. The vessel was attached to the metallic head plate by eight bolts, and pressure integrity was achieved by use of a Viton seal.

A metal impeller connected to a metal stirrer shaft agitated the contents of the reactor. This shaft was magnetically coupled to a drum connected to a Planetrol motor, capable of variable speeds up to 2200 rpm. The reactor contained a baffle to ensure thorough mixing and operation outside of diffusion control limits.

Temperature control of the reactor was achieved by pumping cryogenic liquid through the space between the reactor and glass jacket. The liquid could be heated to temperature up to 523 K by use of a Julabo HC8 heating unit. This unit consisted of heating elements submerged in a large reservoir of dimethyl polysiloxane, and a recirculator to pump the liquid through the reactor. The temperature of the liquid was monitored by use of a PT100 sensor, the feedback from which determined the amount of heating supplied to the liquid. If the operating temperature was between 293 and 313 K, the circulating liquid was cooled by flowing water through the internal coils in the reservoir. This helped counteract the heating effect from the circulator pump.

A thermocouple probe connected to the Julabo's digital temperature display monitored the temperature within the reactor.

The hydrogen pressure in the reactor was controlled by a dosing system, designed and built in-house by Dr I M Sutherland (Fig 2.2.3). The pressure differential across S_1 and S_2 was measured by a South East Labs pressure transducer, supplied with a constant 24V power supply (RS). When the transducer detected an increase in the pressure differential of 10 Torr caused by hydrogen consumption in the reactor, RS relays activated S_1 and S_2 in a sequence which first dosed hydrogen from the constant volume

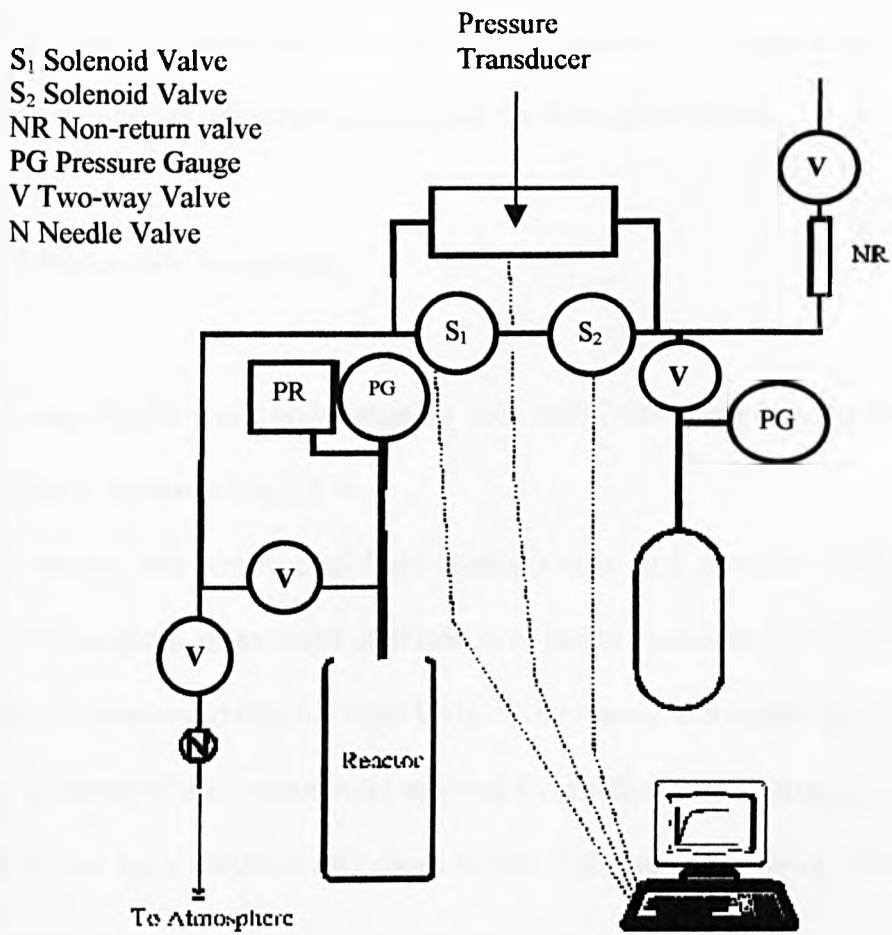


Figure 2.2.3 Gas Dosing System

into the reactor and then recharged the volume to its reference pressure. Pressure in the reactor was therefore kept constant throughout the reaction.

The gas dosing system was controlled, and the dosed volume of hydrogen recorded, by a BBC computer connected to the pressure transducer. Hydrogen uptake was displayed on the monitor as a function of time and the data saved to disk.

2.2.5 Baskerville Autoclave

The majority of work undertaken in this study was carried out using the Baskerville autoclave, shown in Fig 2.2.4.

The reactor was constructed from stainless steel and pressure rated to 100 bar. The reactor consisted of an outer stainless steel jacket containing a 100 ml glass liner. The reactor was screwed into the main body of the reactor and sealed using a PTFE seal.

The contents of the reactor were agitated by a teflon paddle attached to the drive shaft and driven by a Parvalux DC shunt motor. This was capable of stirring speeds up to 1400 rpm.

The gas pressure within the reactor was maintained by a Büchi Pressflow Controller, model 9901 interfaced to a PC. This monitored hydrogen consumption from the reaction and when necessary dosed a calibrated quantity of gas. Post reaction data processing was carried out using Microsoft Excel 97 software.

2.2.6 Other reactor vessels

Reactions involving deuterium in place of hydrogen and the study of deuteriated compounds were carried out using a 30 ml glass reaction vessel (Fig. 2.2.5).

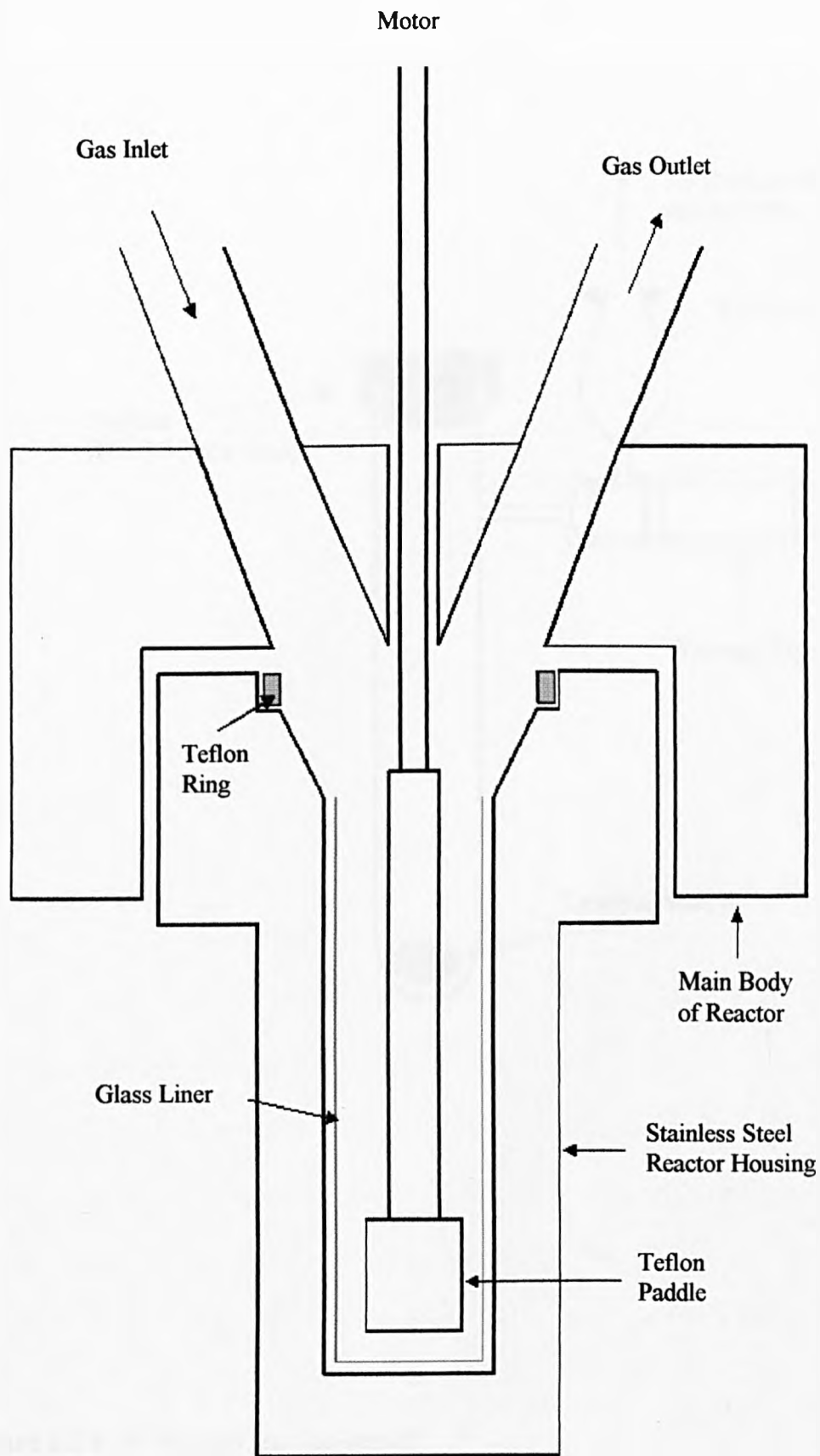


Figure 2.2.4 The Baskerville Autoclave

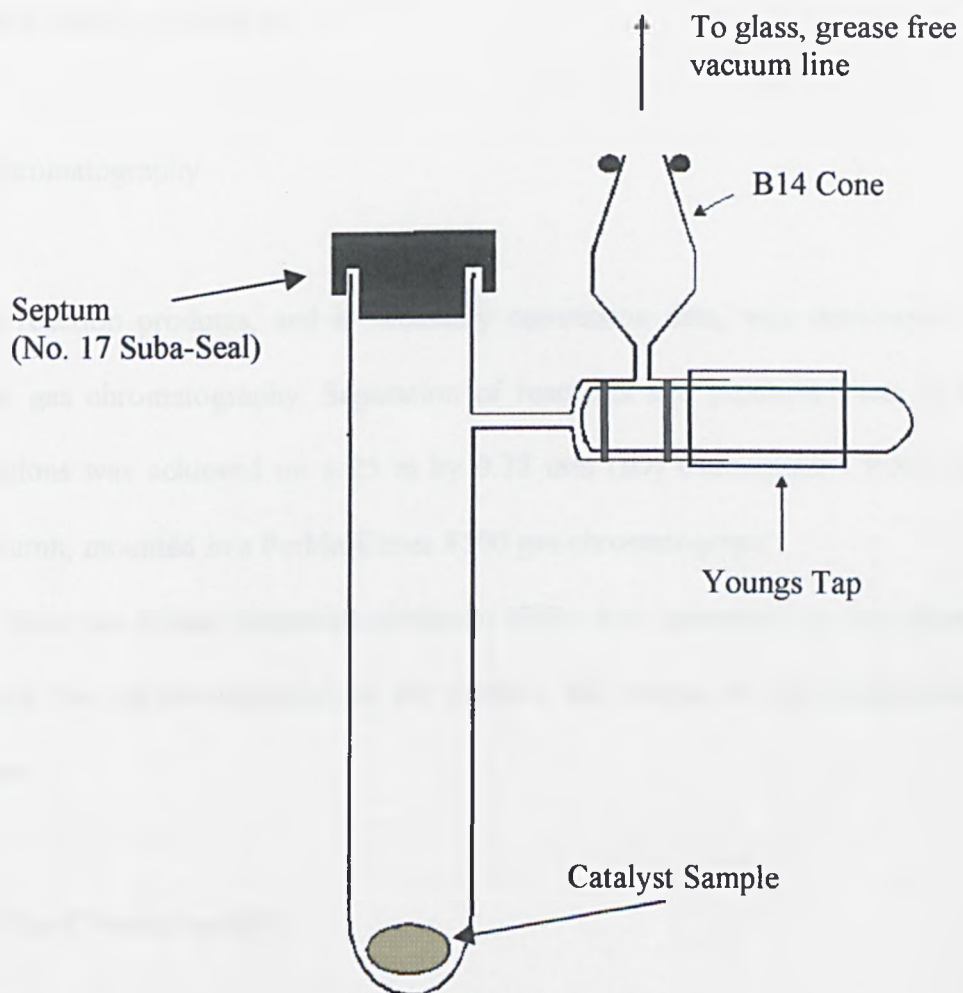


Figure 2.2.5 30 ml glass reaction vessel

2.2.7 Product Separation

Products and reactants were separated from the catalyst by suction filtration using a Pyrex sintered funnel, porosity No. 4.

2.2.8 Gas Chromatography

Analysis of reaction products, and if necessary conversion data, was determined by conventional gas chromatography. Separation of reactants and products from all the studied reactions was achieved on a 25 m by 0.32 mm (ID) Chrompack CP-Sil 5CB capillary column, mounted in a Perkin-Elmer 8500 gas chromatograph.

The signal from the Flame Ionisation Detector (FID) was measured by the internal integrator and the results displayed to the monitor and output to the Perkin-Elmer GP100 printer.

2.2.9 Chiral Gas Chromatography

The products from enantioselective reactions were analysed, where possible, by chiral chromatography. A Chrompack CP9001 chromatograph was fitted with a FID and a Chrompack 25m x 0.25mm Chirasil-Dex CB capillary column. The internal integrator running in conjunction with the package Chrom-Card for Windows, processed the signal from the FID. The resulting data were captured on a PC for manipulation.

2.2.10 Polarimetry

When chiral chromatography wasn't feasible, an Optical Activity AA-10 polarimeter was used to measure the optical rotation of products from possible enantioselective reactions. The sample cell length was 20 cm and the rotation measured at the sodium D-line at ambient temperature.

2.2.11 Mass Spectrometry and Gas Chromatography Mass Spectrometry (GCMS)

Conventional probe mass spectrometry was performed using a Finnigan MAT automated quadropole mass spectrometer. Analysis was additionally carried out on a Thermoquest Finnigan GCQ ion trap GCMS operating at a fixed voltage of 70 eV. The column used in the GC was a SGE BPX5, 30m by 0.25mm capillary.

2.2.12 ^1H NMR and FTIR

^1H NMR analysis was predominantly performed on a Jeol JNM LA400MHz FTNMR and to a lesser extent, a Jeol 270MHz FTNMR. Analysis by FTIR was undertaken using a Perkin Elmer Paragon 1000 FTIR spectrometer interfaced to a PC running PE Spectrum for Windows software.

2.2.13 Catalyst Characterisation

The morphology of the catalyst was investigated using a Jeol Jem 100C High Resolution Transmission Electron Microscope operating at 100KeV.

The single point BET surface areas of the catalyst were determined using a Micromeritics Pulse Chemisorb 2700 instrument.

2.2.14 Molecular Modelling

Two software packages were used. Initial investigations were carried out using HyperChem 4.5 for Windows, and later investigations used Cerius 2 operating under Unix software on a Silicon Graphics workstation.

2.3 Procedures

2.3.1 Catalyst Activation

2.3.1.1 Pd/C

Samples of the as-received catalyst (0.1g) were placed into the reduction vessel described in section 2.2.2. A small amount of glass wool was gently pushed into the tube, just above the catalyst to prevent any catalyst particles being withdrawn while under vacuum. The vessel was attached to the vacuum line, evacuated for 30 min at approximately 10^{-4} Torr and isolated from vacuum by the closing of the Youngs tap. The vacuum line was flushed three times with hydrogen, to completely purge any air from the system and then filled with hydrogen (~ 1 atm).

The Youngs tap was opened and the catalyst exposed to hydrogen at near atmospheric pressure and room temperature for 40 min. Sometimes the reduction was carried out at elevated temperatures, for which a furnace was placed around the vessel.

2.3.1.2 Other PGM catalysts

The reduction of PGM catalysts other than Pd/C used the method described in section 2.3.1.1, the only difference being an elevated reduction temperature of 403 K.

2.3.1.3 Raney Ni

The Raney Ni catalyst was prepared by the digestion of 1.9 g Al/Ni alloy (50/50 or 42/58 powder) in 20 ml 5M NaOH, for 1 h over a hot-plate. The catalyst was allowed to cool and then washed with distilled water (20 x 30 ml). At this point the catalyst, if

allowed to dry, was highly pyrophoric so it was imperative to leave under water until used.

2.3.2 Catalyst Modification

2.3.2.1 PGM catalysts

When a reaction presented a possible enantioselective outcome, a modified catalyst was used. The standard procedure for catalyst modification involved dissolving the alkaloid (0.5g) in 50 ml of solvent and then injecting a sample (5 ml) onto the catalyst, via a suba-seal, into the reduction vessel. The mixture was then shaken to ensure a thoroughly wetted catalyst and added to the remaining modifier solution. This was normally stirred in air for 1h at room temperature.

The reactant (5 mmol) was dissolved in the solution, which was then added to the reactor.

When a reaction required an unmodified catalyst, a sample (5 ml) of the reaction solvent was injected in place of the modifier solution. This was shaken and added to the reactor.

2.3.2.2 Raney Ni

The activated Raney Ni catalyst was stored under water (see Section 2.3.1.3). The water was decanted and the catalyst added to a solution of 1 g tartaric acid (either R, R or S, S) and NaBr (6 g) in 100 ml distilled water. The pH of the solution was adjusted to 3.2 with 1 M NaOH solution and heated for 1 h at 100°C. The catalyst was allowed to cool and magnetically decanted from the solution. This was then washed with distilled water

(50 ml), methanol (50 ml, twice) and then the reaction solvent (25 ml). The catalyst was washed into the reactor with the reaction solvent (30 ml).

The reactant (5 mmol) was dissolved in 5 ml of reaction solvent and added to the reactor followed by 5 ml of pivalic acid.

2.3.3 Büchi Autoclave

The catalyst slurry and reaction solution was added to the reactor. The vessel was sealed into place and, for reaction at ambient temperature, the water-cooled circulating oil started to maintain a constant temperature.

The solenoid valves were opened, and the system purged with hydrogen three times (2 x 5 bar, 1 x 10 bar). The vessel was then pressurised to 10.4 bar, the solenoids closed and the pressure of the reactor reduced to the operating pressure of 10 bar.

Information about the date, experiment name, and ambient temperature was entered into the computer. The computer then calculated the difference between the regulator and reactor pressure and performed an internal calibration so it could accurately perform the dosing volume.

The contents of the reactor were then stirred at a speed of 1200 rpm and the hydrogen dosing system activated to maintain a constant pressure and record the hydrogen consumption against time. The reaction was allowed to continue until it had reached the desired conversion.

2.3.4 Baskerville Autoclave

The Baskerville Autoclave was used when hydrogen pressures greater than 10 bar were required. The standard hydrogenation procedure involved as above, the addition of the reactant/catalyst/solvent mixture to the glass liner of the reactor, which was, then placed into the reactor. The reactor was sealed, purged with hydrogen three times and charged to its operating pressure.

The contents were stirred at 1200 rpm and room temperature unless otherwise stated.

The hydrogen dosing system was activated to maintain a constant pressure and a PC recorded the hydrogen consumption against time.

2.3.5 Product Separation and Analysis

The catalyst was separated from the reaction mixture by suction filtration using a Pyrex sintered funnel (porosity No. 4). Normally, a 2 μ l sample was injected onto the GC column (non-chiral) as described in section 2.2.11, to analyse for product conversion. The temperature of the oven was kept constant at 423 K for 40 min and the conversion calculated by peak integration.

If a new compound was being hydrogenated, GCMS was used to analyse the reaction products. A typical injection volume was 1 μ l at an isothermal analysis temperature of 453 K.

The products from a reaction involving a modified catalyst were typically analysed by chiral GC. This was only carried out on the products from methyl pyrazine-2-carboxylate hydrogenation. The procedure involved the evaporation of a sample (10 ml) to near dryness in a stream of nitrogen, followed by the addition of trifluoroacetic

anhydride (1 ml). This was shaken and left to stand at room temperature for 1 h. Again this was evaporated to near dryness in a stream of nitrogen, and ethanol (2 ml) added.

A 0.2 μ l portion was injected onto the chiral column described in section 2.2.11 operated at an isothermal temperature of 407 K. The enantiomeric excess was measured from the integrated eluted enantiomer peaks.

The enantiomeric excess (%) = $[X_R - X_S] / [X_R + X_S] \times 100$

Where X_R = Int. area of R-enantiomer and X_S = Int. area of S-enantiomer

2.3.6 Intermediate Investigation

The intermediate reaction products formed in methyl pyrazine-2-carboxylate (PCME) and 2-cyanopyrazine hydrogenation were investigated after a two-mole uptake.

A typical unmodified hydrogenation was carried out, as described in section 2.2.3 but the reaction terminated after a 2-mole uptake. The catalyst was removed by suction filtration and a 0.1 μ l portion analysed by GCMS. An additional volume of reaction solution (10 ml) was carefully evaporated to near dryness (stream of nitrogen) leaving the ester in a suitable state for ^1H NMR analysis.

2.3.7 Catalyst Characterisation

The Pd/C was characterised using the techniques described in section 2.2.13.

The total surface area of the catalyst was measured using the BET apparatus. In order for the apparatus to display surface area in m^2 directly, the instrument has to be

calibrated using a 1 ml N₂ injection. This volume of gas represents the amount required to physisorb as a monolayer surface of area = 2.84 m², under standard conditions. However, small deviations had to be accounted for, as laboratory conditions are not standard.

Once the instrument was calibrated, a known mass of catalyst was placed in the sample U-tube, connected to the apparatus and degassed in a 30% N₂/He stream at 533 K for 20 min then allowed to cool to room temperature. Once cool, the tube was immersed in liquid nitrogen and the volume of nitrogen gas adsorbed shown on the output display. The Dewar was removed and the sample allowed to return to room temperature, yielding the volume of desorbed gas. This procedure was repeated several times and an average value used to obtain the surface area, taking into account the final weight of the catalyst.

2.3.8 Competitive Reactions

An investigation into the rates of hydrogenation of pyridine, pyridazine, pyrimidine, pyrazine and triazine over an unmodified 5% Pd/C catalyst was undertaken.

The hydrogenation of each heterocycle (5 mmol) was undertaken using the standard reaction procedure described in section 2.2.3.

2.3.9 Deuterium Tracer/Exchange investigation

2.3.9.1 Reaction of pyrazine with deuterium

The catalyst (0.1g) was placed in the static reduction vessel and activated as described in Section 2.3.1 except molecular deuterium was used in place of hydrogen. A 5 ml portion of $\text{CH}_3\text{CH}_2\text{OD}$ was injected onto the catalyst via a suba-seal and the slurry shaken. The resulting slurry and pyrazine (5 mmol) were added to the Büchi autoclave (Section 2.2.4), whereupon the reactor was sealed, flushed twice with 3 bar deuterium, pressurised to 5 bar, and stirring started (1200rpm). Reaction was terminated at the desired degree of conversion. The catalyst was quickly separated from the mixture by suction filtration and the resulting solution analysed by GCMS.

2.3.9.2 Reaction of pyrazine- h_4 with pyrazine- d_4 .

The catalyst (0.1g) was placed in the glass vessel shown in Fig 2.25 and connected to the glass vacuum line (Section 2.21). The standard procedure, unless otherwise stated, involved activating the catalyst as described in Section 2.3.1.

Stock solutions of pyrazine- h_4 and pyrazine- d_4 , each 0.12 M in ethanol were prepared. A 5 ml portion of each solution was added to the catalyst via a Suba-Seal and the magnetic stirrer started. Samples (0.5 ml) were extracted at regular intervals over a period of 5 h. The catalyst was removed from the sample by gravity filtration and the solution analysed by GCMS.

2.3.9.3 Mass spectrometric analysis of deuteriated pyrazine

Mass spectra of samples of pyrazine ($C_4N_2H_4$) were obtained using GCMS. Ions in the parent ion region were as shown in Table 2.1.5.

Table 2.1.5 Mass spectra of $C_4N_2H_4$ in solution in C_2H_5OH (A), and of $C_4N_2D_4$ in solution in C_2D_5OD (B).

		Ion Abundances						
	m/z=79	80	81	82	83	84	85	86
A	1.6	100.0	19.6	1.2				
A ^a	1.6	100.0	14.5	0.2				
B				1.0	5.6	100.0	4.8	4.0
B ^a				1.0	5.6	100.0	-0.5	3.7

^a. after isotope correction [$^{13}C = 1.1\%$; $^{15}N = 0.36\%$; ^{14}N]

Pyrazine gave only one fragment ion by loss of one hydrogen atom, as shown in Table 2.1.5, the extent of that loss being 1.6 % ($f_1 = 0.016$, see below). The ion at mass 81 should have been zero after isotope correction. The observation that ions were present at $m/z = 81$ with an intensity of 14.5 indicates the acquisition of H^+ by pyrazine molecules in the source. The trace abundance of ions at $m/z = 82$ is attributed to background. Support for the occurrence of such ion reactions in the source was obtained by examination of the spectrum of $C_4N_2D_4$ in C_2D_5OD . Here, the ion at $m/z = 85$ becomes zero after isotope correction within experimental error (as expected), but a significant



Ions at $m/z = 83$ are attributable to $\text{C}_4\text{N}_2\text{HD}_3$ impurity in the $\text{C}_4\text{N}_2\text{D}_4$.

Determination of the relative parent ion concentrations from the mass spectrum after isotope correction was achieved by use of the following equations, where a, b...e represent the required parent ion intensities $\text{C}_4\text{N}_2\text{D}_4^+$, $\text{C}_4\text{N}_2\text{HD}_3^+$... $\text{C}_4\text{N}_2\text{H}_4^+$, and A, B...E the ion intensities at $m/z = 84, 83 \dots 80$ respectively.

<u>-d_x</u>	<u>m/z</u>	
-d ₄	84	a = A
-d ₃	83	b = B
-d ₂	82	c = C - f ₁ (a + 0.25b)
-d ₁	81	d = D - f ₁ (0.75b + 0.50c)
-d ₀	80	e = E - f ₁ (0.50c + 0.75d)
	79	g = f ₁ (0.25d + e)

Table 2. 1. 5 shows $f_1 = 0.016$ and it is assumed that C - H and C - D bonds undergo identical fragmentation in the mass spectrometer. Thus, taking the entry for time = 40 minutes in Table 3.1 of the Results Section as an example:

<u>-d_x</u>	<u>m/z</u>	
-d ₄	84	a = A = 38.0
-d ₃	83	b = B = 39.0
-d ₂	82	c = 18.0 - 0.016(38.0 + 9.7(5)) = 17.2
-d ₁	81	d = 4.0 - 0.016(0.75(39.0) + 0.50(17.2)) = 3.4
-d ₀	80	e = 1.0 - 0.016(0.50(17.2) + 0.75(3.4)) = 0.8
	79	f = 0.016(0.25(3.4) + 0.8) = 1.6

[The observed ion current at $m/z = 79$ was zero]

[The observed ion current at $m/z = 79$ was zero]

A comparison of the ion currents before and after application of the fragmentation correction is as follows.

	$m/z = 84$	83	82	81	80
Before fragmentation correction	38	39	18	4	1
After fragmentation correction	39	39	18	3	1

It is therefore concluded that fragmentation can be neglected, and that the spectra for pyrazine samples containing deuterium, after correction for ^{13}C and ^{15}N , give the relative parent ion abundances directly within experimental error.

2.3.9.4 Mass spectrometric analysis of deuteriated piperazine

The parent ion for piperazine, $\text{C}_4\text{N}_2\text{H}_{10}$ ($m/z = 86$) was small compared to the fragment ion formed by the loss of one hydrogen atom $f_1 = 14.1$ ($m/z = 85$, Section 3.3.2). The ion at mass 87 was zero (within experimental error), indicating no H^+ addition by ion reaction in the source.

The extent of fragmentation of piperazine is so large that it cannot be used quantitatively.

The scheme for application of the fragmentation correction is as follows (where $a, b \dots m$ represent the required parent ion intensities, and $A, B \dots M$ are the ion intensities (after isotope correction) at $m/z = 96, 95 \dots 86$ respectively).

<u>-d_x</u>	<u>m/z</u>	
-d ₁₀	96	a = A
-d ₉	95	b = B
-d ₈	94	c = C - f ₁ (a + 0.10b)
-d ₇	93	d = D - f ₁ (0.90b + 0.20c)
-d ₆	92	e = E - f ₁ (0.80c + 0.30d)
-d ₅	91	g = G - f ₁ (0.70d + 0.40e)
-d ₄	90	h = H - f ₁ (0.60e + 0.50g)
-d ₃	89	j = J - f ₁ (0.50g + 0.60h)
-d ₂	88	k = K - f ₁ (0.40h + 0.70j)
-d ₁	87	l = L - f ₁ (0.30j + 0.80k)
-d ₀	86	m = M - f ₁ (0.20k + 0.90l)

Taking the entry for time = 60 minutes in Table 3.7 of the Results Section as an example:

<u>-d_x</u>	<u>m/z</u>	
-d ₁₀	96	a = 0
-d ₉	95	b = 0
-d ₈	94	c = 0
-d ₇	93	d = 0
-d ₆	92	e = 5 - 0 = 5
-d ₅	91	g = 15 - 14.1(0.7(0) + 0.4(5)) = -13.2
-d ₄		[no way forward]

It is concluded that fragmentation cannot be allowed for quantitatively when it is so extensive. Thus, in the discussion of results, quantitative statements will be made which make approximate allowance for the extensive fragmentation.

References

1. Schurch, M., Heinz, T., Aeschimann, T., Mallat, T., Pfaltz, A., and Baiker, A.,
J. Catal. 173 187 (1998)
2. Meheux, P. A., PhD Thesis, University of Hull (1991)

Chapter Three

Hydrogenation of Pyrazine

3.1 Introduction

The catalytic hydrogenation of pyrazine has been studied with a view to gaining an understanding of the mode of adsorption and the surface reactivity of this N-heterocycle. First, pyrazine hydrogenation has been studied over a range of metals having a common support. Second, reactions of perdeuteriopyrazine with hydrogen, and of pyrazine with perdeuteriopyrazine, have been studied over Pd.

Third, the relative activity of Pd for the hydrogenation of five N-heterocycles is compared.

Product analysis indicated that no intermediates or high molecular weight products were being formed during pyrazine hydrogenation, and the total hydrogen uptake was as expected, indicating no hydrogenolysis.

3.2 Results

3.2.1 Hydrogen Uptake Curve

The hydrogenation of pyrazine (5 mmol in 40 ml ethanol) at 293 K and 10 bar hydrogen pressure was investigated over Pd, Pt, Rh and Ru, each supported on carbon at 5% loading. The most active catalyst was Pd/C, which converted this concentration of pyrazine to piperazine within 60 min, at an initial rate (r_i) of $260 \text{ mmol h}^{-1} \text{ g}^{-1}$ (Figure 3.1). The other catalysts were less efficient, Ru showing the lowest activity. The order of activity was $\text{Pd} > \text{Rh} > \text{Pt} > \text{Ru}$.

3.2.2 Orders of Reaction

A common method for quantifying the kinetics of reaction is by using the initial rate (r_i), which in this chapter is equivalent to the maximum rate (r_{\max}). However, r_i does not always give the most accurate results due to reaction conditions, therefore in subsequent chapters, r_{\max} replaces r_i .

The kinetics of reaction were studied. Hydrogen uptake curves showed continuously decreasing rates. First order behaviour was tested by plotting of $\ln(a - x)$ against time as shown in Figure 3.2 (where a is the expected final uptake of 15 mmol, and x is the uptake at time t). Linear behaviour was observed up to 75 % conversion, indicating the decreasing rate was first order in remaining pyrazine.

Initial rates at 293 K varied with hydrogen pressure over the range 2 to 10 bar as shown in Figure 3.3. The order in hydrogen, determined from Figure 3.4 was 0.5.

The initial rate varied with pyrazine concentration over the range 5 to 20 mmol as shown in Figure 3.5. The order in pyrazine was approximately -0.4 (Figure 3.6). These initial rate orders are indicative of strong pyrazine adsorption and relatively weak hydrogen adsorption.

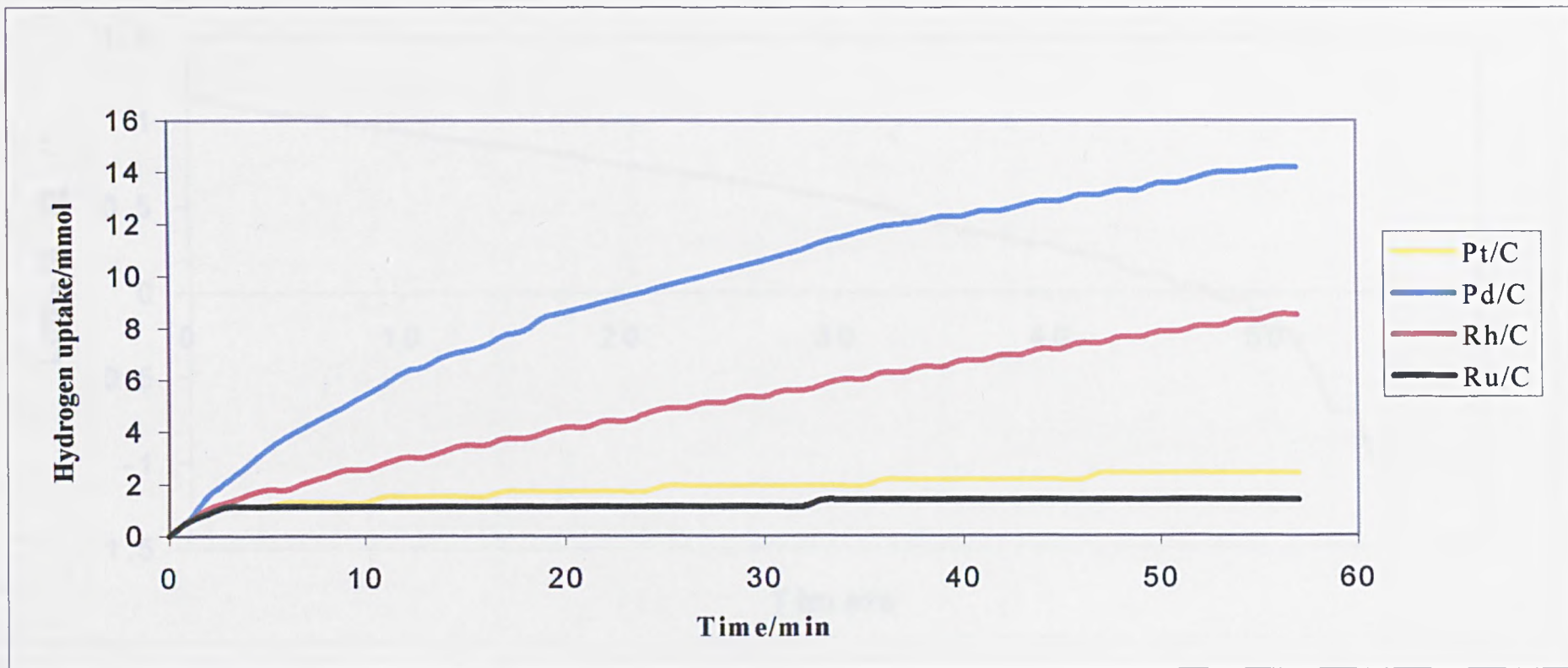


Figure 3.1 Pyrazine hydrogenation at 293 K. Hydrogen uptake against time curves

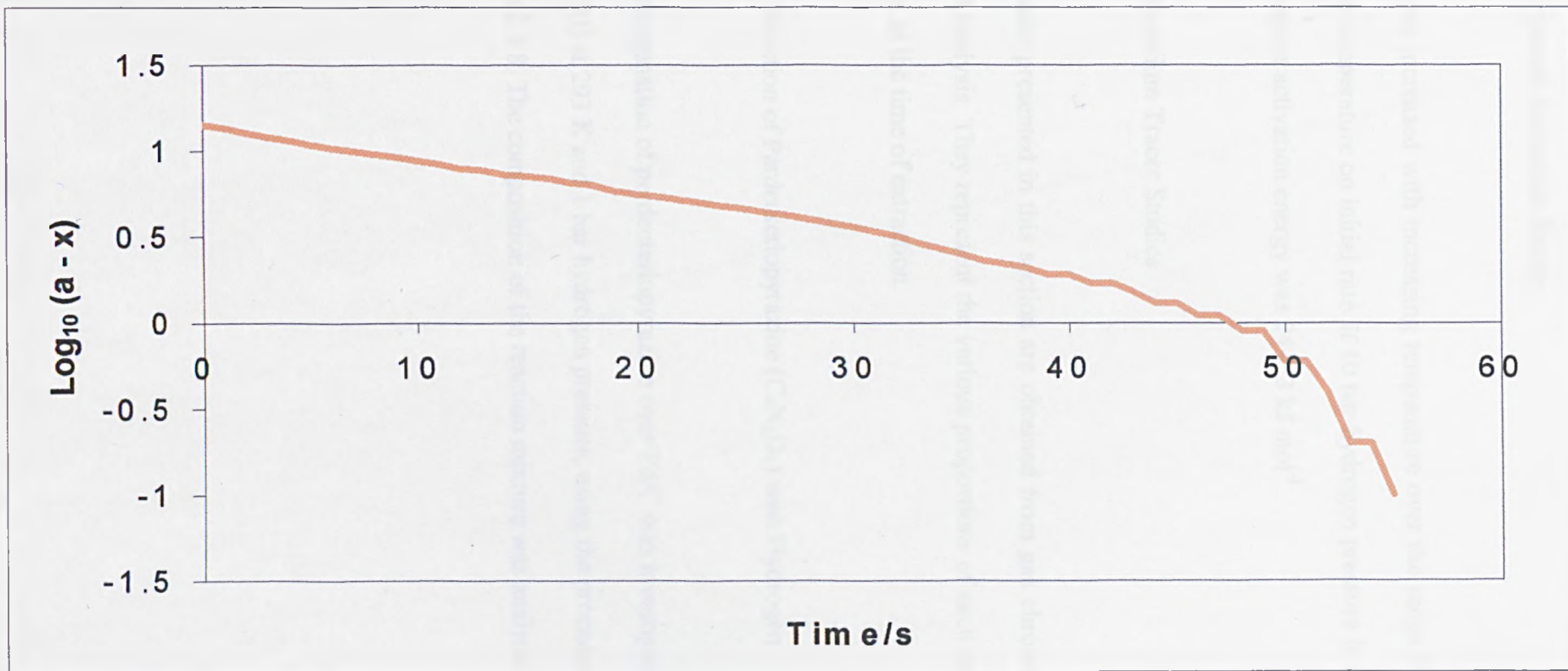


Figure 3.2 Pyrazine hydrogenation over Pd at 293 K. First order test plot

3.2.3 Apparent Activation Energy

Initial rate increased with increasing temperature over the range 297 K to 325 K. The effect of temperature on initial rate at 10 bar hydrogen pressure is shown in Figure 3.7.

The apparent activation energy was $24 \pm 3 \text{ kJ mol}^{-1}$.

3.2.4 Deuterium Tracer Studies

The results presented in this section are obtained from gas chromatographic and mass spectral analysis. They represent the various proportions of each species in the reaction mixture, at the time of extraction.

3.2.4.1 Reaction of Perdeuteriopyrazine ($\text{C}_4\text{N}_2\text{D}_4$) with Hydrogen

The hydrogenation of perdeuteriopyrazine over Pd/C was investigated in ethanol ($\text{C}_2\text{D}_5\text{OD}$) at 293 K and 1 bar hydrogen pressure, using the procedures described in Section 2.3.8. The composition of the reaction mixture was analysed at intervals by GC-MS.

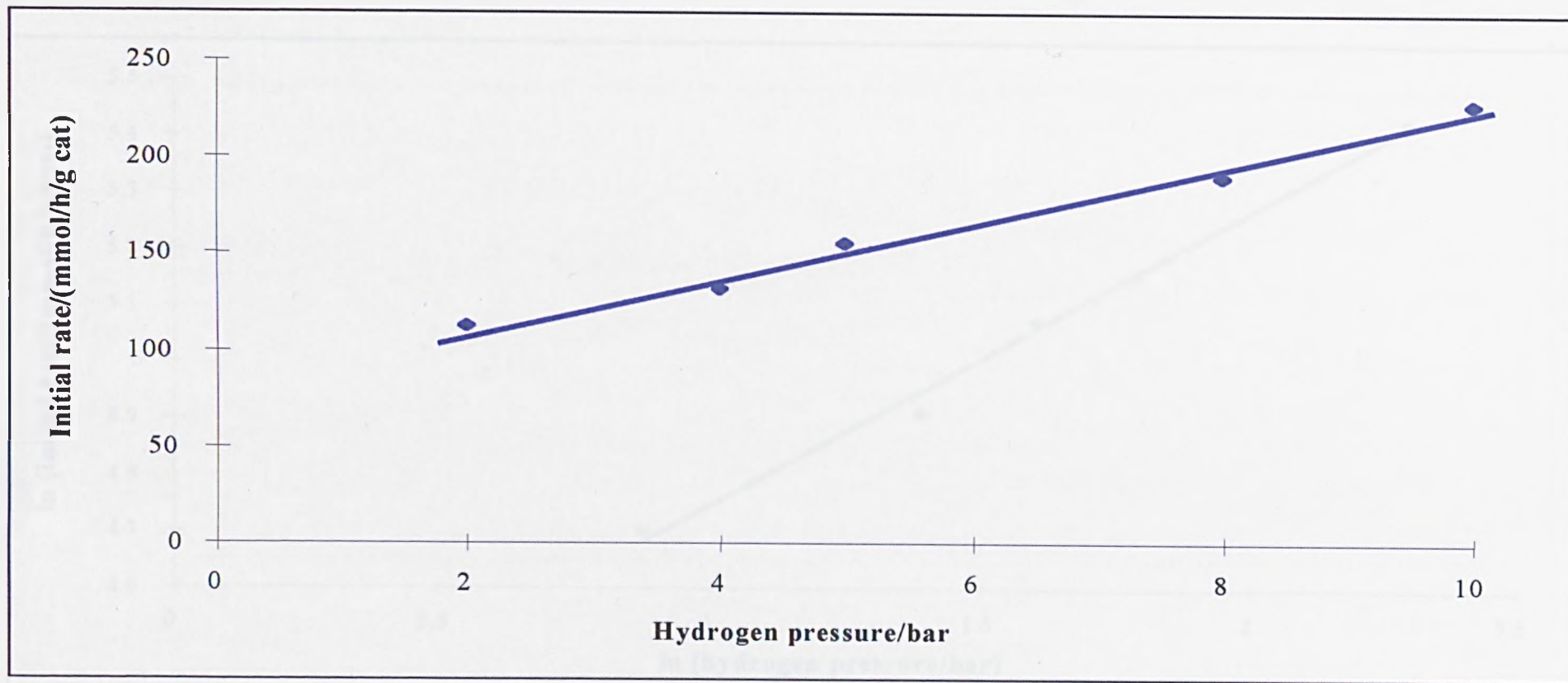


Figure 3.3 Pyrazine hydrogenation over Pd/C at 293 K. Variation of initial rate with hydrogen pressure

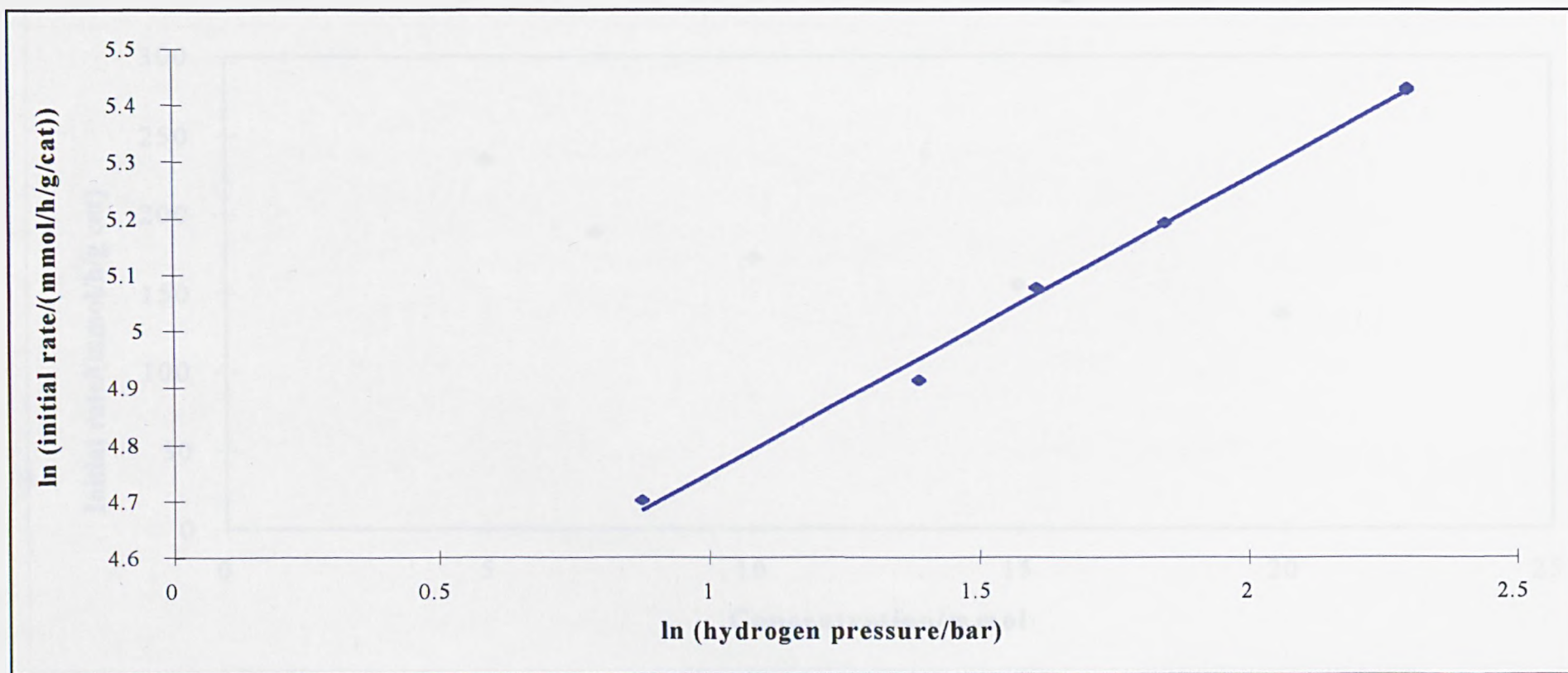


Figure 3.4 Pyrazine hydrogenation over Pd/C at 293 K. Logarithmic plot of initial rate against hydrogen pressure

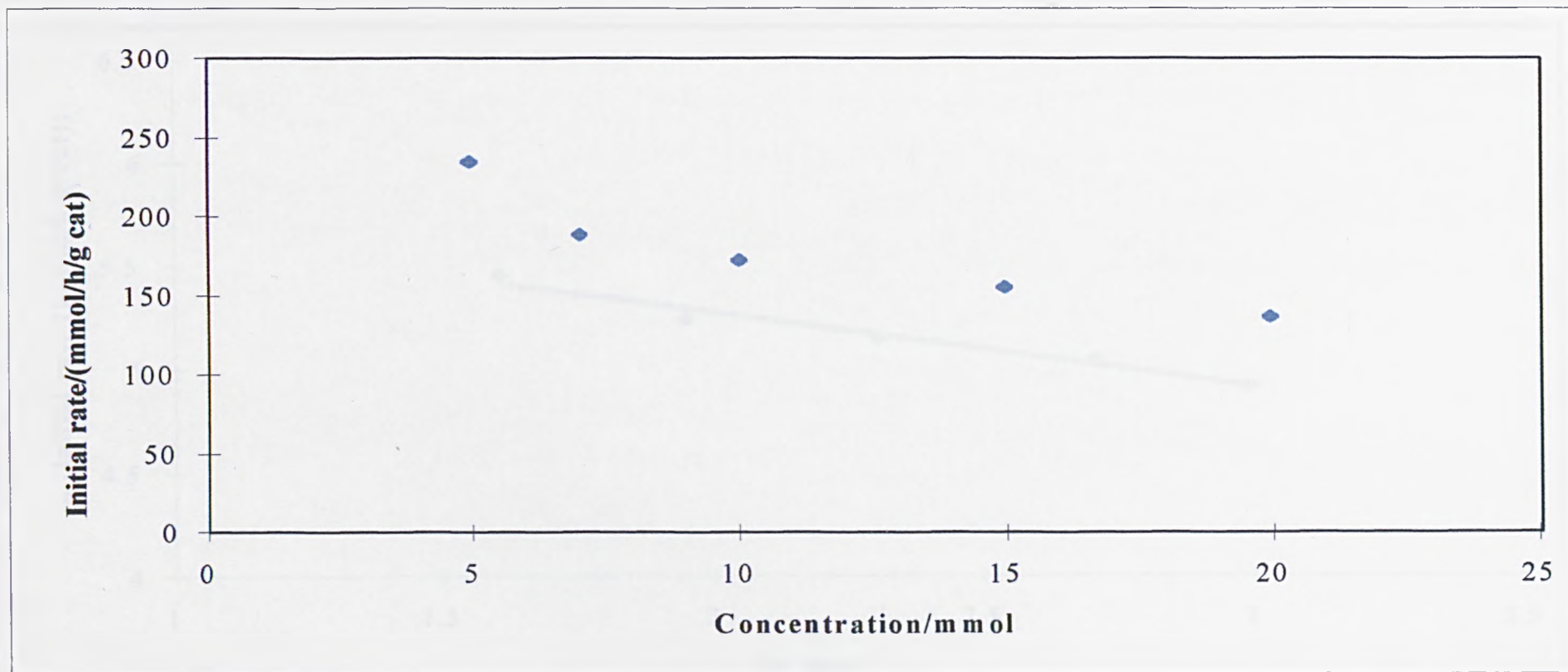


Figure 3.5 Pyrazine hydrogenation over Pd/C at 293 K. Variation of initial rate with pyrazine concentration

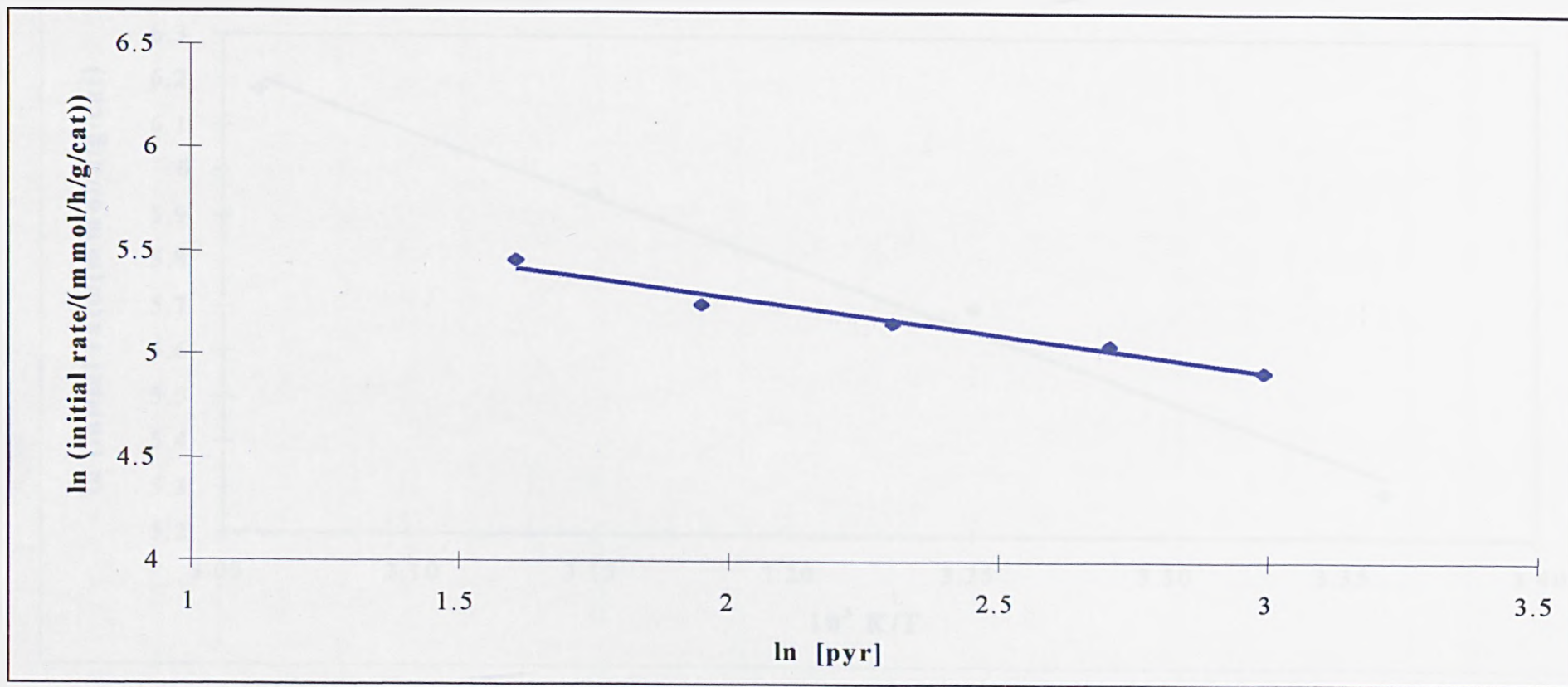


Figure 3.6 Pyrazine hydrogenation over Pd/C at 293 K. Logarithmic plot of initial rate against pyrazine concentration

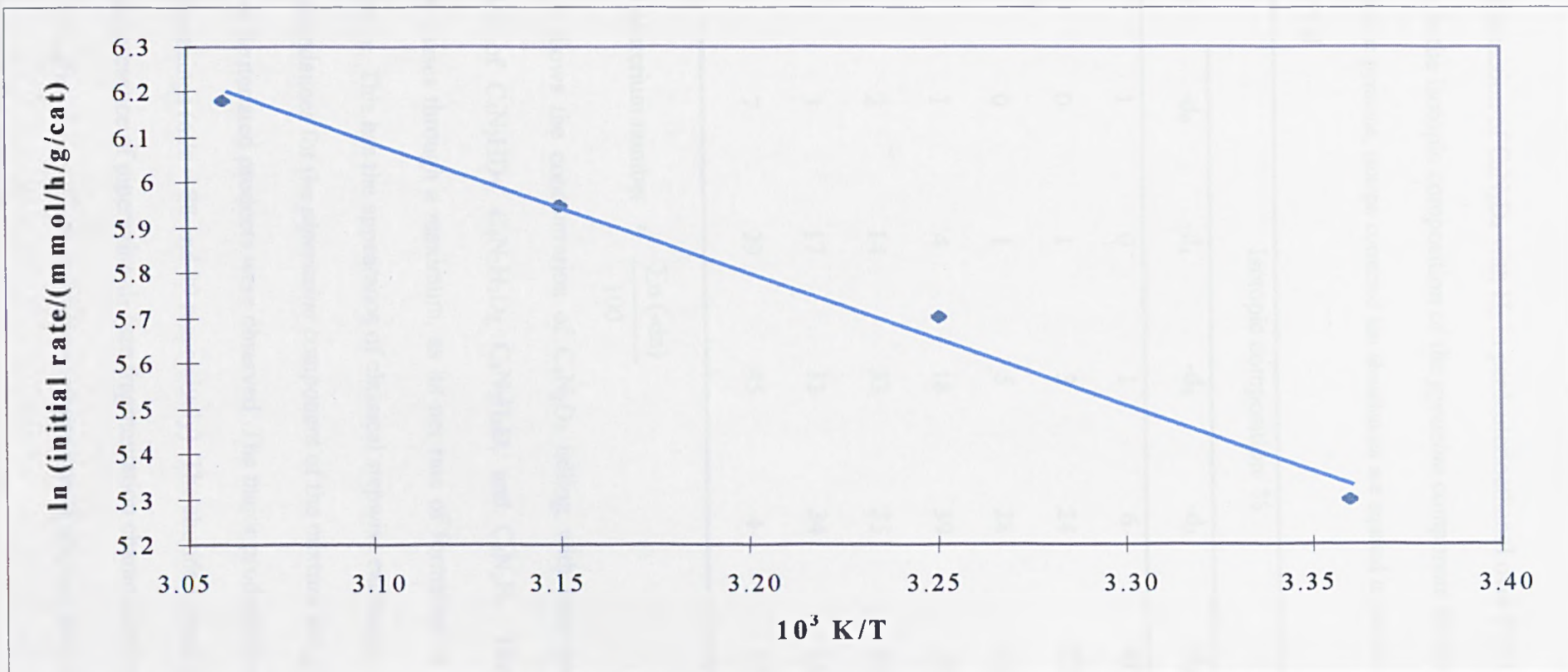


Figure 3.7 Pyrazine hydrogenation over Pd/C. Variation of rate with reciprocal temperature

Table 3.1 Reaction of C₄N₂D₄ with H₂ in perdeuterioethanol over Pd/C at 293 K.

Variation in the isotopic composition of the *pyrazine* component of the reaction mixture with time. [For pyrazine, isotope corrected ion abundances are equated to parent ion abundances, see Section 2.3.9.3]

t /min	Isotopic composition/ %					DN ^a
	-d ₀	-d ₁	-d ₂	-d ₃	-d ₄	
0	1	0	1	6	92	3.9
10	0	1	3	24	72	3.7
20	0	1	5	28	66	3.6
40	1	4	18	39	38	3.1
70	2	14	33	35	16	2.5
130	3	17	33	34	13	2.4
190	7	29	45	4	15	1.9

a.
$$\text{DN} = \text{deuterium number} = \frac{\sum n (-dn)}{100}$$

Table 3.1 shows the concentration of C₄N₂D₄ falling with time and the successive appearance of C₄N₂HD₃, C₄N₂H₂D₂, C₄N₂H₃D, and C₄N₂H₄. The contribution of C₄N₂HD₃ passes through a maximum, as its net rate of formation is first positive and later negative. This has the appearance of classical stepwise exchange.

The ion abundances for the *piperazine* component of the mixture are given in Table 3.2. A range of deuteriated products were observed. The major products formed were the d₂ and d₃ piperazines (m/z = 88 and 89 respectively). The abundant peak at m/z = 90 implies the presence of piperazine-d₅ (see fragmentation characteristics, Section 2.3.9.4). The abundance of non-deuteriated piperazine (C₄N₂H₁₀, m/z = 86) remained low throughout the reaction.

Table 3.2 Reaction of $C_4N_2D_4$ with H_2 in perdeuterioethanol over Pd/C at 293 K.

Isotope corrected ion abundances for the *piperazine* component of the sample extracted at varying times.

t/min	Ion abundances/%					
	m/z = 85	86	87	88	89	90
0	*	*	*	*	*	*
10	*	*	*	*	*	*
20	5	1	4	21	45	24
40	2	2	9	26	42	19
70	2	3	15	31	34	15
130	2	3	11	28	38	18
190	2	5	15	30	34	14

* indicates no detectable piperazine yield

3.2.4.2 Isotope Exchange between Pyrazine ($C_4N_2H_4$) and Perdeuteriopyrazine ($C_4N_2D_4$).

The exchange between pyrazine and perdeuteriopyrazine in ethanol over Pd/C at 293 K was investigated using the procedures presented in Section 2.3.9. The catalyst was pre-reduced in hydrogen (H_2), but prior to reaction the vessel was evacuated. The purpose of the experiment was to determine whether exchange occurred spontaneously, or whether it required the presence of molecular hydrogen.

Samples of the reaction mixture were analysed at regular intervals by GCMS; the results are given in Table 3.3.

Table 3.3 C₄N₂D₄ - C₄N₂H₄ exchange over Pd/C at 293 K

[For pyrazine, isotope corrected ion abundances are equated to parent ion abundances, see Section 2.3.9.3]

t / min	Isotopic composition/%					DN ^a
	-d ₀	-d ₁	-d ₂	-d ₃	-d ₄	
0	39	1	1	3	56	2.4
20	49	4	3	3	41	1.8
40	48	2	2	3	45	1.9
70	39	2	2	3	54	2.3
130	40	2	2	3	53	2.3

a. $DN = \text{deuterium number} = \frac{\sum n(-dn)}{100}$

The reaction was carried out in the absence of molecular hydrogen and no hydrogenation occurred. Samples analysed after 0, 70, and 130 minutes showed similar ion abundances (the deuterium number remained constant) which indicates no exchange occurred. [The sample compositions obtained after 20 and 40 minutes show an apparent increase in the amount of C₄N₂H₄ present and a decrease in the amount of C₄N₂D₄. This cannot be a real effect and is attributed to some perturbation in the mass spectrometer].

3.2.4.3 Isotope Exchange Reaction between Pyrazine (C₄N₂H₄) and Perdeuteriopyrazine (C₄N₂D₄) in the presence of hydrogen (H₂).

The reaction of pyrazine with perdeuteriopyrazine was investigated in the presence of hydrogen using the same procedures.

The catalyst was again reduced with hydrogen and the reaction was carried out in the presence of 1 bar hydrogen. A degree of pyrazine and perdeuteriopyrazine hydrogenation was observed. The isotopic composition of the *pyrazine*, as a function of time, is given in Table 3.4

Table 3.4 C₄N₂D₄ - C₄N₂H₄ exchange over Pd/C at 293 K in the presence of hydrogen
Variation in the isotopic composition of the *pyrazine* component of the reaction mixture with time.

[For pyrazine, isotope corrected ion abundances are equated to parent ion abundances, see Section 2.3.9.3]

Isotopic Composition/%						
t /min	-d ₀	-d ₁	-d ₂	-d ₃	-d ₄	DN ^a
0	39	1	1	3	56	2.4
5	43	4	3	8	42	2.0
10	42	5	6	14	33	1.9
20	43	8	6	18	25	1.7
35	42	11	13	18	16	1.5
95	38	16	18	19	9	1.4
165	42	23	19	13	3	1.1
230	47	23	19	9	2	1.0

^a. DN = deuterium number = $\frac{\sum n(-dn)}{100}$

In the early stages of reaction, the major components of the reaction were $C_4N_2H_4$ and $C_4N_2D_4$. However, with increasing reaction time, the concentration of $-d_4$ decreased, and that of $-d_3$, $-d_2$, $-d_1$ and (eventually) $-d_0$ increased. The variation of the deuterium number indicated an overall loss of D from the pyrazine and its replacement by H.

The ion abundances for the piperazine component of the sample are given in Table 3.5. Piperazine was detected after 95 minutes. Thus, substantial pyrazine exchange occurred before hydrogenation became evident. Piperazine molecules containing up to three deuterium atoms were observed. The most abundant products were those containing 0, 1, and 2 D atoms.

Table 3.5 $C_4N_2D_4$ - $C_4N_2H_4$ exchange over Pd/C at 293 K in the presence of hydrogen
Isotope corrected ion abundances for the *piperazine* component of the sample extracted at varying times

t/min	Ion Abundances/%					
	m/z = 85	86	87	88	89	90
0	*	*	*	*	*	*
5	*	*	*	*	*	*
10	*	*	*	*	*	*
20	*	*	*	*	*	*
35	*	*	*	*	*	*
95	38	16	18	19	9	0
165	42	23	19	13	3	0
230	46	23	18	10	3	0

* indicates no detectable piperazine yield

3.2.4.4 Isotope Exchange between Pyrazine (C₄N₂H₄) and Perdeuteriopyrazine

(C₄N₂D₄) in the presence of deuterium (D₂).

The exchange reaction between pyrazine and perdeuteriopyrazine was investigated over Pd/C under 1 bar deuterium. The catalyst was pre-reduced under deuterium before use.

Pyrazine exchange occurred as shown in Table 3.6. The concentrations of -d₀ and -d₄ pyrazine decreased with time. The deuterium number however, remained fairly constant unlike that previously observed (Table 3.4).

The concentrations of -d₁ and -d₃ pyrazine increased in a similar fashion with time and that of -d₂ increased later, indicating again the occurrence of step-wise addition.

Table 3.6 C₄N₂D₄ - C₄N₂H₄ exchange over Pd/C at 293 K in the presence of deuterium

Variation in the isotopic composition of the *pyrazine* component of the reaction mixture with time.

[For pyrazine, isotope corrected ion abundances are equated to parent ion abundances, see Section 2.3.9.3]

t /min	Isotopic composition/%					DN ^a
	-d ₀	-d ₁	-d ₂	-d ₃	-d ₄	
0	39	1	1	3	56	2.4
5	33	9	2	7	49	2.3
10	29	13	4	9	45	2.3
20	25	12	6	12	45	2.4
40	20	18	9	16	37	2.3
60	17	20	14	19	30	2.3
90	14	21	19	23	23	2.2
130	15	24	19	24	18	2.1

a. $DN = \text{deuterium number} = \frac{\sum n(-dn)}{100}$

This reaction produced a quantity of piperazine the ion abundances for which are given in Table 3.7. A noticeable difference between reaction under deuterium and that under hydrogen was an increased mass range in the former. Piperazine products were observed ranging from -d₁ (m/z = 87) to -d₆ (m/z = 92), and the presence of traces of -d₇ are thereby implied.

The -d₁ to -d₅ products (m/z = 87-91) were the most abundant throughout the reaction

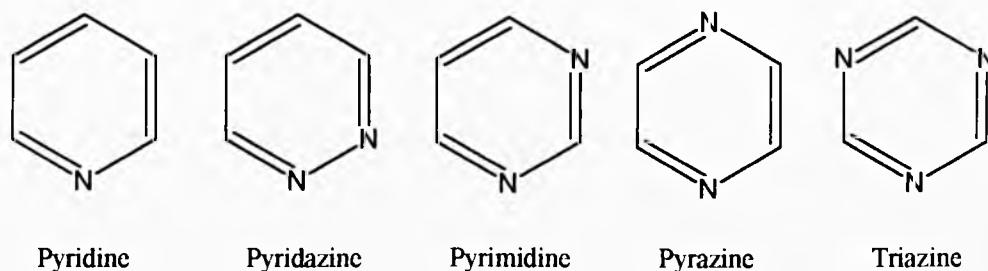
Table 3.7 C₄N₂D₄ - C₄N₂H₄ exchange over Pd/C at 293 K in the presence of deuterium
Isotope corrected ion abundances for the *piperazine* component of the sample extracted at varying times

Ion Abundances/%								
t/min	m/z = 85	86	87	88	89	90	91	92
0	*	*	*	*	*	*	*	*
5	*	*	*	*	*	*	*	*
10	7	14	15	10	14	21	13	6
20	4	8	10	10	18	26	18	6
40	6	17	16	11	14	19	12	5
60	4	9	14	14	18	21	15	5
90	5	13	16	16	18	20	9	3
130	3	9	15	16	20	21	12	4

* indicates no detectable yield of piperazine

3.2.5 Comparative Reactivities of five N-Heterocycles

An investigation into the relative rates of hydrogenation of pyridine, pyridazine, pyrimidine, pyrazine and triazine in ethanol over the standard Pd/C catalyst at 293 K and 10 bar pressure was undertaken.



The hydrogenation of each N-heterocycle was carried out using the catalyst preparation and reaction procedures described in Section 2.3.7. The results are shown in Table 3.8 and in Figures 3.8.

Table 3.8 Hydrogenation of 5 mmol of various N-heterocycles in ethanol over Pd/C at 293 K and 10 bar hydrogen pressure.

Reactant	Reaction time/min	Hydrogen uptake/mmol	Initial rate/ mmol h ⁻¹ g ⁻¹	t ^{1/2} /min
Pyridine	1100	16.8	45	140
Pyridazine	1200 ^a	8.8	18	750
Pyrimidine	1200	15.6	52	128
Pyrazine	70	15.0	200	18
Triazine	1200 ^a	7.8	12	1220

^a reaction complete after 4000 minutes

The results presented in Table 3.8 indicate the position of the N-atom (s) in the ring is important for catalytic hydrogenation. Pyrazine was hydrogenated most rapidly with full conversion to piperazine occurring after about 1 h. Pyridine and pyrimidine were hydrogenated at similar rates achieving saturation after 16 h. Triazine and pyridazine showed very low rates of hydrogenation, but were eventually fully hydrogenated after 66 h.

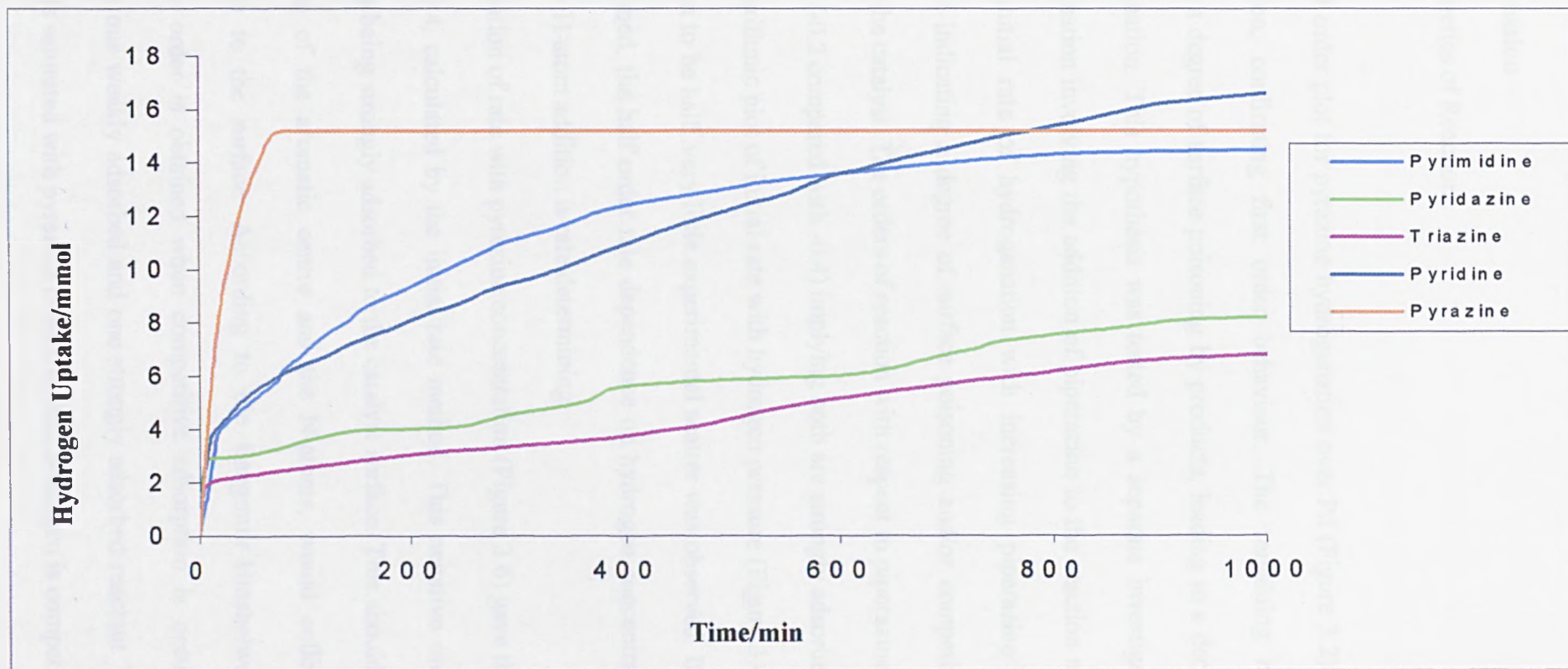


Figure 3.8 Comparison of hydrogen uptake curves for N-heterocycle hydrogenation at 293 K and 10 bar pressure (5 mmol reactant)

3.3 Discussion

3.3.1 Kinetics of Reaction

The first order plot for pyrazine hydrogenation over Pd (Figure 3.2) was linear to 75% conversion, confirming first order behaviour. The remaining non-linearity could indicate a degree of surface poisoning by products, leading to a decrease in the rate of hydrogenation. This hypothesis was tested by a separate investigation into pyrazine hydrogenation involving the addition of piperazine to the reaction mixture. A decrease in the initial rate of hydrogenation with increasing piperazine concentration was observed indicating a degree of surface poisoning and/or competition for adsorption sites on the catalyst. The orders of reaction with respect to piperazine and pyrazine were similar, (-0.2 compared with -0.4) implying both are strongly adsorbed to the surface.

The logarithmic plot of initial rate with hydrogen pressure (Figure 3.4) gave the order in hydrogen to be half; very little experimental scatter was observed. If Langmuir kinetics are assumed, the half order rate dependence on hydrogen concentration could indicate that first H-atom addition is rate determining.

The variation of rate with pyrazine concentration (Figure 3.6) gave the order in pyrazine to be -0.4, calculated by the initial rate method. This negative order is indicative of pyrazine being strongly adsorbed to the catalyst surface. This should be expected as the π -system of the aromatic centre and the N-atoms, would collectively anchor the molecule to the surface. According to the Langmuir-Hinshelwood mechanism, a negative order is obtained when competitive adsorption is occurring and reaction involves one weakly adsorbed and one strongly adsorbed reactant. We can assume the surface is saturated with pyrazine molecules and hydrogen is competing for

adsorption sites.

The variation of initial rate with temperature followed the Arrhenius relationship, and the equation was well obeyed throughout the investigated temperature range (Figure 3.7). The calculated value for the activation energy was $24 \pm 3 \text{ kJ mol}^{-1}$.

The activation energy was investigated at an agitation speed of 1200 rpm, which has shown to be in the region of kinetic control in a separate study (1).

3.3.2 Mechanisms of Pyrazine Exchange and Hydrogenation

Pyrazine is an aromatic organic compound, and therefore its modes of adsorption and hydrogenation may have features in common with those of benzene and pyridine. Benzene adsorption occurs associatively as a π -complex and dissociatively as a σ -bonded intermediate (Figures 3.9 (a) and (b)) (2), whereas pyridine adsorption is generally considered to involve a N-metal chemisorption bond, with the plane of the molecule inclined at an angle to the surface (Figure 3.9 (c), (3)).

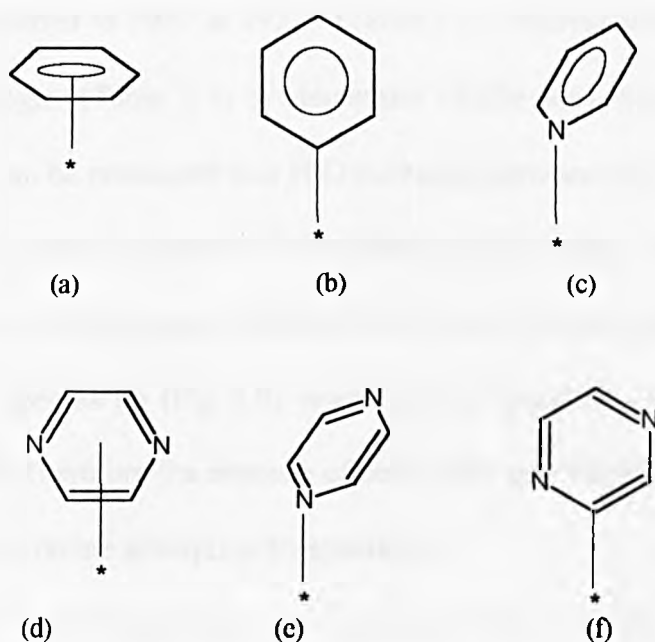


Figure 3.9 Modes of aromatic adsorption

By analogy, pyrazine might be adsorbed with the ring parallel to the surface as a π -adsorbed state (Figure 3.9 (d)) involving the interaction of only one N-atom with the surface (Figure 3.9 (e)) or as a state involving carbon-metal σ -bonding (Figure 3.9 (f)). State (f) is a dissociatively adsorbed state; states (d) and (e) are non-dissociatively adsorbed states. Adsorption of benzene by mode (b) or of pyrazine by mode (f) implies that, initially, one adsorbed H-atom exists at the surface for every species (b) or (f) created. Such adsorbed H-atoms may subsequently combine and undergo desorption as H_2 molecules, or (at the Pd surface only) become dissolved-H in the bulk of the metal if the solubility limit of the metallic phase for hydrogenation has not been previously been attained.

There is no spectroscopic evidence for the nature of adsorbed pyrazines, and therefore states (d), (e), and (f) are speculative. However, adsorbed states can be probed by D-tracer techniques. In particular, the occurrence or non-occurrence of isotope exchange between a reactant and its isotopically labelled variant provides significant information.

In the case of pyrazine, no exchange occurred when a 2:3 mixture of $C_4N_2H_4$ and $C_4N_2D_4$ was admitted to Pd/C at 293 K (Table 3.3), whereas exchange occurred when molecular hydrogen (Table 3.4) or deuterium (Table 3.6) was present. From these observations it can be concluded that H/D exchange between pyrazine molecules occurs when adsorbed -H and/or adsorbed -D are present at the surface, and (more importantly) no exchange occurs in the absence of adsorbed -H and -D. Now, dissociative adsorption of pyrazine by species (f) (Fig 3.9) would release adsorbed -H onto the surface, as indicated above. Therefore the absence of self-exchange (Table 3.3) argues against the participation of pyrazine adsorption by species (f).

In the ($C_4N_2D_4 + H_2$) experiment described in Table 3.1, the concentration of the reactant $C_4N_2D_4$ diminishes, that of $C_4N_2HD_3$ rises, passes through a maximum, and

falls. The concentrations of $C_4N_2H_2D_2$, $C_4N_2H_3D$ and $C_4N_2H_4$ each rise progressively slowly. These results represent stepwise exchange, that is, the major process occurring is the sequential exchange of D for H one atom at a time.

Table 3.4 describes the reaction of a ($C_4N_2H_4 + C_4N_2D_4$) mixture with H_2 . Here the same stepwise exchange is observed with $C_4N_2HD_3$ being formed from $C_4N_2D_4$. Later, $C_4N_2H_2D_2$ and $C_4N_2H_3D$ are formed sequentially, and by extension, the concentration of $C_4N_2H_4$ finally rises. The concentration of $C_4N_2H_2D_2$ rises more slowly than $C_4N_2HD_3$ confirming the simultaneous exchange of two X – atoms ($X = H$ or D) in the reactant is not significant.

The reaction of a ($C_4N_2H_4 + C_4N_2D_4$) - mixture with deuterium shows similar features (Table 3.6); here the H/D pool of X – atoms on the surface is richer in deuterium, and therefore the concentration of $C_4N_2D_4$ falls more slowly and that of $C_4N_2H_4$ rises more quickly.

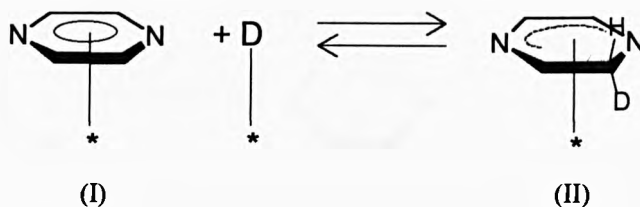
The inability to determine parent ion concentrations for product piperazine limits the information that can be gleaned from Tables 3.2, 3.5, and 3.7. However, the absence of piperazine formation when a ($C_4N_2H_4 + C_4N_2D_4$) - mixture was admitted to the catalyst (Table 3.3) confirms that adsorbed $-X$ ($X = H$ or D) was not formed by dissociative adsorption of the reactant (a conclusion drawn above from the absence of exchange in the reactant). In each reaction involving 1 bar molecular hydrogen or deuterium, piperazine was not detected in the early stages, by which time considerable exchange in the reactant had occurred.

The initial product of the $C_4N_2D_4/H_2$ reaction (Table 3.2) was rich in $C_4N_2H_6D_4$ as expected with some $C_4N_2H_5D_5$ being present as the implied by the substantial contribution at $m/z = 90$. However, the initial product of the reaction of a ($C_4N_2H_4 +$

$C_4N_2D_4$) - mixture with deuterium contained piperazine ranging from $C_4N_2H_{10}$ to $C_4N_2H_4D_6$ (and, by implication, $C_4N_2H_3D_7$).

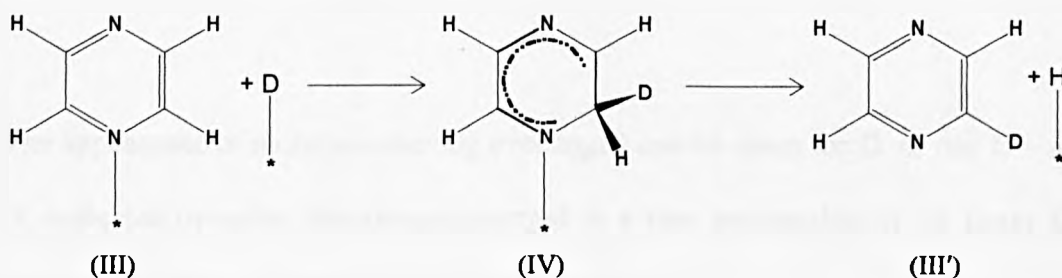
The simplest mechanisms for exchange and hydrogenation consistent with these observations are as follows.

D atom addition to pyrazine adsorbed as species (d) does not lead to exchange because reversal of the step regenerates the reactants with their original isotope composition.



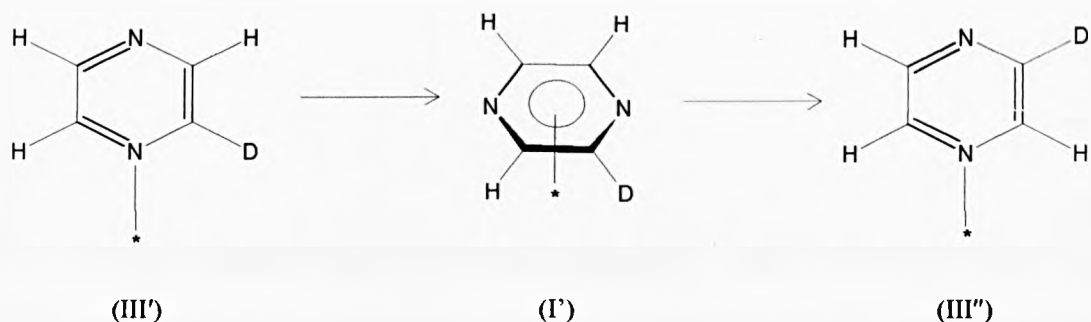
Exchange would require ring turnover or interaction of (II) with molecular deuterium, as originally proposed by Rooney for H/D exchange in substituted cyclopentanes over Pd (4).

Consider the pyrazine molecule adsorbed as species (e) and oriented at right angles to the surface. D – atom addition to one side of the ring, and H – atom abstraction from the other side achieves stepwise exchange.



Repetition of this process would achieve exchange at the other α - position; this is

Repetition of this process would achieve exchange at the other α - position; this is analogous to the mechanism originally proposed for pyridine exchange by Moyes and Wells (5). Exchange of the third and fourth hydrogen atoms would require desorption and re-adsorption by the other N - atom, or interconversion of species (III') and (I).



If the pyrazine ring is inclined at an angle to the surface, as is observed for pyridine, then a fluxional change in orientation is required to facilitate the H - atom loss step of the exchange process.



The appearance of molecules having exchanged one H- atom for D, or one D - atom for H, indicates pyrazine desorption occurred at a rate comparable to, or faster than the process of further exchange and of hydrogenation.

The mechanism of hydrogenation is not clearly defined by these experiments. Successive addition of six D - or H - atoms to pyrazine $C_4N_2H_4$ adsorbed as structure (I) would lead to piperazine containing up to, but not more than six D - atoms.

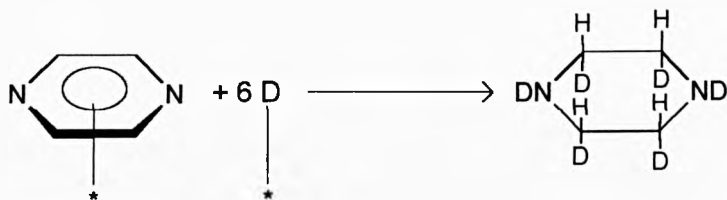
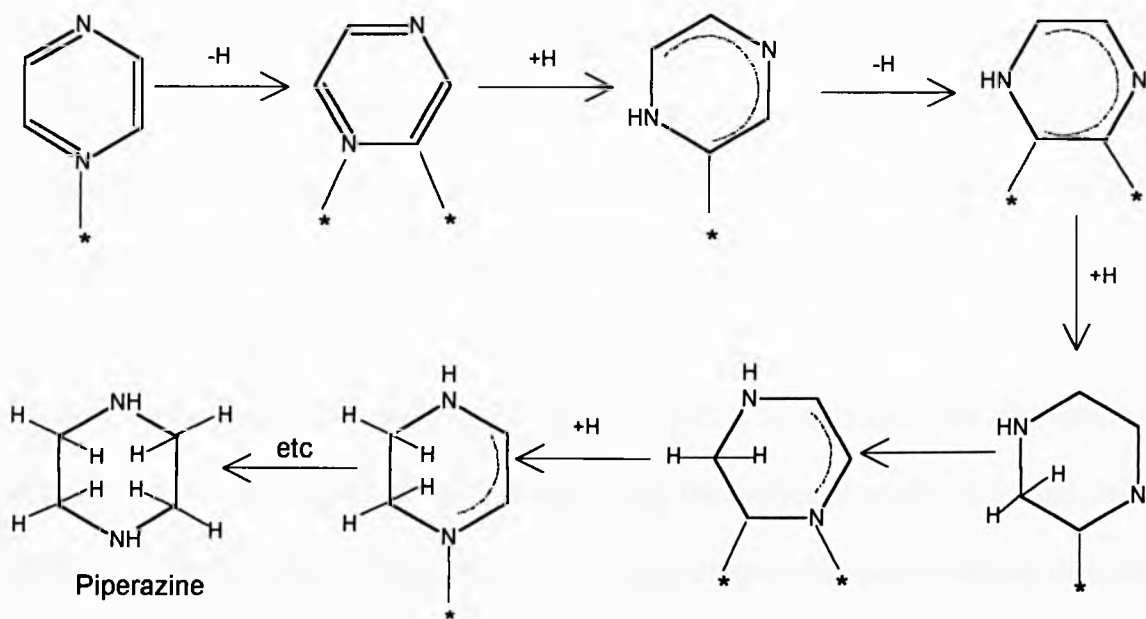


Table 3.7 is not consistent with this proposal; the small amount of $C_4N_2H_3D_7$ implied as present by the results would have been formed by addition of six D - atoms to exchange pyrazine ($C_4N_2H_3D$). More definitive results would have been obtained had the reaction of $C_4N_2H_4$ with a very large excess of D_2 been examined and had a mass spectrometer method been available that avoided excessive fragmentation to piperazine product.

Alternative mechanisms of hydrogenation would require the participation of intermediates σ - bonded to the surface by both carbon and nitrogen atoms of the pyrazine ring.

A possible mechanism for the saturation of successive carbon atoms could occur as follows:



Although complex, the mechanism is equivalent to that proposed for pyridine hydrogenation and, taken in conjunction with the proposed mechanism for exchange, would permit the formation of all isotopically distinguishable piperazines in the $C_4N_2H_4/D_2$ reaction

3.3.3 Comparative Reactions of N-Heterocycles

The position of the N-atom(s) in the ring clearly effects the rate of catalytic hydrogenation (Table 3.8).

The work in the previous section discussed how co-planar adsorption of pyrazine to the catalyst surface may occur. It is thought that this permits efficient hydrogenation with fast initial rates (as experimentally observed).

Pyridine and pyrimidine was hydrogenated over the same Pd catalyst as for pyrazine hydrogenation, but longer reaction times and lower initial rates were observed.

Deuterium exchange studies of pyridine over a range of Group VIII metals mainly

displayed exchange at positions 2 and 6, with extensive exchange observed over Pt only at 373 K (6). It was proposed that chemisorption occurs by the formation of a coordinate bond between the pyridine-N and a metal atom at the surface. At elevated temperatures, further interaction between the π -electrons of the aromatic ring and the surface were observed.

Modern surface techniques such as NEXAFS and EELS have studied the adsorption of pyridine on Pt (111) and found the ring inclined to the surface at angles of 52 and 74° at different temperatures (7). This would make ring hydrogenation more difficult than that observed with pyrazine.

If this N-atom adsorption theory is correct, pyrimidine would be expected to tilt away from the catalyst surface, with a smaller angle than pyridine but enough to make ring hydrogenation more difficult than pyrazine. This was reflected in the initial rates of reaction; pyridine hydrogenation gave an initial rate of 45 mmol/h/g cat, whereas pyrimidine gave a slightly higher rate of 52 mmol/h/g cat.

Calf and Garnett reported the deuterium exchange of pyridazine over Pt (8). The orientation of deuterium was analogous to that observed in pyridine exchange i.e. predominantly in the α -position. This would indicate pyridazine, like pyridine and pyrimidine, adsorbs to the surface at an incline. The presence of two adjacent N-atoms may collectively have a stronger poisoning effect than the other diazines, giving the lower rate of hydrogenation.

On the basis of the above interpretations, triazine would be expected to adsorb very strongly to the surface, making the frequency of adsorption/desorption processes very low. It would effectively be acting as a poison giving the observed low rate of hydrogenation.

References

1. Carroll, J. R. First Year Report, University of Hull (1997)
2. Moyes, R. B., and P. B. Wells., *Advances in catalysis*, **23** (1973)
3. Johnson, A. L., Muetterties, E. L., Stohr, J., and Sette, F., *J. Phys. Chem.*, **89**, 4071 (1985)
4. Rooney, J J., *J. Catal.*, **2**, 3 (1963)
5. Moyes, R. B., and P. B. Wells., *J. Catal.*, **20**, 86 (1971)
6. Calf, G. E., Garnett, J. L., and Pickles, V. A., *Aust. J. Chem.*, **21**, 961 (1968)
7. Johnson, A. L., Muetterties, E. L., Stohr, J., and Sette, F., *J. Phys. Chem.*, **89**, 4071 (1985)
8. Calf, G. E., Garnett, J. L., and Pickles, V. A., *Aust. J. Chem.*, **21**, 961 (1968)

Chapter Four

Hydrogenation of Substituted Pyrazines

4.1 Introduction

The hydrogenation of a range of mono-substituted pyrazines was investigated over Pd/C. It was thought to be essential to study a variety of compounds to gain an understanding of their chemistry prior to attempting enantioselective hydrogenation (see Chapter 5).

4.2 Results

4.2.1 Pyrazine-2-carboxylic acid

4.2.1.1 Reactant solubility

At the start of this investigation, problems with the solubility of pyrazine-2-carboxylic acid (PCA) in many solvents became apparent. As the nature of the project dictated reactions to be in the liquid phase, this difficulty had to be overcome.

PCA was virtually insoluble in all of the usual reaction solvents, even ethanol, which historically was the reaction solvent of choice for the Hull group. It was therefore necessary to undertake an investigation into the solubility of PCA in a range of potential reaction solvents. The results are presented in Table 4.1.

Table 4.1 Solubility of pyrazine-2-carboxylic acid in solvents of various dielectric constant. Scale of solubility — (virtually insoluble) to +++ (fully soluble)

Solvent	Dielectric constant at 25°C	KOH added	Solubility
Water	79	X	+
Water	79	√	+++
DMSO	49	X	—
Methanol	33	X	— —
Ethanol	24	X	— —
Acetone	21	X	— —
Propan-2-ol	18	X	—
Butan-2-ol	16	X	— —
Acetic acid	6	X	— —
Water:Ethanol (80:20)	—	X	+
Water:Propan-2-ol (80:20)	—	X	+

PCA was most soluble in solutions containing water. The best solubility was obtained when potassium hydroxide was added to the PCA/water solution, thereby making the potassium salt of the acid.

4.2.1.2 Hydrogen uptake curve

After establishing PCA was most soluble in an aqueous solution of KOH, its hydrogenation over Pd/C to piperazine-2-carboxylic acid was attempted at 293 K and 10 bar hydrogen pressure (PCA 5 mmol, and KOH 5 mmol, in 50 ml water).

The hydrogen uptake against time curve is shown in Figure 4.1.

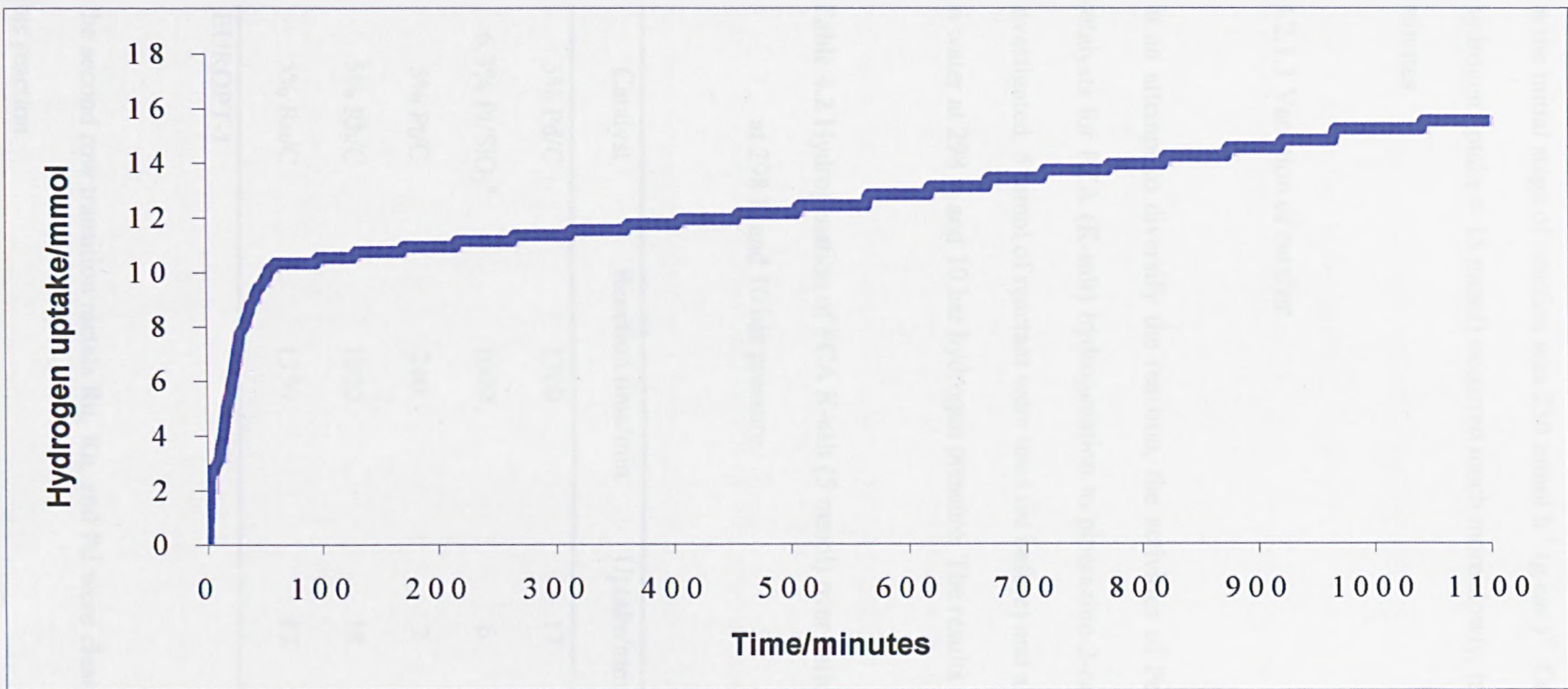


Figure 4.1 Hydrogenation of PCA K-salt (5 mmol) over 5% Pd/C in water

After 60 minutes, two moles of hydrogen had been consumed, the maximum rate (r_{\max}) in the initial stage of reaction was $250 \text{ mmol h}^{-1} (\text{g cat.})^{-1}$. Complete reaction (i.e. 3 mole hydrogen uptake \equiv 15 mmol) occurred much more slowly, taking approximately 1000 minutes.

4.2.1.3 Variation of catalyst

In an attempt to diversify the reaction, the activities of Pd, Pt, Rh and Ru metals as catalysts for PCA (K-salt) hydrogenation to piperazine-2-carboxylic acid (K-salt) were investigated. 5 mmol of reactant were used (as before) and all reactions were undertaken in water at 298 K and 10 bar hydrogen pressure. The results are given in Table 4.2.

Table 4.2 Hydrogenation of PCA K-salt (5 mmol) over various catalysts in water at 298 K and 10 bar pressure.

Catalyst	Reaction time/min	Uptake/mmol	Max rate /mmol h ⁻¹ g ⁻¹
5% Pd/C	1300	17	250
6.3% Pt/SiO ₂ ^a	1000	6	3
5% Pt/C	240	2	2
5% Rh/C	1300	18	180
5% Ru/C	1350	17	11

^a EUROPT-1

The second row transition metals Ru, Rh, and Pd were clearly more efficient than Pt for this reaction.

4.2.2 Pyrazine-2-carboxylic acid methyl ester

After encountering further difficulties with PCA, particularly with post-reaction analysis, it was decided that pyrazine-2-carboxylic acid methyl ester (PCME) should be used for further investigations. Unlike PCA, initial tests showed PCME to be completely soluble in all the commonly used reaction solvents.

4.2.2.1 Hydrogen uptake curve

The hydrogenation of pyrazine-2-carboxylic acid methyl ester (PCME, 5 mmol) in ethanol at 293 K and 10 bar hydrogen pressure was investigated over 5% Pd/C; the hydrogen uptake against time curve is shown in Figure 4.2.

Reaction occurred at a faster rate than that observed for PCA. A two mole hydrogen uptake was observed after 20 minutes at a r_{\max} of around $1000 \text{ mmol h}^{-1} (\text{g cat.})^{-1}$. However, after this 2 mole uptake, reaction slowed considerably and eventually stopped.

4.2.2.2 Orders of reaction

The variation of r_{\max} with hydrogen pressure and PCME concentration was studied to determine the orders of reaction. Rate varied with hydrogen pressure, giving an order of approximately +0.9 (Figure 4.3), and with PCME concentration (Figure 4.4), giving an order in PCME of -0.1.

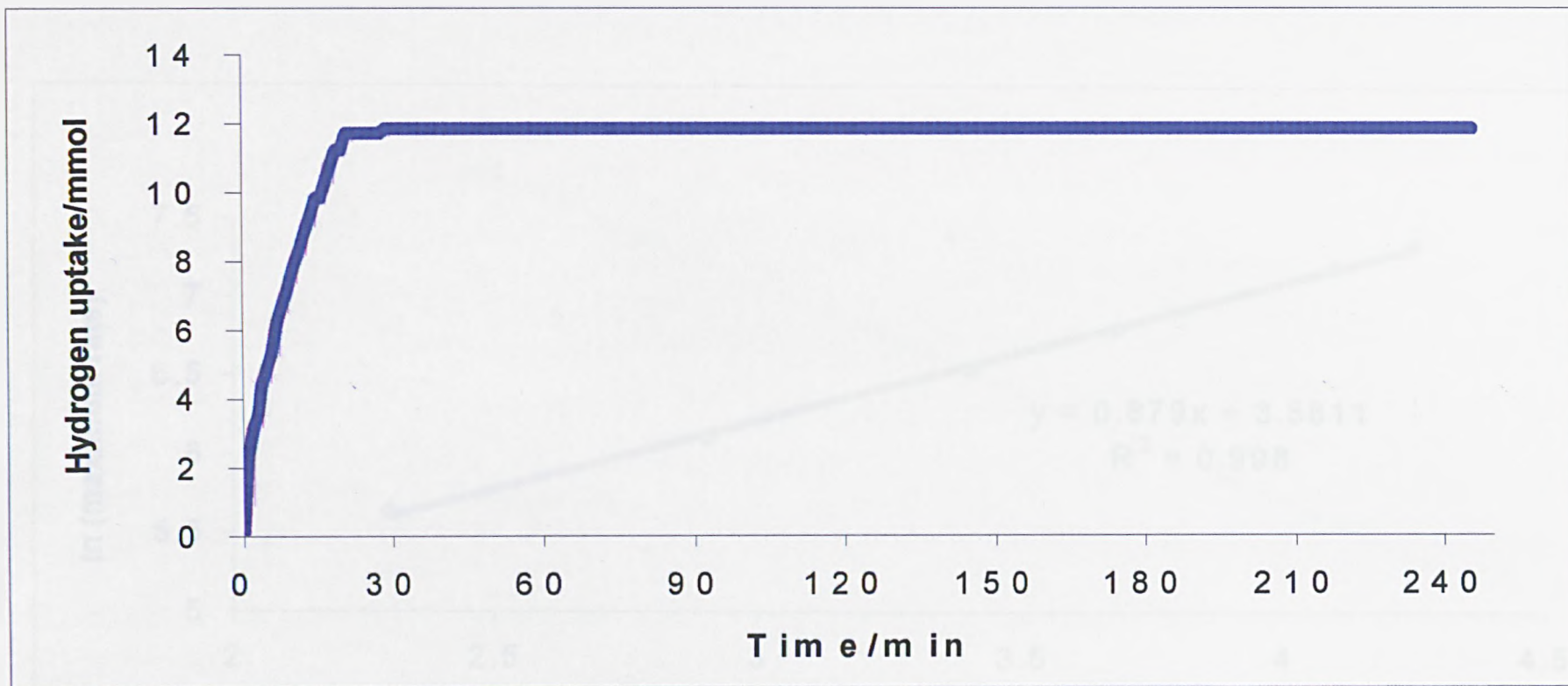


Figure 4.2 Hydrogenation of PCME (5 mmol) over 5% Pd/C in ethanol

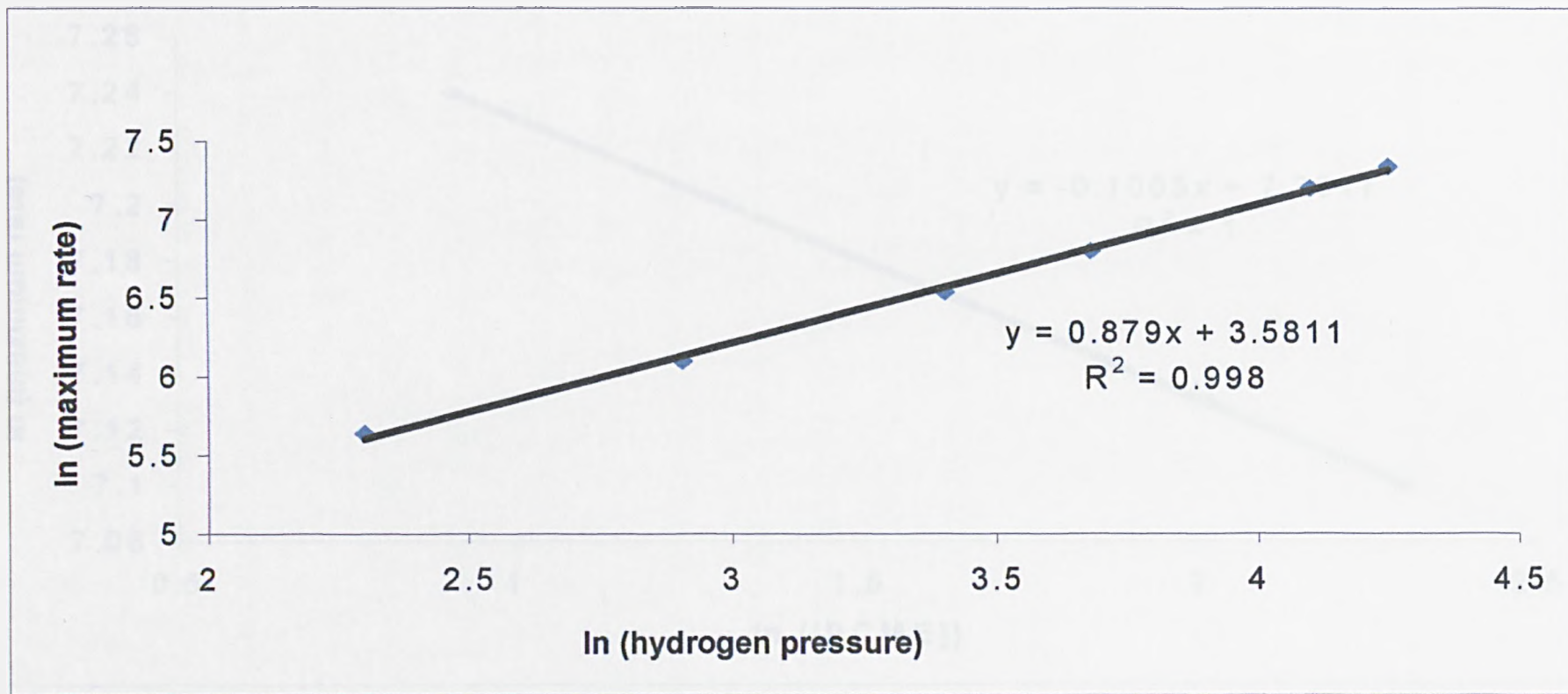


Figure 4.3 PCME hydrogenation over unmodified Pd/C at 293 K. Logarithmic plot of rate against hydrogen pressure.

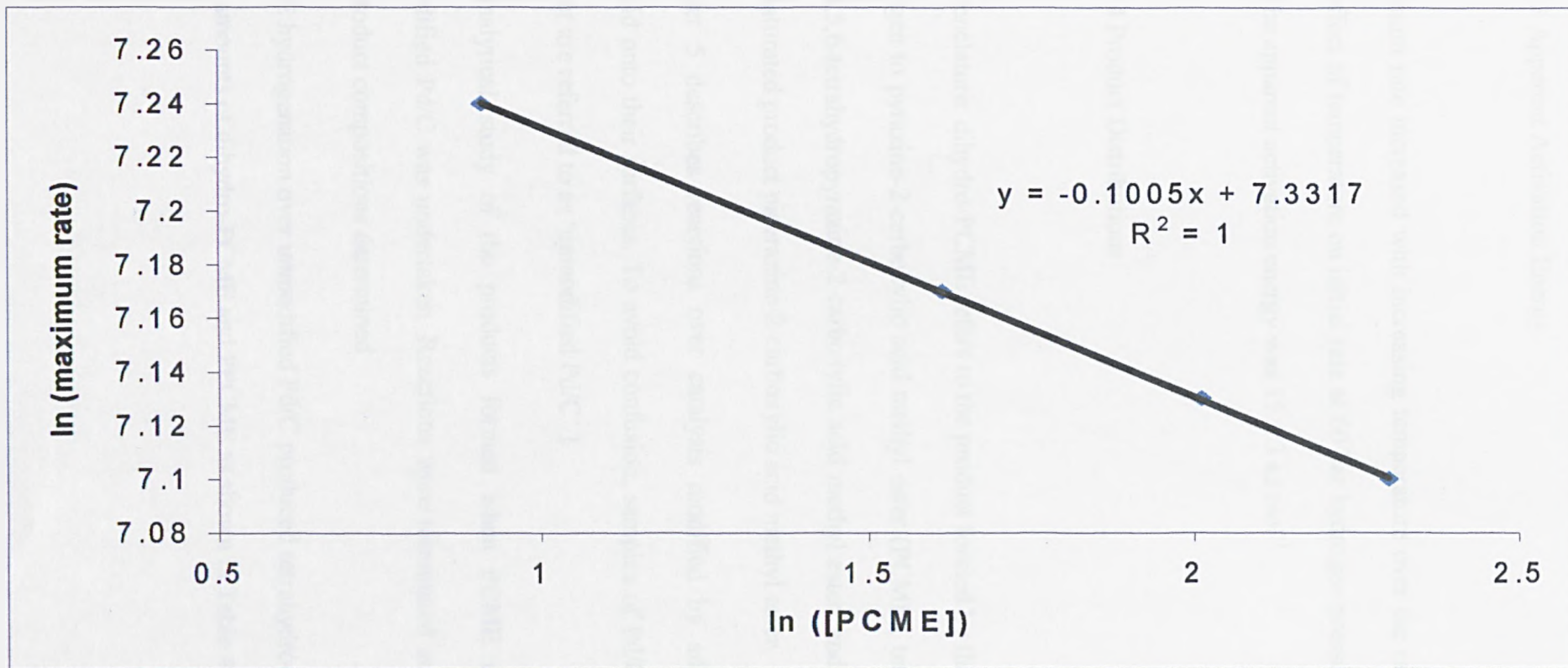


Figure 4.4 PCME hydrogenation over unmodified Pd/C at 293 K. Logarithmic plot of rate against PCME concentration.

4.2.2.3 Apparent Activation Energy

Maximum rate increased with increasing temperature over the range 283 K to 319 K. The effect of temperature on initial rate at 60 bar hydrogen pressure is shown in Figure 4.5. The apparent activation energy was $15 \pm 3 \text{ kJ mol}^{-1}$.

4.2.2.4 Product Distributions

[Nomenclature: dihydro-PCME refers to the product formed by the addition of one mole hydrogen to pyrazine-2-carboxylic acid methyl ester (PCME), tetrahydro-PCME refers to 1,4,5,6-tetrahydropyrazine-2-carboxylic acid methyl ester, and PPCME refers to the ring-saturated product piperazine-2-carboxylic acid methyl ester.

Chapter 5 describes reactions over catalysts modified by adsorption of cinchona alkaloid onto their surfaces. To avoid confusion, samples of Pd/C catalyst used in this chapter are referred to as 'unmodified Pd/C'.]

An analytical study of the products formed when PCME is hydrogenated over unmodified Pd/C was undertaken. Reactions were terminated at different conversions and product compositions determined.

PCME hydrogenation over unmodified Pd/C produced tetrahydro-PCME in excess with trace amounts of dihydro-PCME and PPCME as shown in Table 4.3 and Figure 4.6.

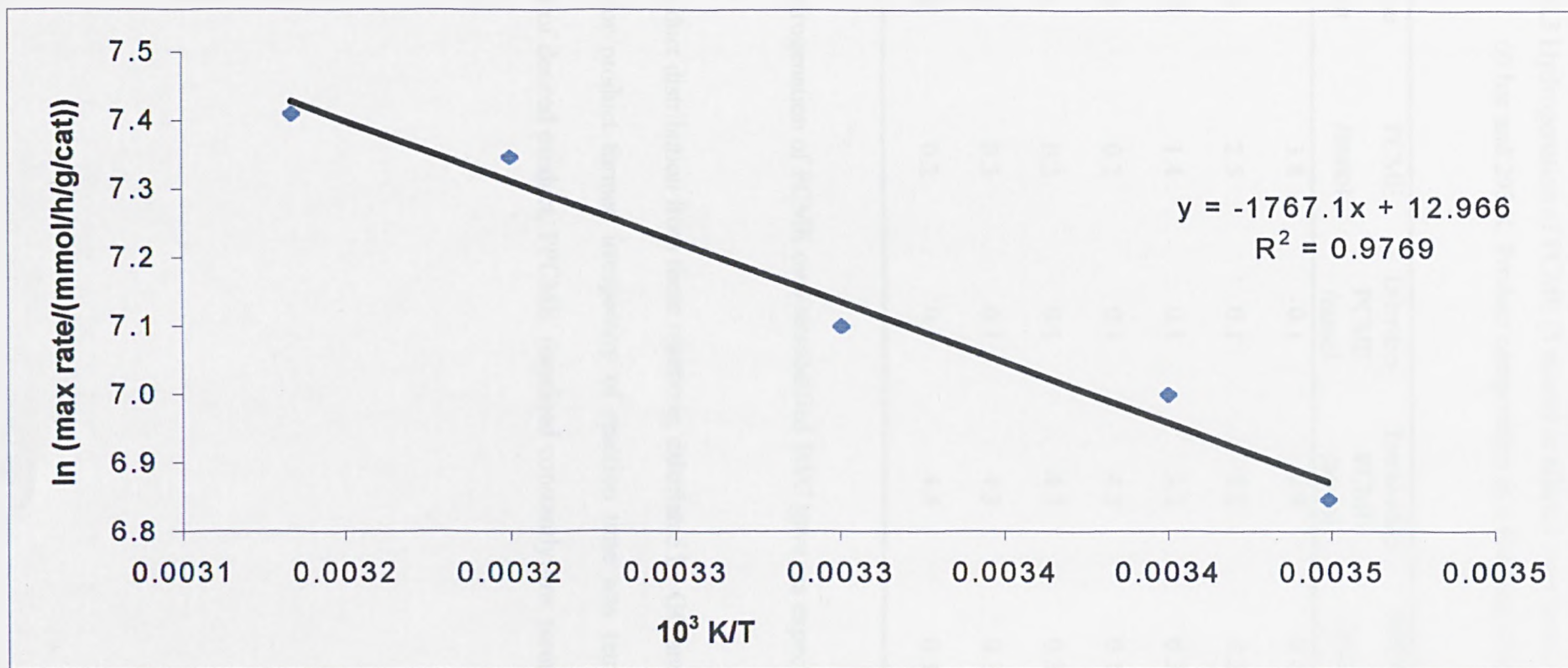


Figure 4.5 PCME hydrogenation over Pd/C. Variation of maximum rate with reciprocal temperature

Table 4.3 Hydrogenation of PCME (5 mmol) in ethanol over unmodified 5% Pd/C at 60 bar and 293 K. Product composition as a function of time.

Time /min	PCME /mmol	Dihydro- PCME /mmol	Tetrahydro- PCME /mmol	PPCME /mmol	ee /%
5	3.8	0.1	0.9	0.2	0
10	2.5	0.1	2.2	0.2	0
15	1.4	0.1	3.2	0.3	0
23	0.2	0.1	4.3	0.4	0
46	0.2	0.1	4.3	0.3	0
61	0.3	0.1	4.3	0.3	0
78	0.2	0.1	4.4	0.3	0

The hydrogenation of PCME over unmodified Pd/C gave, as expected, no enantiomeric excess.

The product distribution from these reactions, calculated by GC analysis, indicated that the major product formed irrespective of reaction time was tetrahydro-PCME. The amount of desired product, PPCME, remained constantly low throughout the course of reaction.

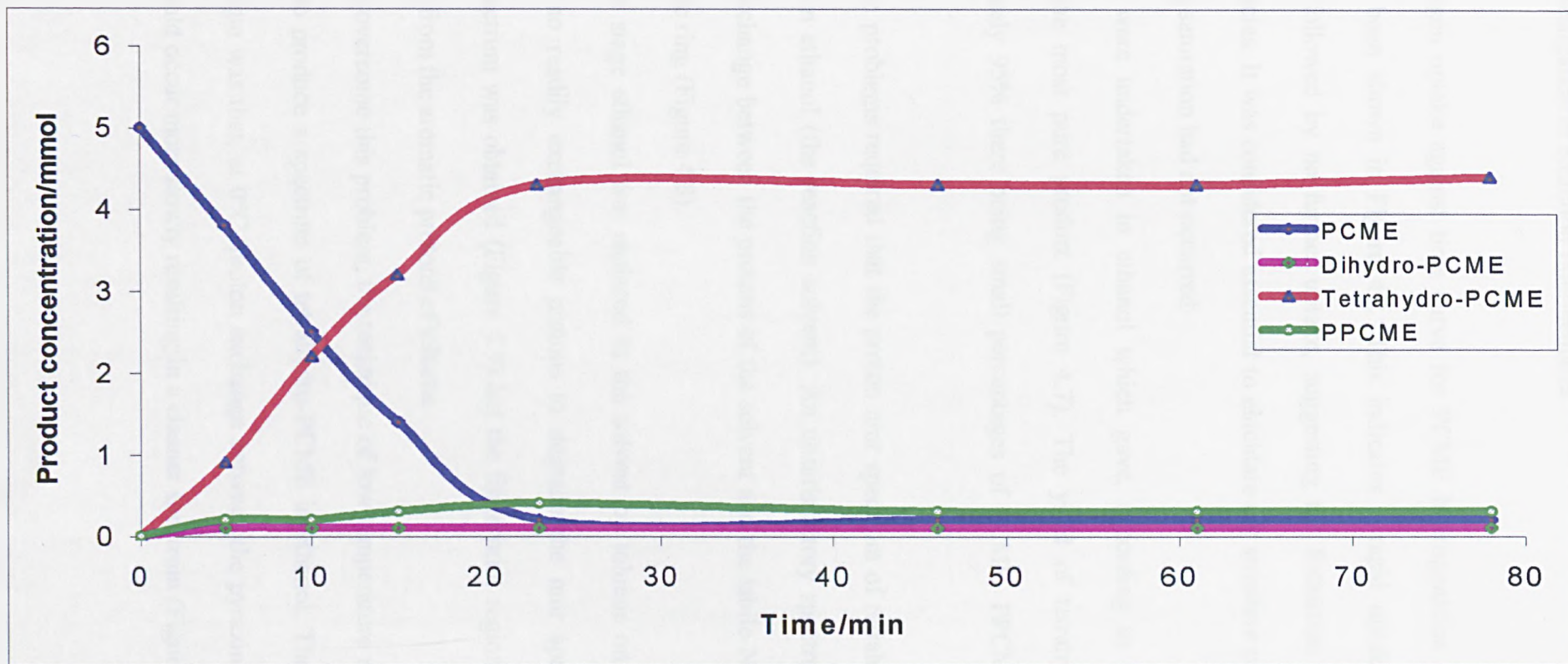


Figure 4.6 PCME hydrogenation over unmodified Pd/C. Product composition against reaction time.

4.2.2.5 Investigation of Reaction Intermediates

The hydrogen uptake against time curve for PCME hydrogenation over unmodified Pd/C has been shown in Figure 4.2. This indicates a rapid uptake of two moles hydrogen followed by no further uptake, suggesting the formation of a tetrahydro-PCME species. It was considered essential to elucidate the structure of this compound, as full ring saturation had not occurred.

Reactions were undertaken in ethanol which gave, according to GC and GCMS analysis, the most pure product (Figure 4.7). The yield of tetrahydro-PCME was approximately 95% there being small percentages of PCME, PPCME and dihydro-PCME.

Purification problems required that the proton nmr spectrum of tetrahydro-PCME was examined in ethanol (the reaction solvent). An unsatisfactory spectrum was obtained showing exchange between the protons of the solvent and the labile-NH protons of the heterocyclic ring (Figure 4.8).

In the next stage ethanol was replaced as the solvent by toluene on the basis that it contained no readily exchangeable protons to degrade the nmr spectrum. A much cleaner spectrum was obtained (Figure 4.9) but the fingerprint region was masked by the signals from the aromatic protons of toluene.

In order to overcome this problem, the technique of low temperature nmr spectroscopy was used to produce a spectrum of tetrahydro-PCME in ethanol. The concept behind this technique was that, at 0°C, proton exchange between the pyrazine compound and ethanol would occur more slowly resulting in a cleaner spectrum (Figure 4.10).

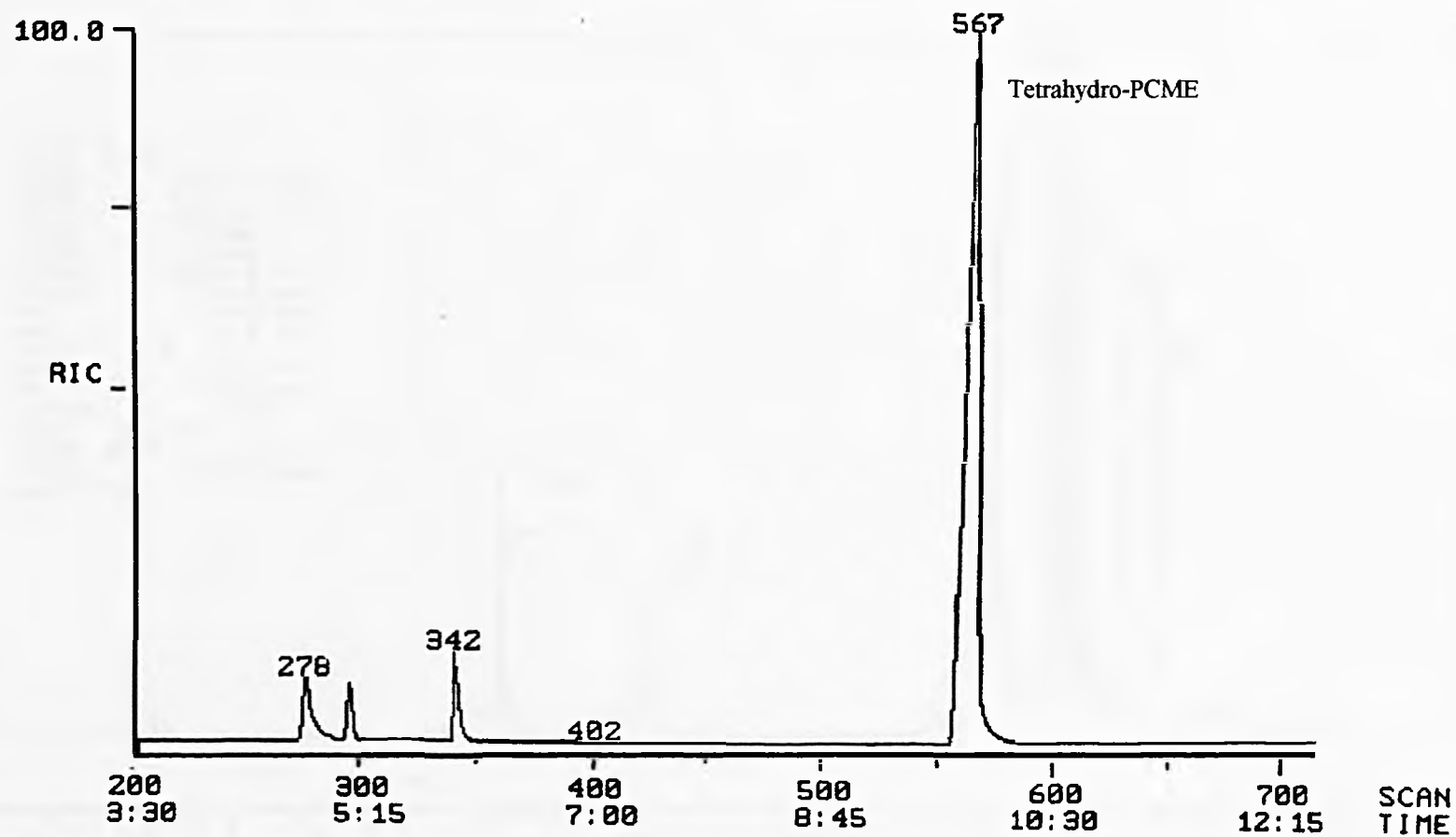


Figure 4.7 PCME hydrogenation over unmodified Pd/C. Chromatogram of products formed after two mole hydrogen uptake.

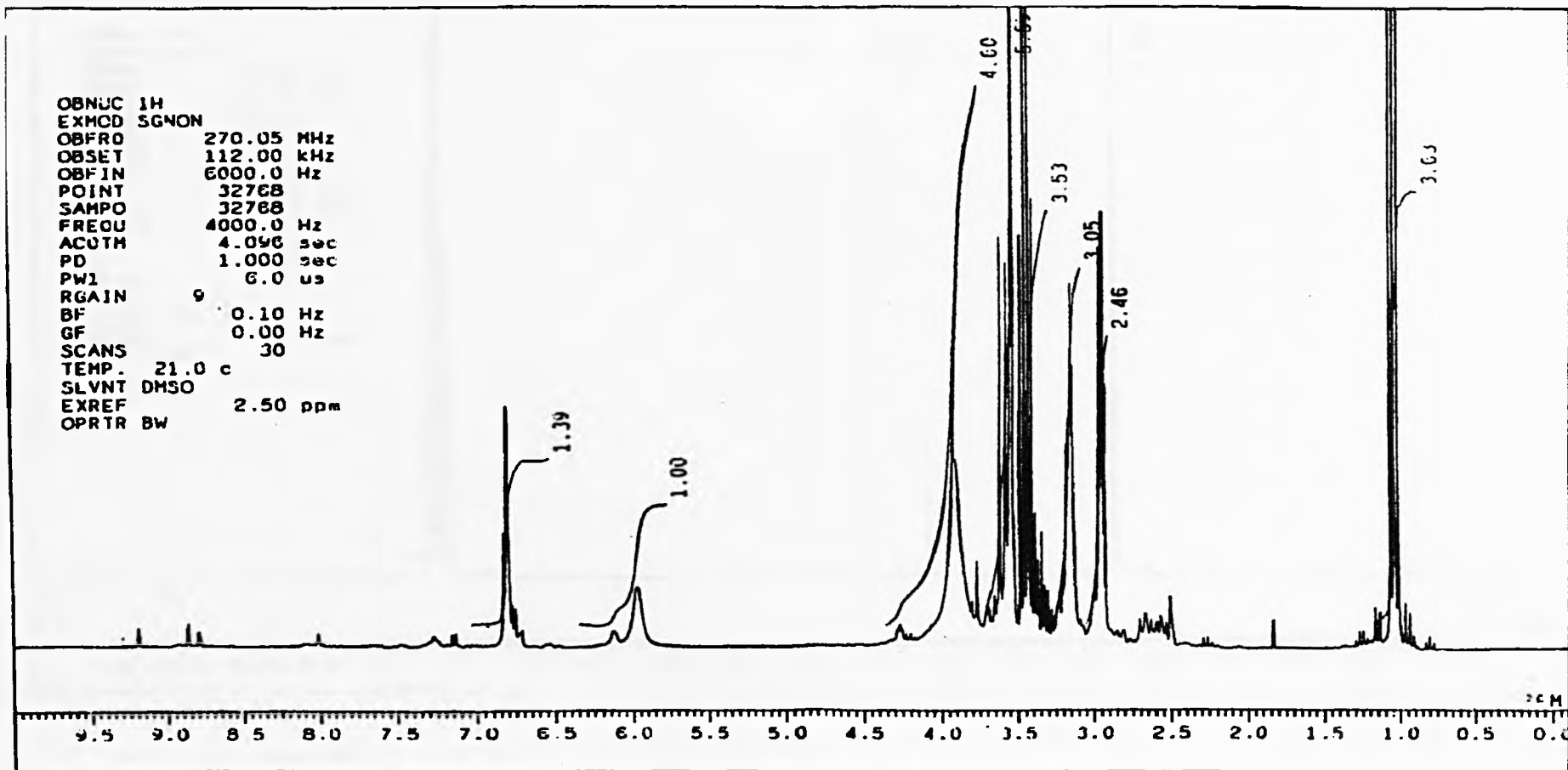


Figure 4.8 PCME hydrogenation over unmodified Pd/C. Proton nmr spectrum of tetrahydro-PCME in ethanol at room temperature.

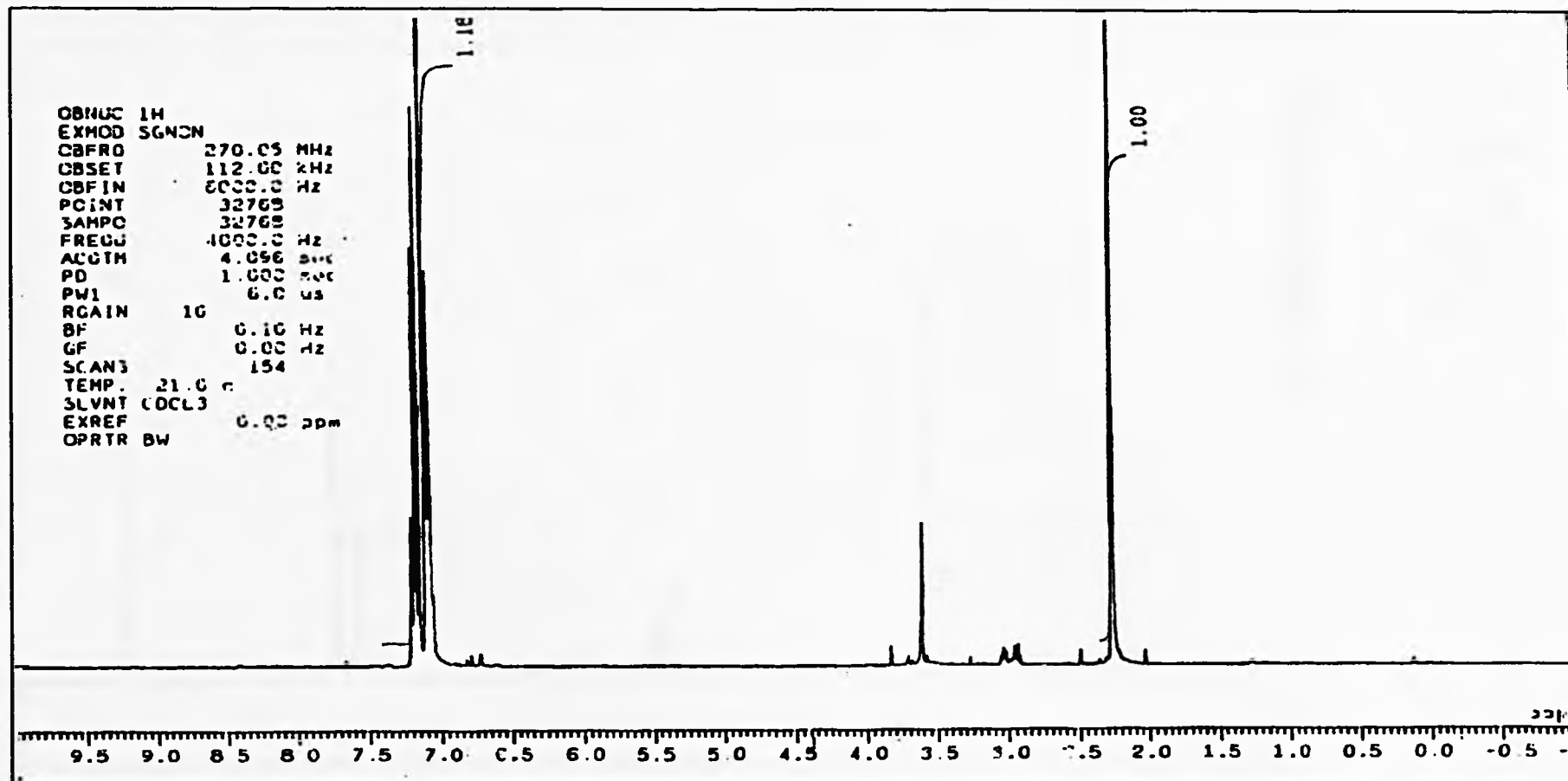


Figure 4.9 PCME hydrogenation over unmodified Pd/C. Proton nmr spectrum of tetrahydro-PCME in toluene at room temperature.

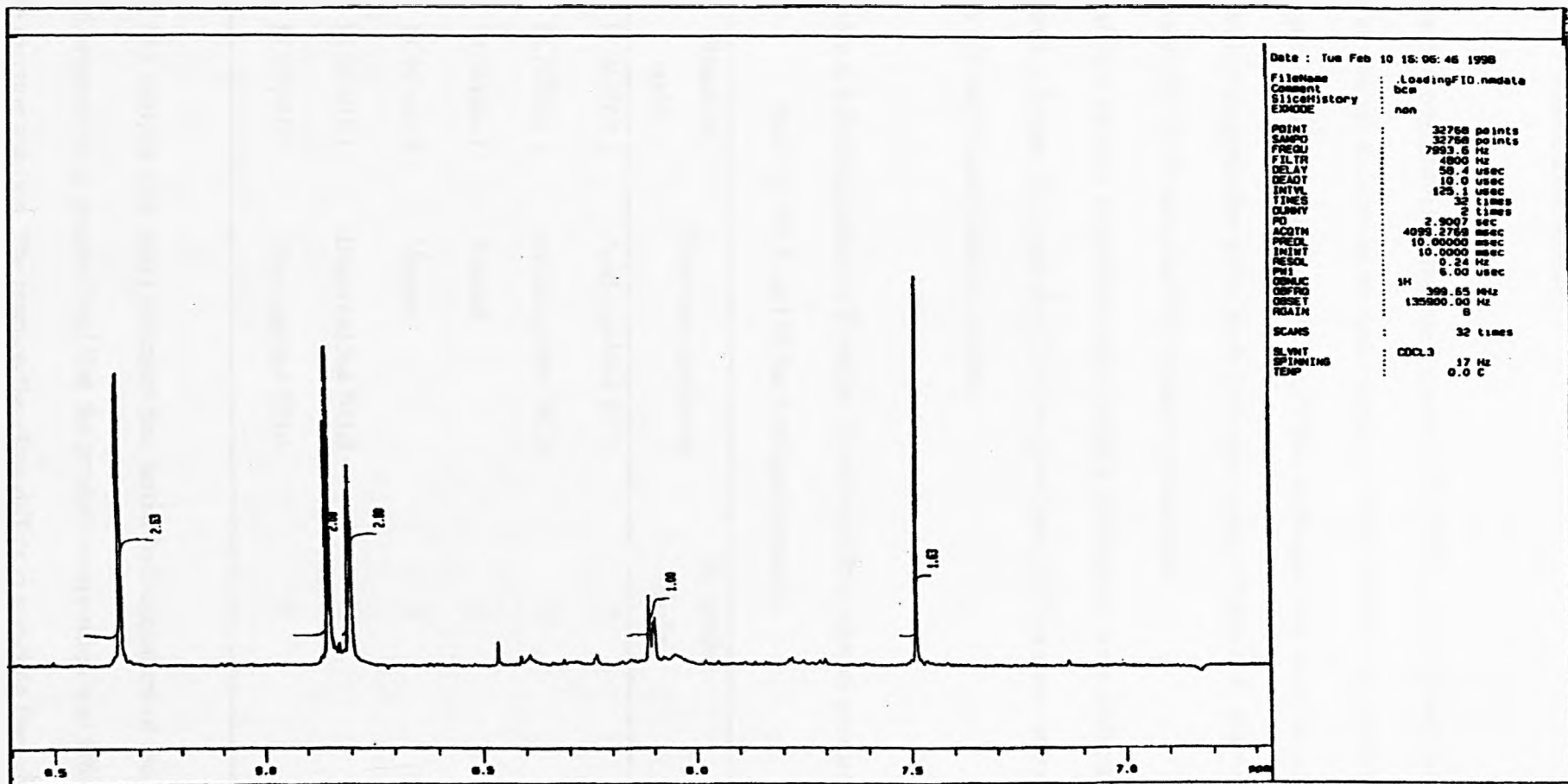


Figure 4.10 PCME hydrogenation over unmodified Pd/C. Proton nmr spectrum of tetrahydro-PCME in ethanol at 0°C.

4.2.3 Pyrazine-2-carbonitrile

The hydrogenation of pyrazine-2-carbonitrile (PCN) over unmodified Pd/C was studied in an attempt to increase the understanding of the chemistry of substituted pyrazines.

Again, as previously observed for PCME hydrogenation over an unmodified catalyst, reaction stopped after a two mole hydrogen uptake (Table 4.4). It seemed appropriate to investigate the structure of this tetrahydro compound.

Standard catalyst preparation and reaction procedures were undertaken as previously stated (Chapter 2), except that 2 ml of either conc. HCl or conc. ammonia was added to the solvent (ethanol) before reaction.

Table 4.4 Hydrogenation of Pyrazine-2-carbonitrile in ethanol over unmodified 5% Pd/C at 298 K and 60 bar hydrogen pressure.

Reaction code	Reaction conditions	H ₂ uptake /moles	Max rate /mmol h ⁻¹ g ⁻¹
PCN/HCl-1	Acidic (added HCl)	2	26
PCN/HCl-2	Acidic (added HCl)	2	19
PCN/neu-1	Neutral	2	40
PCN/neu-2	Neutral	2	47
PCN/NH-1	Basic (added NH ₃)	2	38
PCN/NH-3	Basic (added NH ₃)	2	44

GCMS analysis (see later) indicated that partial hydrogenation of the cyano substituent and aromatic ring occurred and that the product composition was affected by the pH of the reaction solution. The reaction therefore differs in principle from that of PCME.

4.3 Discussion

4.3.1 Pyrazine-2-carboxylic acid

4.3.1.1 Reactant Solubility

The results in Table 4.1 show PCA was of low solubility in most of the common solvents tested except water, and that water had to be a component of the solvent if any appreciable solubility was to be achieved. Improved solubility was obtained when the solvent was a mixture of water and a protic solvent. In this investigation, water/ethanol and water/propan-2-ol mixtures were tested, but reasonable solubility required a large excess of water. Complete solubility in water was only obtained when the acid was converted to a salt, in this case its potassium salt.

Hydrogenation of the acid as a salt caused no problems over an unmodified catalyst. However, in hydrogenation over an alkaloid modified catalyst, where a desired interaction between the free acid and the basic modifier is critical, use of a salt was expected to cause problems. This is discussed in Chapter 5.

The reason for PCA being so insoluble is attributable to its structure. If the aromatic ring was not heterocyclic, as in benzoic acid, there would be no problem as substituted benzoic acids are soluble in common solvents. However, as the acid group is allylic to a nitrogen function, the molecule is susceptible to zwitterion formation. A similar example exists with amino acids such as methionine (1). Thus, it is likely that PCA forms the zwitterion in solution and that a lattice is formed involving ensembles of these ions, thus making it insoluble. On this basis, when water is a component of the solvent, this lattice effect is reduced, and reactant solubility is improved.

4.3.1.2 Catalytic Hydrogenation

Hydrogenation over a range of unmodified catalysts gave some interesting results (Table 4.2). It is evident that supported Pt catalysts are inefficient for PCA hydrogenation, whereas Pd/C is the most active. The Rh catalyst also showed high hydrogenation activity but the reaction was not investigated in detail because general experience shows that Rh cannot be rendered enantioselective by the methods currently available, and this was the eventual goal. The Ru catalyst fully hydrogenated PCA but reaction times were long and maximum rates low.

The hydrogen uptake curves for reaction over Rh and Ru catalysts were very similar in form to those for the Pd/C catalysed hydrogenation shown in Figure 4.1.

4.3.2 Pyrazine-2-carboxylic acid methyl ester

The hydrogenation of this ester (denoted PCME) was investigated because the reactant is soluble in a variety of common solvents.

4.3.2.1 Variation of reaction variables

Orders of reaction over unmodified Pd/C were +0.9 in hydrogen and -0.1 in PCME.

This is indicative of weak adsorption of hydrogen and strong adsorption of PCME.

The variation of maximum rate with temperature followed the Arrhenius relationship and the equation appeared to be well obeyed throughout the investigated temperature range. The calculated value for the activation energy was $15 \pm 3 \text{ kJ mol}^{-1}$. This value is rather low and may be indicative of a diffusion controlled reaction.

4.3.2.2 Analysis of Product Distributions

PCME was hydrogenated over unmodified Pd/C at a reproducible r_{\max} of approximately $1000 \text{ mmol h}^{-1} (\text{g cat.})^{-1}$ to yield a small quantity of racemic PPCME. The product distribution shown in Figure 4.6 indicates that the product formed in excess, irrespective of reaction time, was tetrahydro-PCME. As the reactant (PCME) was consumed, the concentration of tetrahydro-PCME immediately increased, reaction rate falling to zero after 25 minutes. The amount of the desired PPCME remained low throughout the reaction, possibly due to the inherent stability of the carbamate-like conjugated tetrahydro-PCME (see later), and its inability to convert to piperazine under the reaction conditions used.

The product formed by addition of one mole hydrogen, dihydro-PCME, was present also in trace quantities throughout the reaction. Its structure was not elucidated but, curiously, it also showed no further reactivity, indicating that it could not compete with tetrahydro-PCME for the surface.

4.3.2.3 Investigation of Reaction Intermediates

The low temperature nmr spectrum of tetrahydro-PCME in ethanol (Figure 4.10) gave a distinct signal at $\delta = 7.5$. Chemical shifts in this area are typically characteristic of olefinic protons and the mass spectrum results (Figure 4.11) supports the assignment of the compound in solution as an α,β -unsaturated ester. This structure would also be expected experimentally, as its conjugation and electronic stability can explain the resistance of tetrahydro-PCME against further hydrogenation.

This proposed structure is in agreement to that proposed by Landau (2).

MASS SPECTRUM

BASE M/E: 54
RIC: 1001470.

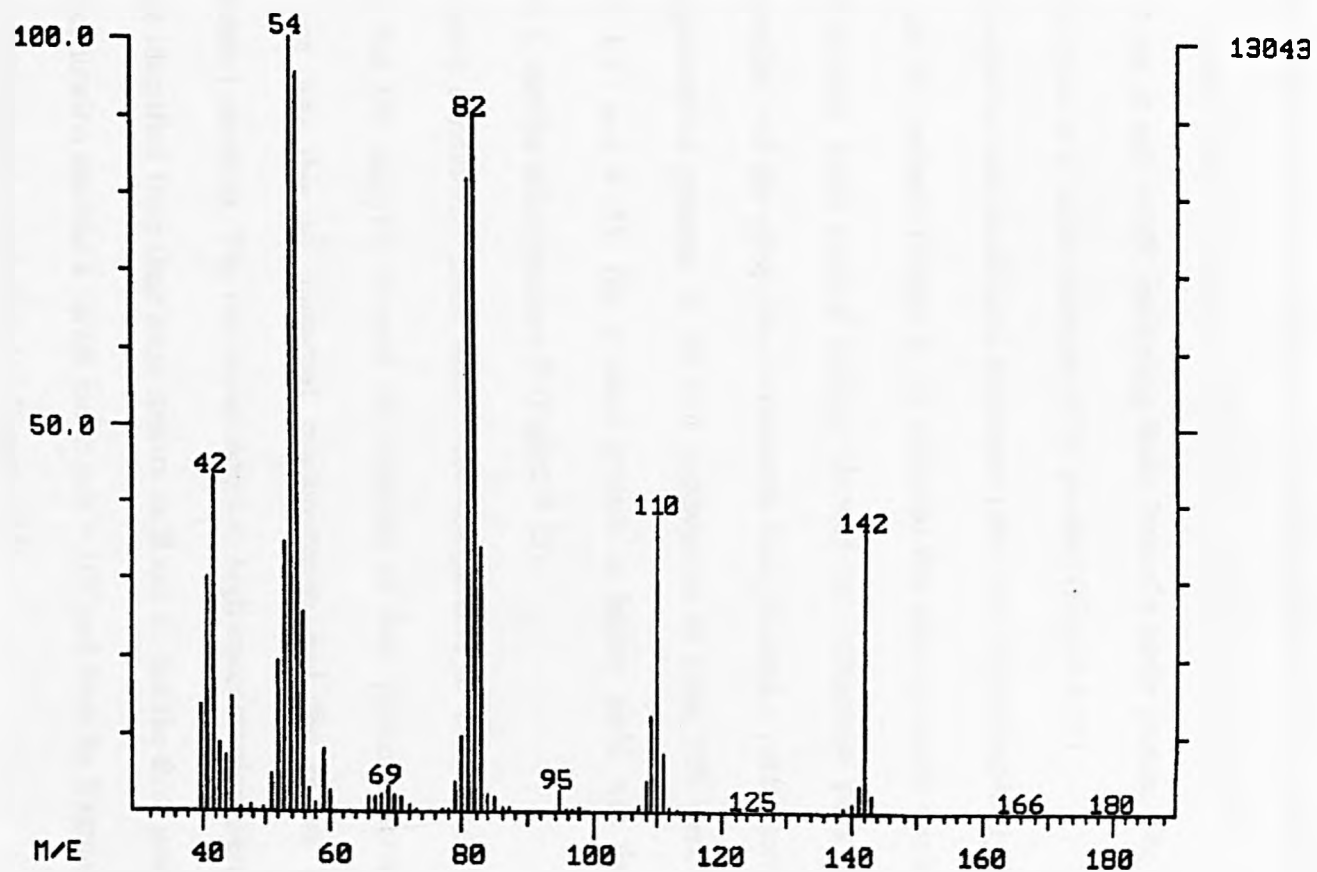


Figure 4.11 PCME hydrogenation over unmodified Pd/C. Mass spectrum of tetrahydro-PCME.

4.3.3 Pyrazine-2-carbonitrile (PCN)

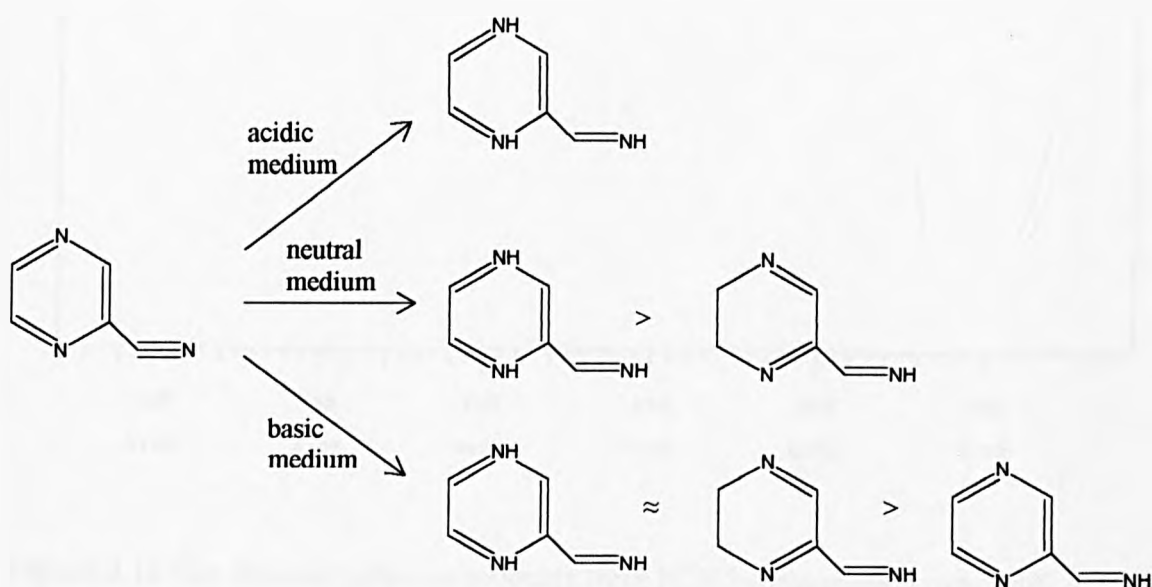
The hydrogenation of pyrazine-2-carbonitrile or 2-cyanopyrazine in acidic media gave low maximum rates (typically ca. $20 \text{ mmol h}^{-1} (\text{g cat.})^{-1}$) and the amount of product evident from the chromatogram (Figure 4.12) was less than expected from the hydrogen uptake. The only components detected by glc were unreacted cyanopyrazine ($m/z = 105$, mass spectrum shown in Figure 4.13) and a product having a parent ion at $m/z = 109$. The fragmentation spectrum of the $m/z = 109$ product (Figure 4.14) showed an abundant ion at $m/z = 108$, indicating facile loss of a labile proton. The fragmentation seemed to point to C as the structure of the product (Figure 4.15).

Under neutral reaction conditions, maximum rates were higher (typically $40 \text{ mmol h}^{-1} (\text{g cat.})^{-1}$) and GC analysis (Figure 4.16) indicated that three products were present in the reaction mixture. Mass spectral analysis showed one component peak to be unreacted cyanopyrazine and the other two components each showed a parent ion at $m/z = 109$. The fragmentation patterns of the two components of mass 109 were very different (Figures 4.17 and 4.18). The product present in higher yield was thought to have structure C and the other structure B (Figure 4.15).

Under basic conditions, initial rates were comparable to those observed in neutral solution but GC analysis showed the presence of four pyrazine derivatives (Figure 4.19); one was due to unreacted cyanopyrazine and the others were partially hydrogenated products. The two components in high concentration were of mass 109, and were identified from their mass spectra as B and C, but the third product present at low concentration showed a parent ion at $m/z = 107$ and from its fragmentation (Figure 4.20) it was assigned structure A (cf. Figure 4.15).

These results show that, as pH was increased, more intermediate species were formed. None of these reactions gave products containing a fully hydrogenated ring, none showed complete hydrogenation of the cyanide group to the primary amine and none gave a product containing an asymmetric carbon atom. Expected nitrile chemistry is not occurring here. Hartung (3) has shown that carrying out hydrogenations in alcohol in the presence of mineral acid can prevent secondary amine formation. Hydrogenation of nitriles in neutral media normally affords mixtures of primary, secondary, and tertiary amines, whereas the addition of ammonia to a nitrile hydrogenation normally prevents secondary or tertiary amine formation (because the imine intermediate is removed from the reaction mixture). Such processes are clearly not happening in the above reactions of cyanopyrazine under basic conditions because the imine is existing as two different detectable intermediates.

The processes identified are shown in Scheme A below.



Scheme A

Chromatogram Plot

Comment: pcnhcl1

Scan No: 233 Retention Time: 5:25 RIC: 425388 Mass Range: 41 - 199

Plotted: 72 to 394 Range: 1 to 1100 100% - 1070185

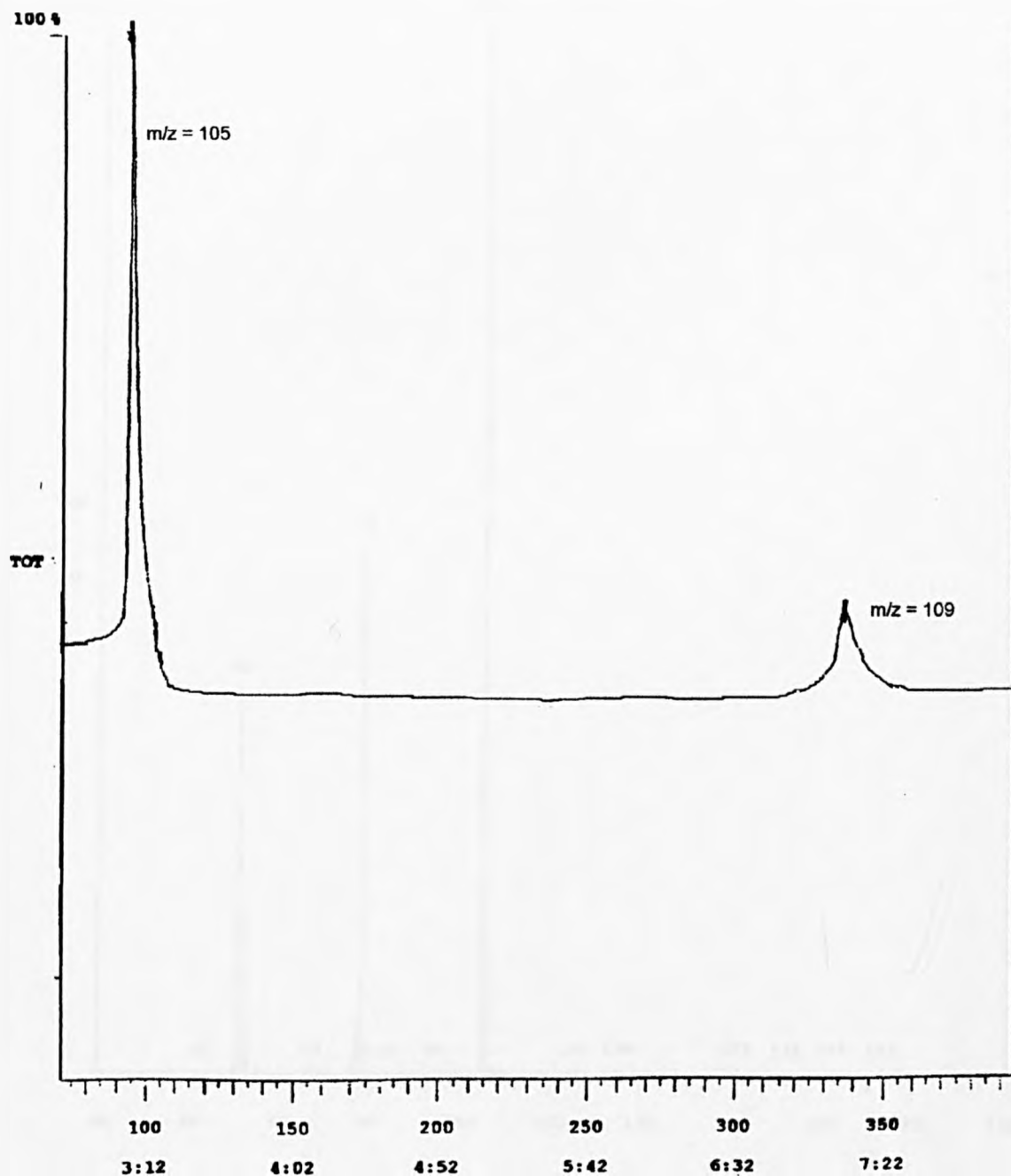


Figure 4.12 Gas chromatogram of products from PCN hydrogenation over Pd/C in acidic medium.

Background Subtract

Comment:

100% - 119753

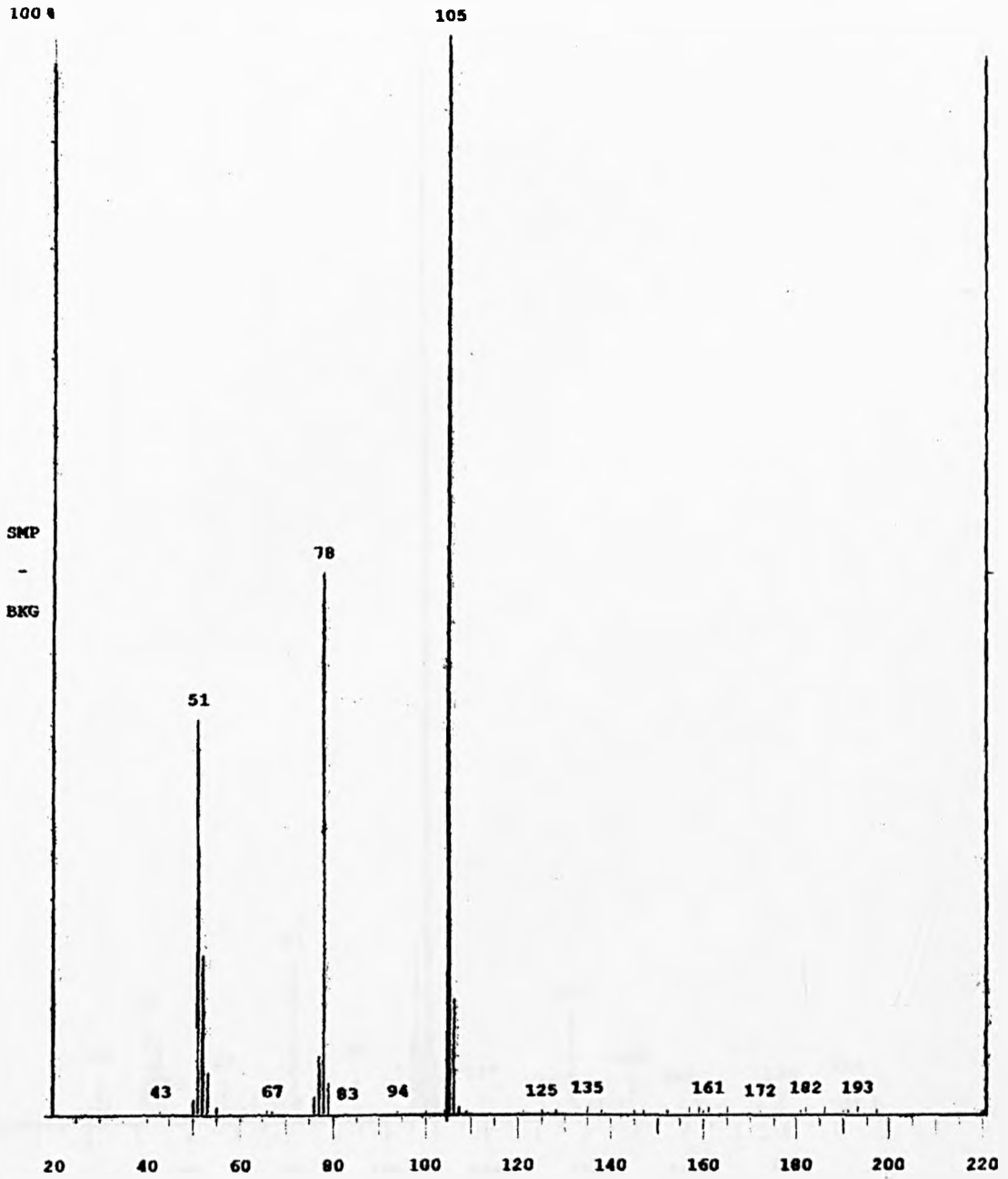


Figure 4.13 Mass spectrum of unreacted PCN.

Background Subtract

Comment: pcnbc11

100% - 19020

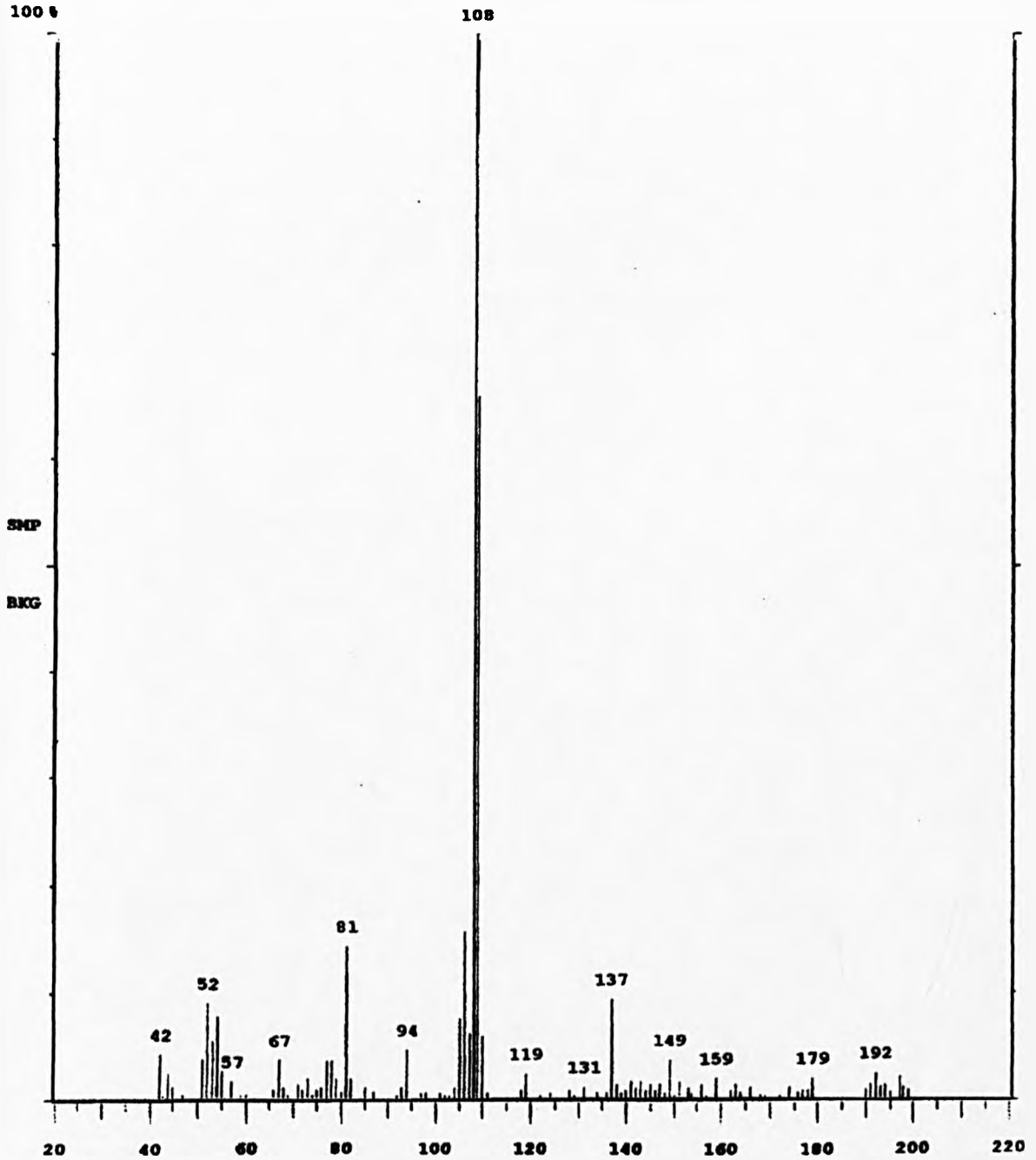
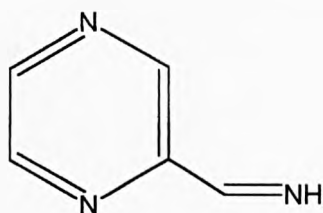
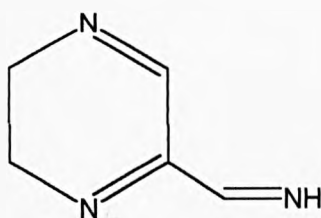


Figure 4.14 PCN hydrogenation in acidic medium. Mass spectrum of the product of apparent mass 109.

Product A



Product B



Product C

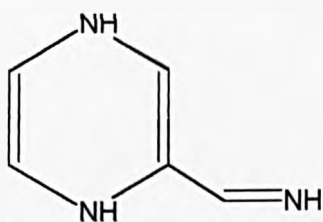


Figure 4.15 Possible products of PCN hydrogenation over Pd/C

Chromatogram Plot

C:\GCQ\DATA\TEMP

Date: 05/06/98 14:33:34

Comment: PCNNEU1

Scan No: 489 Retention Time: 10:41 RIC: 357092 Mass Range: 41 - 199

Plotted: 1 to 978 Range: 1 to 978 100% = 876509

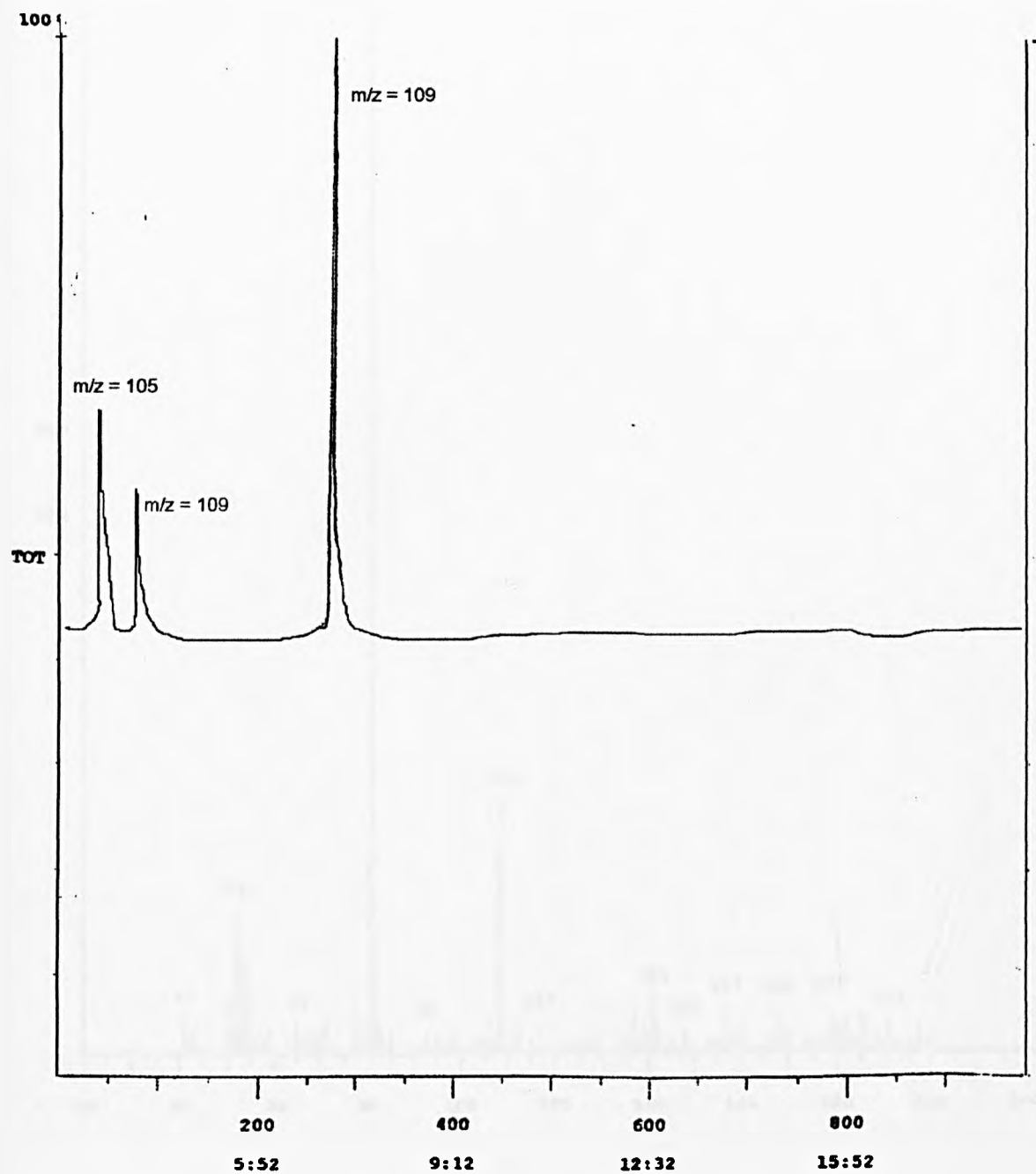


Figure 4.16 Gas chromatogram of products from PCN hydrogenation in neutral medium

Average of: 78 to 82 Minus: 104 to 108

100% - 31875

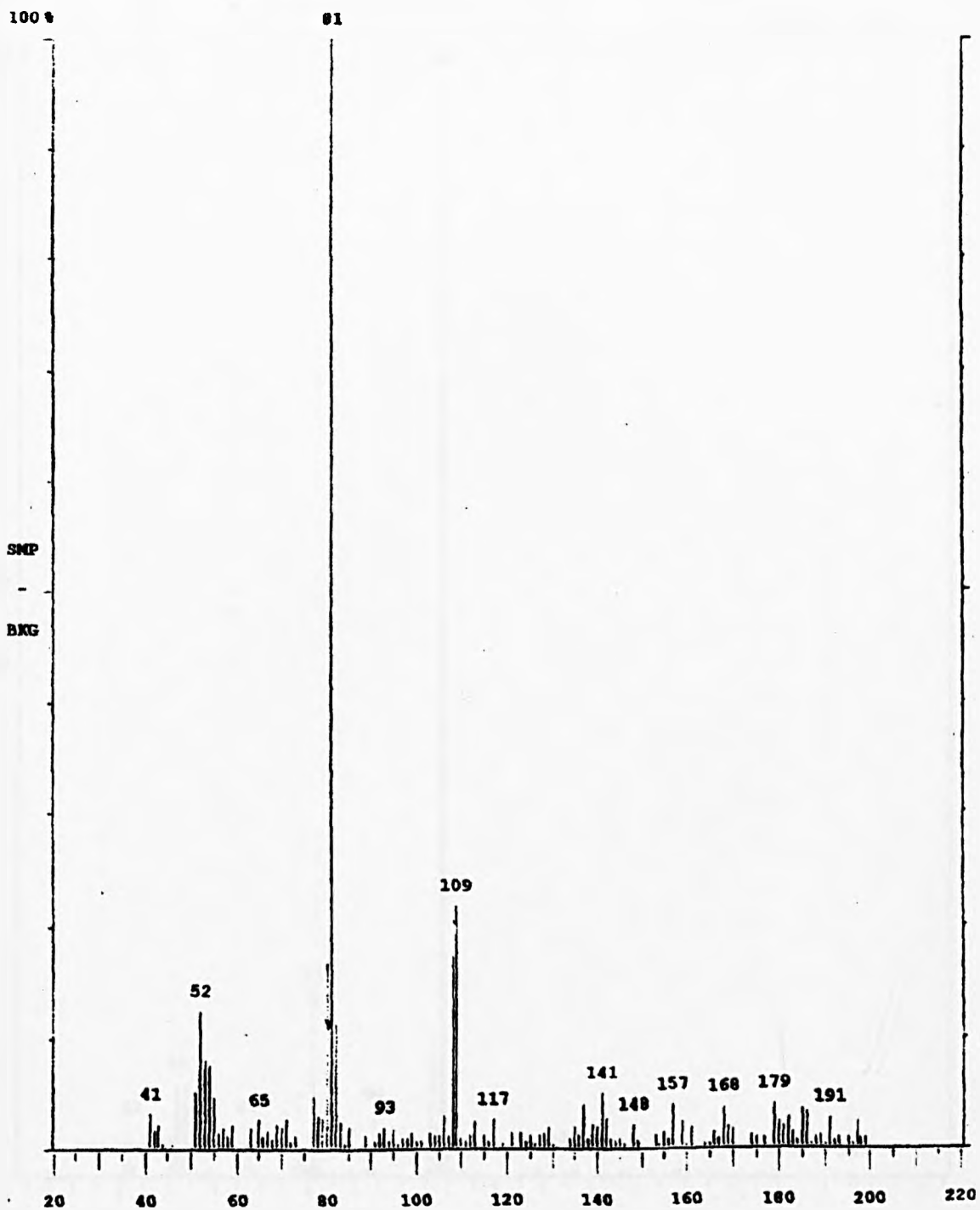


Figure 4.17 PCN hydrogenation in neutral medium. Mass spectrum of the minor product of apparent mass 109.

Comment: PCNNEU1

100% - 75467

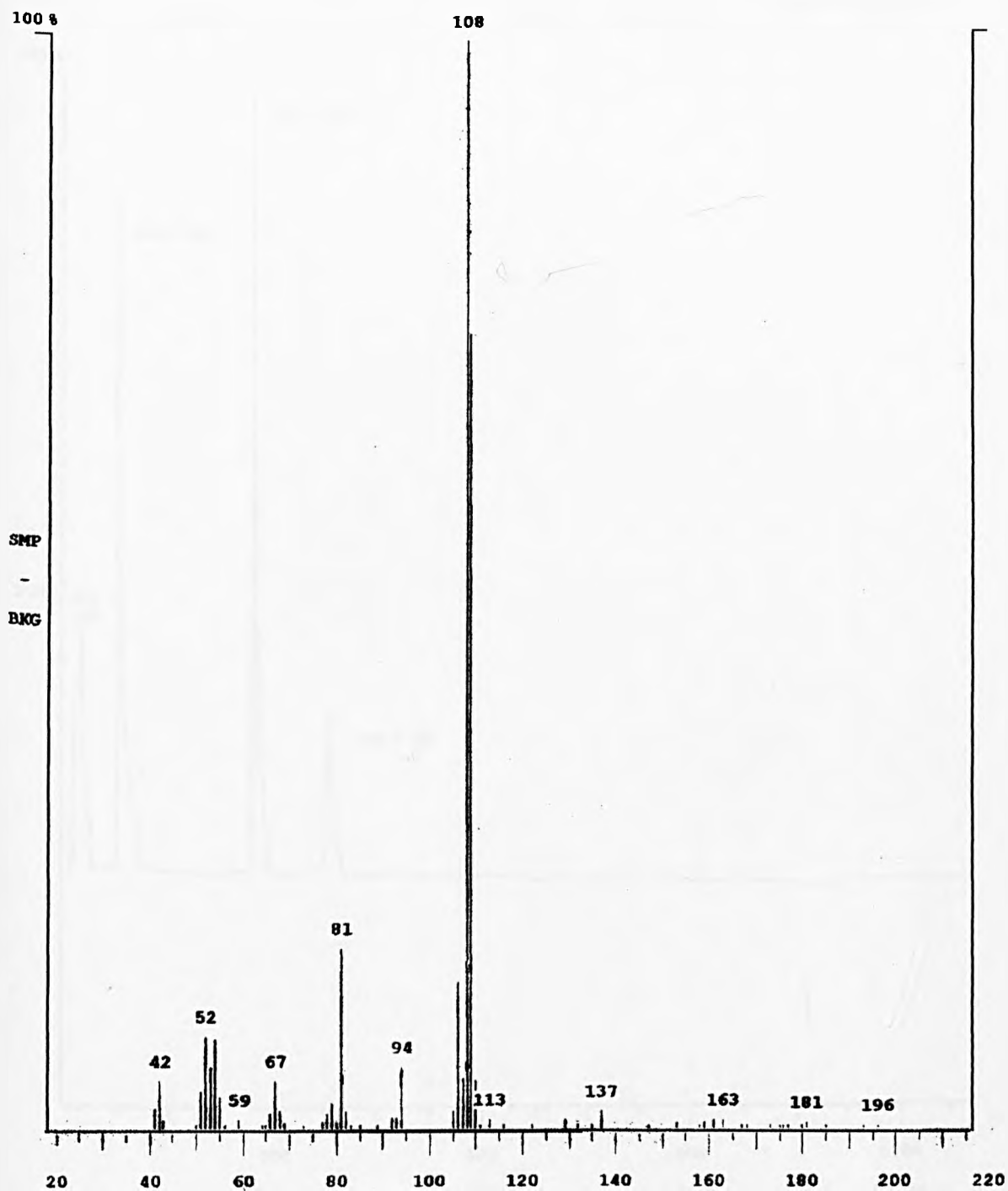


Figure 4.18 PCN hydrogenation in neutral medium. Mass spectrum of the major product of apparent mass 109.

Comment: pcnnh3

Scan No: 659

RIC: 392756 Mass Range: 41 - 199

Plotted: 1 to 1318

Range: 1 to 1318 100% = 1783967

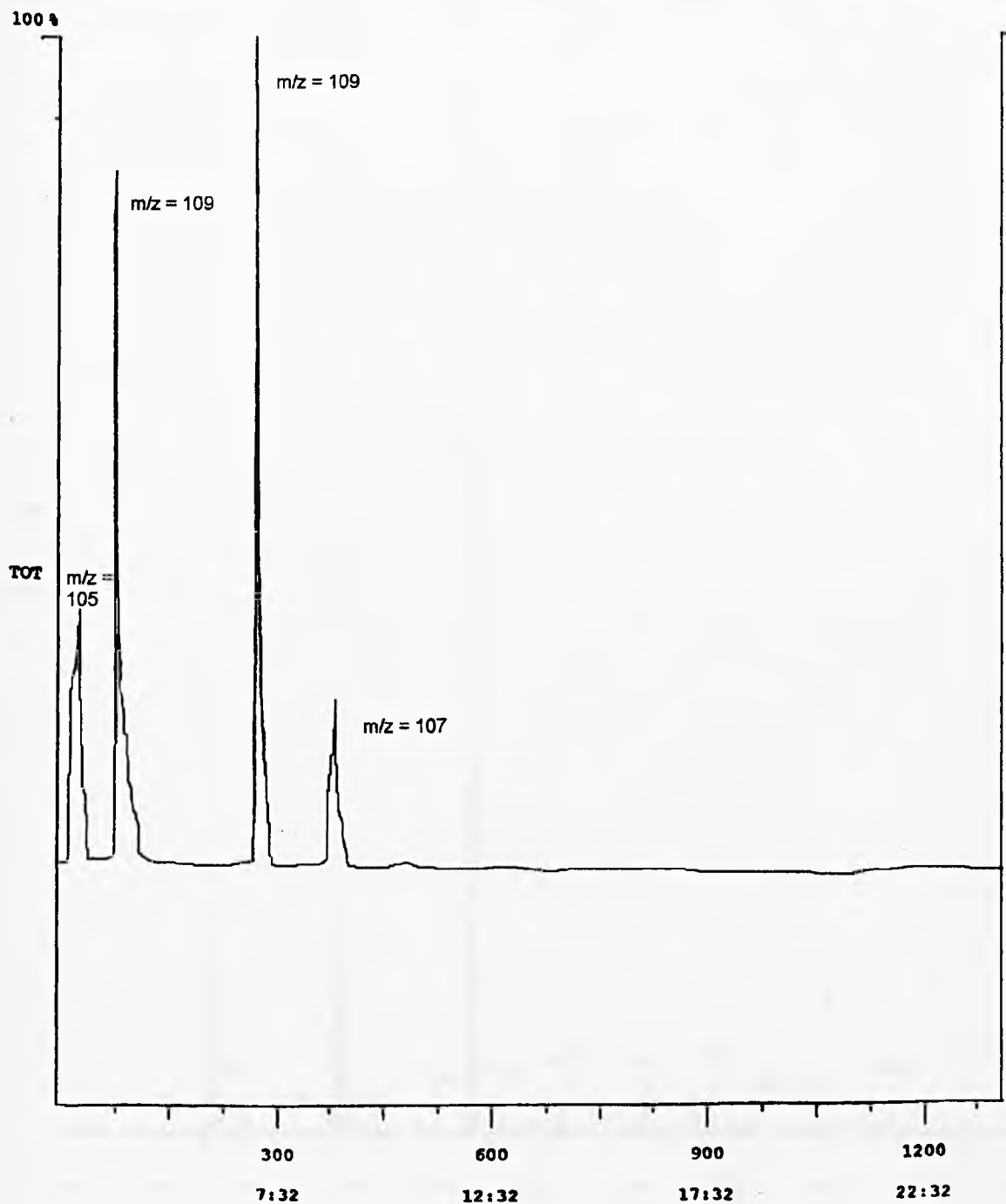


Figure 4.19 GC of products from PCN hydrogenation in basic medium.

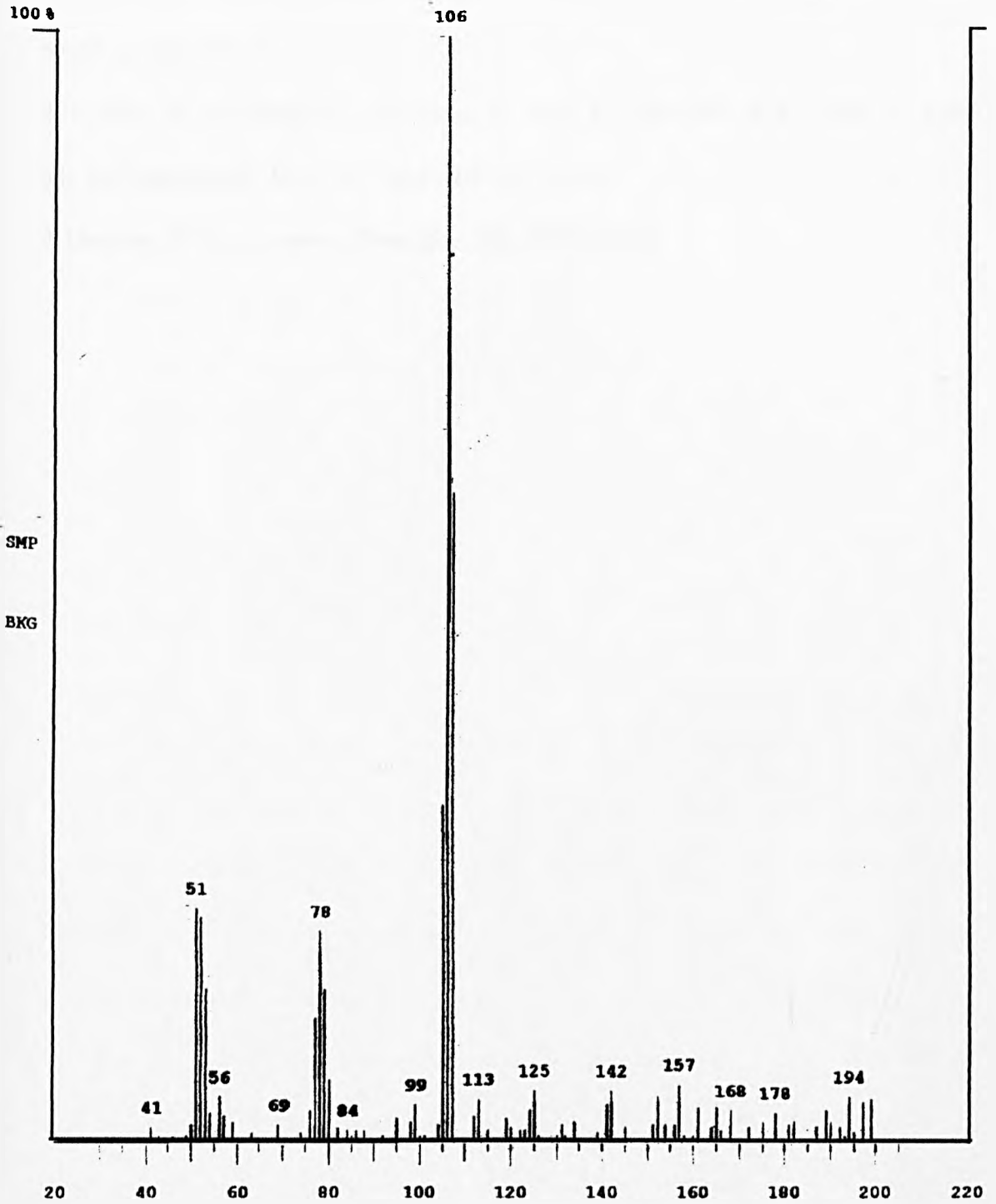


Figure 4.20 PCN hydrogenation in basic medium. Mass spectrum of the product of apparent mass 107.

References

1. Cooper, E., Krebs, F., Smith, M., and Raval, R., *Journal of Electron Spectroscopy*, 64/65, p. 469 (1993)
2. Landau, R. N., Singh, U., Gortsema, F., Sun, Y., Gomolka, S. C., Lam, T., Futran, M., and Blackmond, D. G., *J. Catal.*, **157**,201 (1995)
4. Hartung, W. H., *J. Amer. Chem. Soc.*, **50**, 3370 (1928)

Enantioselective Hydrogenation of Pyrazine -2- Carboxylic Acid Methyl Ester

5.1 Introduction

The hydrogenation of pyrazine-2-carboxylic acid methyl ester was studied over chirally modified Pd and Ni catalysts in an attempt to induce an enantioselective outcome in the product.

In this chapter the terms *unmodified* and *modified* catalysts, refer to the absence or presence of a chiral modifier adsorbed onto the catalyst.

5.2 Results: Catalysis by Pd

5.2.1 Pyrazine-2-carboxylic acid

5.2.1.1 Hydrogen uptake curve

The hydrogenation of pyrazine-2-carboxylic acid (PCA, 5 mmol in 40 ml water) at 293 K and 10 bar hydrogen pressure was investigated over cinchonidine-modified 5% Pd/C; the hydrogen uptake against time curve is shown in Figure 5.1. The insolubility problem associated with PCA was mentioned in Chapter 4, this again was overcome by the addition of 40 mg potassium hydroxide to the reaction solution (water, 40 ml).

The two-stage uptake curve, previously seen in Chapter 4 was again obtained; reaction over an unmodified catalyst achieved the completion of its first stage before reaction over modified catalyst, but the second stage proceeded at a slower rate. Analysis of the reaction products by probe GCMS and polarimetry showed *racemic* piperazine-2-carboxylic acid as the sole product.

When the quantity of cinchonidine was varied, no positive effect on product enantioselectivity was observed (Table 5.1).

Table 5.1 Hydrogenation of PCA (5 mmol) over cinchonidine modified 5% Pd/C (0.1g) in water.

Mass of cinchonidine/g	Reaction time/minutes	Uptake /mmol	Max rate /mmol h ⁻¹ g ⁻¹	ee /%
0.00	1100	16	251	0
0.03	1000	16	191	0
0.07	1000	16	139	0
0.11	1100	16	162	0
0.20	1000	15	125	0
0.30	1000	17	124	0
0.50	1100	17	90	0
0.70	1350	17	33	0

5.2.2 Pyrazine-2-carboxylic acid methyl ester

5.2.2.1 Hydrogen uptake curve

The enantioselective hydrogenation of pyrazine-2-carboxylic acid methyl ester (PCME), or methyl pyrazine-2-carboxylate as it is more commonly called, was investigated in ethanol over a range of modified catalysts.

In this section, all reactions of PCME refer to hydrogenation over cinchonidine-modified 5% Pd/C unless otherwise stated. The typical conditions and quantities of

reactant/reagents for a standard reaction were as follows. The reduced catalyst (0.1 g) modified aerobically with alkaloid (0.5 g.), was used to hydrogenate the reactant (5 mmol) in solvent (50 ml) at 60 bar hydrogen pressure and ambient temperature (293 K).

The hydrogen uptake against time curves for reaction over both unmodified and modified catalysts are given in Figure 5.2.

After a two-mole hydrogen uptake, reaction over the unmodified catalyst slowed considerably and eventually stopped, whereas reaction over the modified catalyst continued smoothly to completion. No induction period was observed for either reaction.

Reaction rates for both reactions were estimated; the r_{\max} was around $1000 \text{ mmol h}^{-1} (\text{g cat.})^{-1}$ for the unmodified reaction compared to $350 \text{ mmol h}^{-1} (\text{g cat.})^{-1}$ for the modified.

Under optimum conditions, the cinchonidine-modified reaction produced methyl piperazine-2-carboxylate (PPCME) with an enantiomeric excess of 25% in favour of the S-enantiomer. When the catalyst was modified with cinchonine, (R)- methyl piperazine-2-carboxylate was produced at a similar rate, but with a lower enantiomeric excess of about 14%.

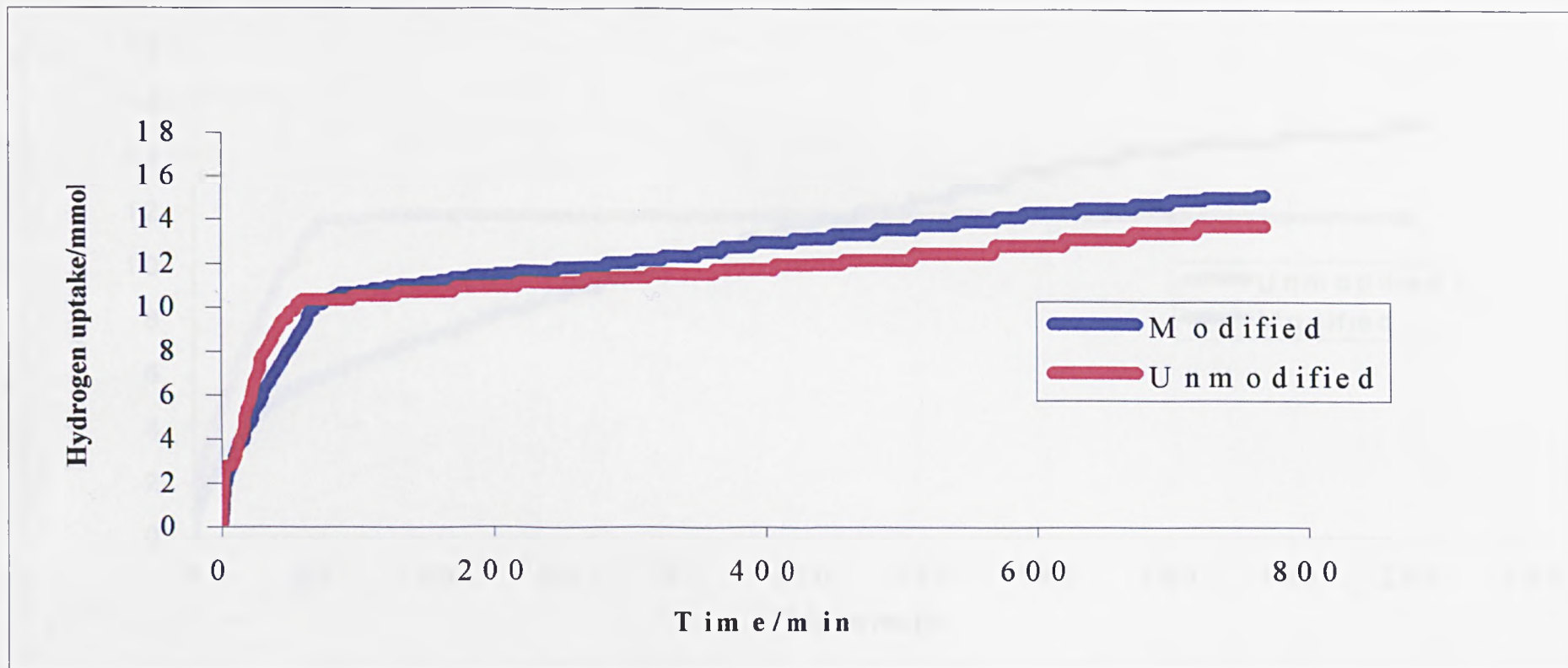


Figure 5.1 Hydrogenation of PCA (5 mmol) over modified and unmodified 5% Pd/C in ethanol

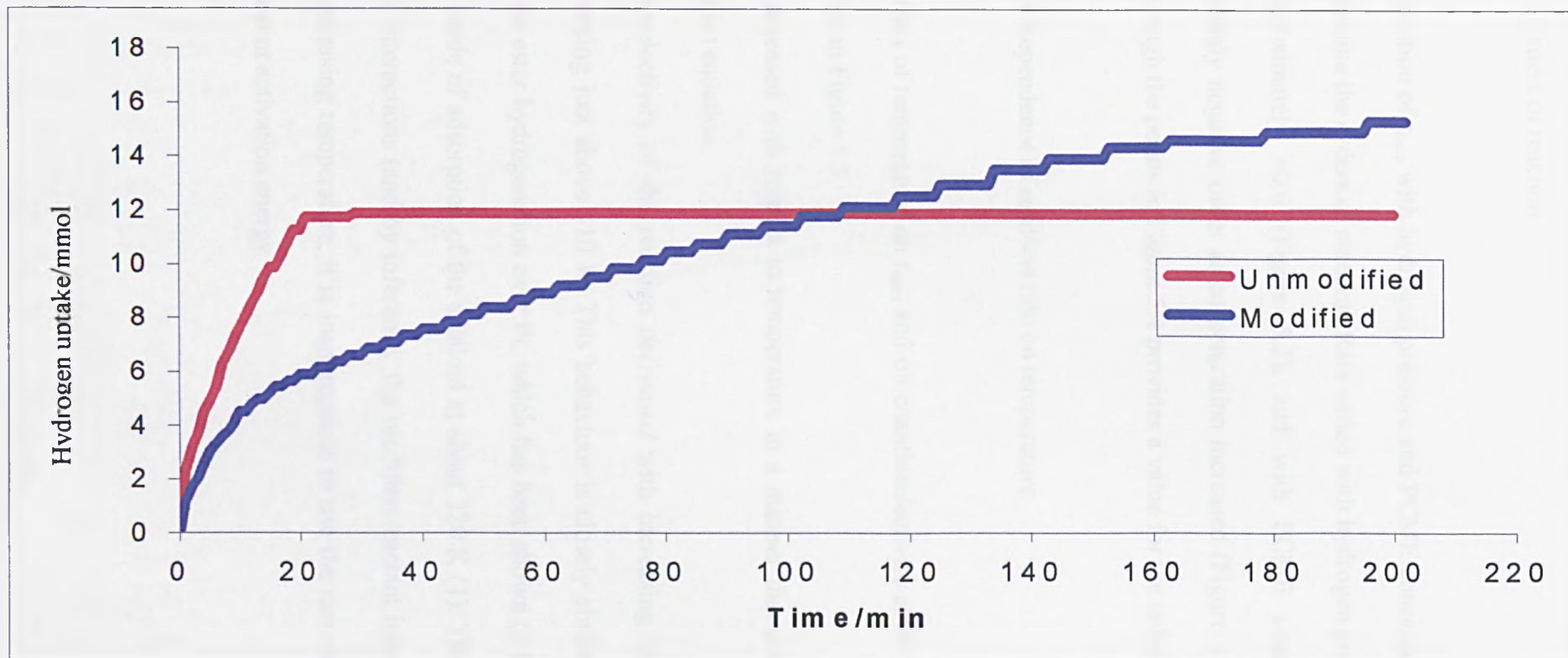


Figure 5.2 Hydrogenation of PCME (5 mmol) over modified and unmodified 5% Pd/C in ethanol

5.2.2.2 Orders of reaction

The variation of r_{\max} with hydrogen pressure and PCME concentration has been studied to determine the orders of reaction. Rate varied with hydrogen pressure, giving an order of approximately +0.6 (Figure 5.3), and with PCME concentration, giving an increasingly negative order as concentration increased (Figure 5.4). The mean straight line through the points in Figure 5.4 provides a value for the order in PCME of -0.2.

5.2.2.3 Dependence of reaction rate on temperature

The effect of temperature on r_{\max} and on enantioselectivity at 60 bar hydrogen pressure is shown in Figure 5.5.

Rate increased with respect to temperature in a manner that does not conform to the Arrhenius equation.

Enantioselectivity of the reaction *decreased* with increasing temperature, a collapse commencing just above 310 K. This behaviour is closely similar to that reported for pyruvate ester hydrogenation over Pt, which has been shown to be caused by a change in the mode of adsorption of the alkaloid at about 320 K (1). Thus, since the modifier-surface interactions (and by inference, the modifier-reactant interactions) are changing with increasing temperature, it is inappropriate to use the rate measurements to obtain an apparent activation energy.

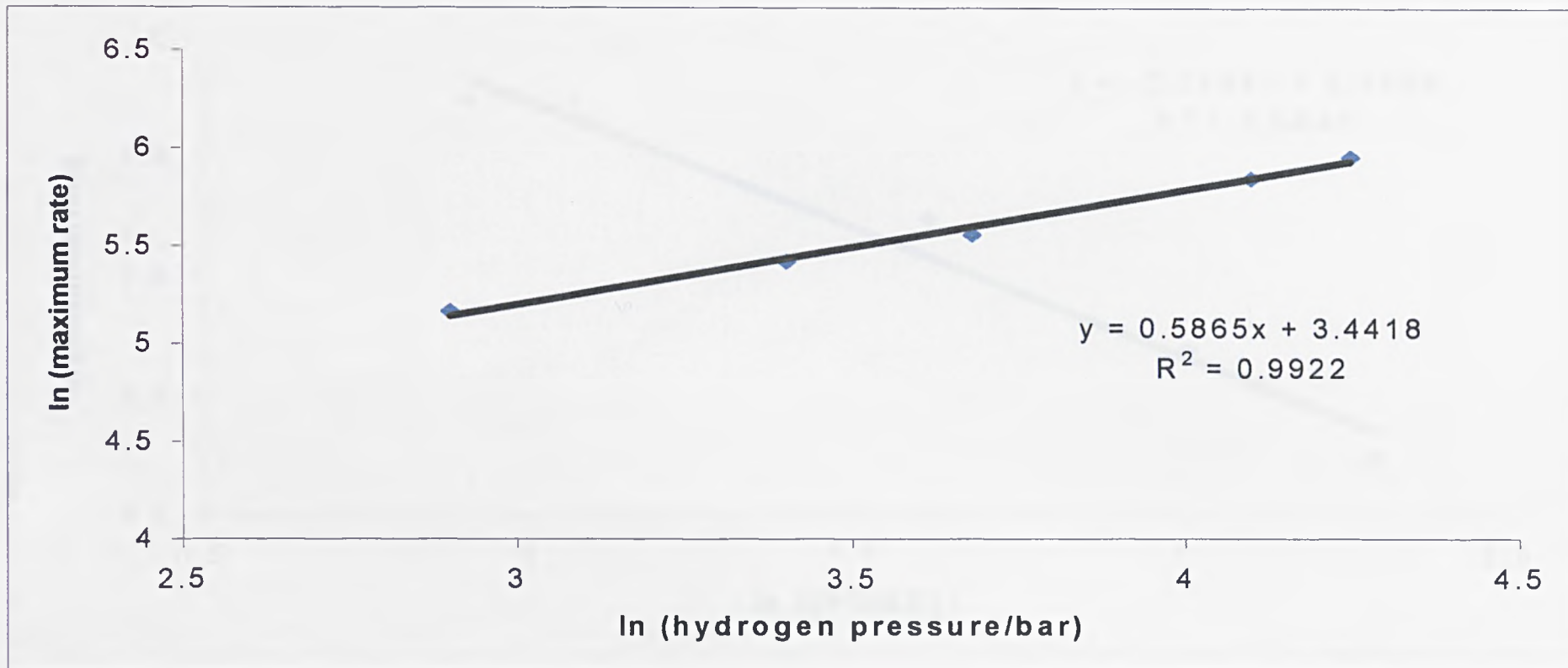


Figure 5.3 PCME hydrogenation over modified Pd/C at 293 K. Logarithmic plot of rate against hydrogen pressure.

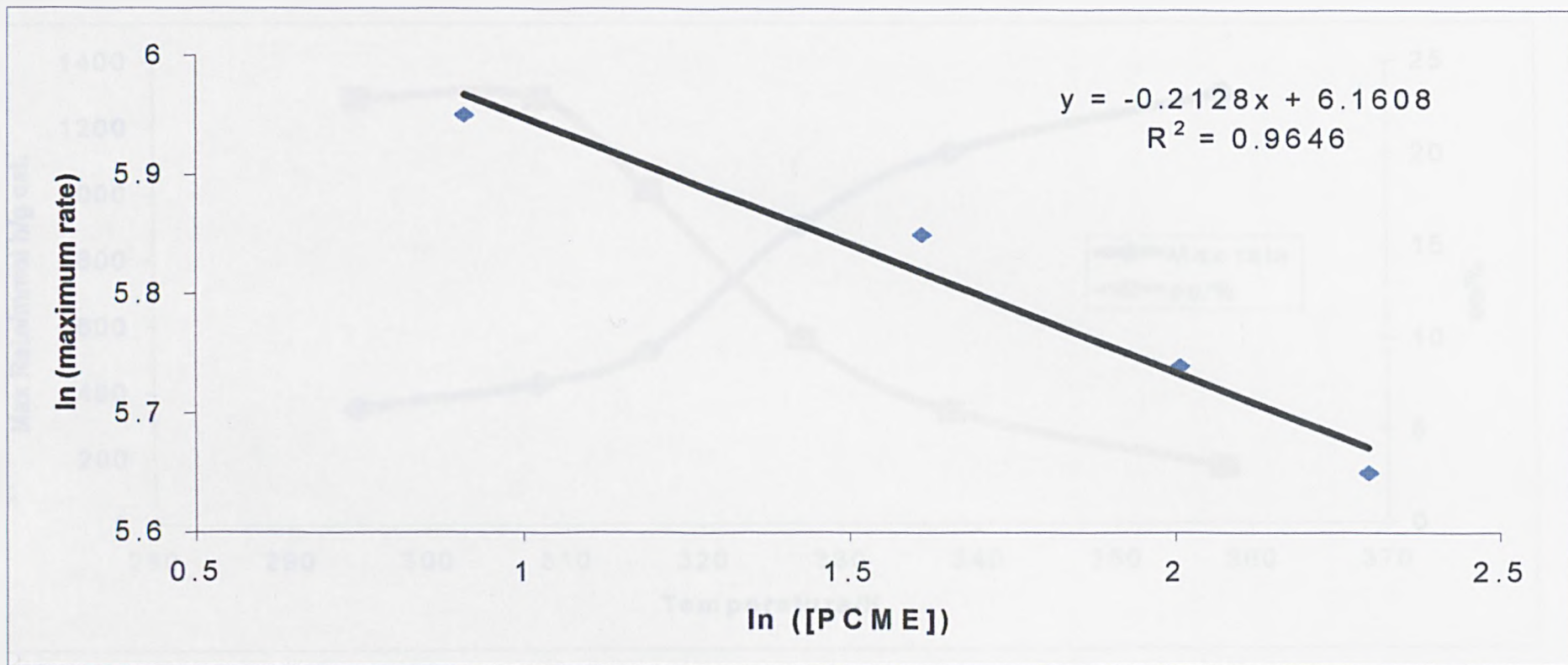


Figure 5.4 PCME hydrogenation over modified Pd/C at 293 K. Logarithmic plot of rate against PCME concentration.

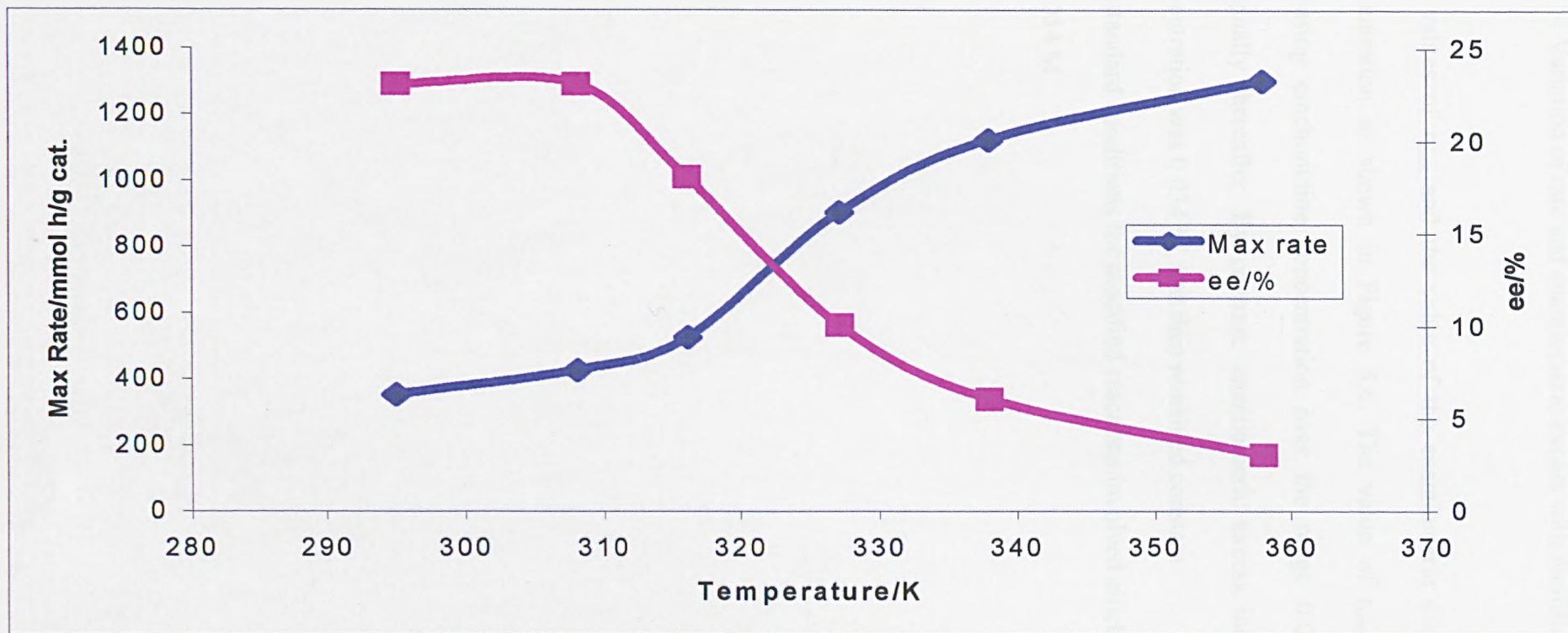


Figure 5.5 PCME hydrogenation over modified Pd/C. Variation of rate and enantiomeric excess with temperature

5.2.2.4 Variation of rate and enantiomeric excess with modifier concentration

The values of r_{\max} and the value of the enantiomeric excess varied with modifier concentration as shown in Figure 5.6. The value of r_{\max} *decreased* rapidly with increasing cinchonidine concentration over the range 0.00 to 0.02 M, and only marginally thereafter. By contrast, enantiomeric excess increased until the alkaloid concentration was 0.034 M, and then remained constant.

The standard conditions for modified reactions involved cinchonidine at a concentration of 0.034 M.

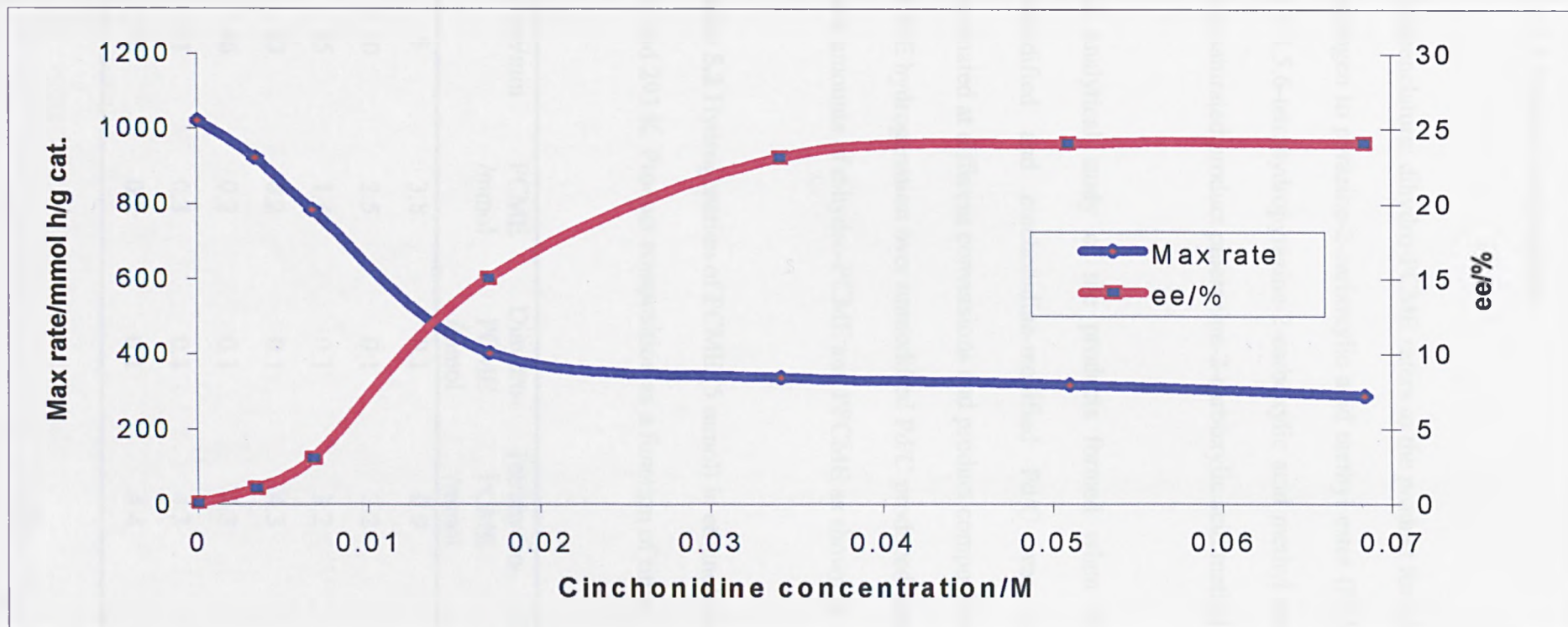


Figure 5.6 PCME hydrogenation over modified Pd/C. Variation of rate and enantiomeric excess with cinchonidine concentration.

5.2.2.5 Product compositions

[Nomenclature: dihydro-PCME refers to the product formed by the addition of one mole hydrogen to pyrazine-2-carboxylic acid methyl ester (PCME), tetrahydro-PCME refers to 1,4,5,6-tetrahydropyrazine-2-carboxylic acid methyl ester, and PPCME refers to the ring-saturated product piperazine-2-carboxylic acid methyl ester].

An analytical study of the products formed when PCME is hydrogenated over unmodified and cinchonidine-modified Pd/C was undertaken. Reactions were terminated at different conversions and product compositions determined.

PCME hydrogenation over unmodified Pd/C produced tetrahydro-PCME in excess with trace amounts of dihydro-PCME and PPCME as shown in Table 5.2 and Figure 5.7.

Table 5.2 Hydrogenation of PCME (5 mmol) in ethanol over unmodified 5% Pd/C at 60 bar and 293 K. Product composition as a function of time.

Time/min	PCME /mmol	Dihydro- PCME /mmol	Tetrahydro- PCME /mmol	PPCME /mmol	ee /%
5	3.8	0.1	0.9	0.2	0
10	2.5	0.1	2.2	0.2	0
15	1.4	0.1	3.2	0.3	0
23	0.2	0.1	4.3	0.4	0
46	0.2	0.1	4.3	0.3	0
61	0.3	0.1	4.3	0.3	0
78	0.2	0.1	4.4	0.3	0

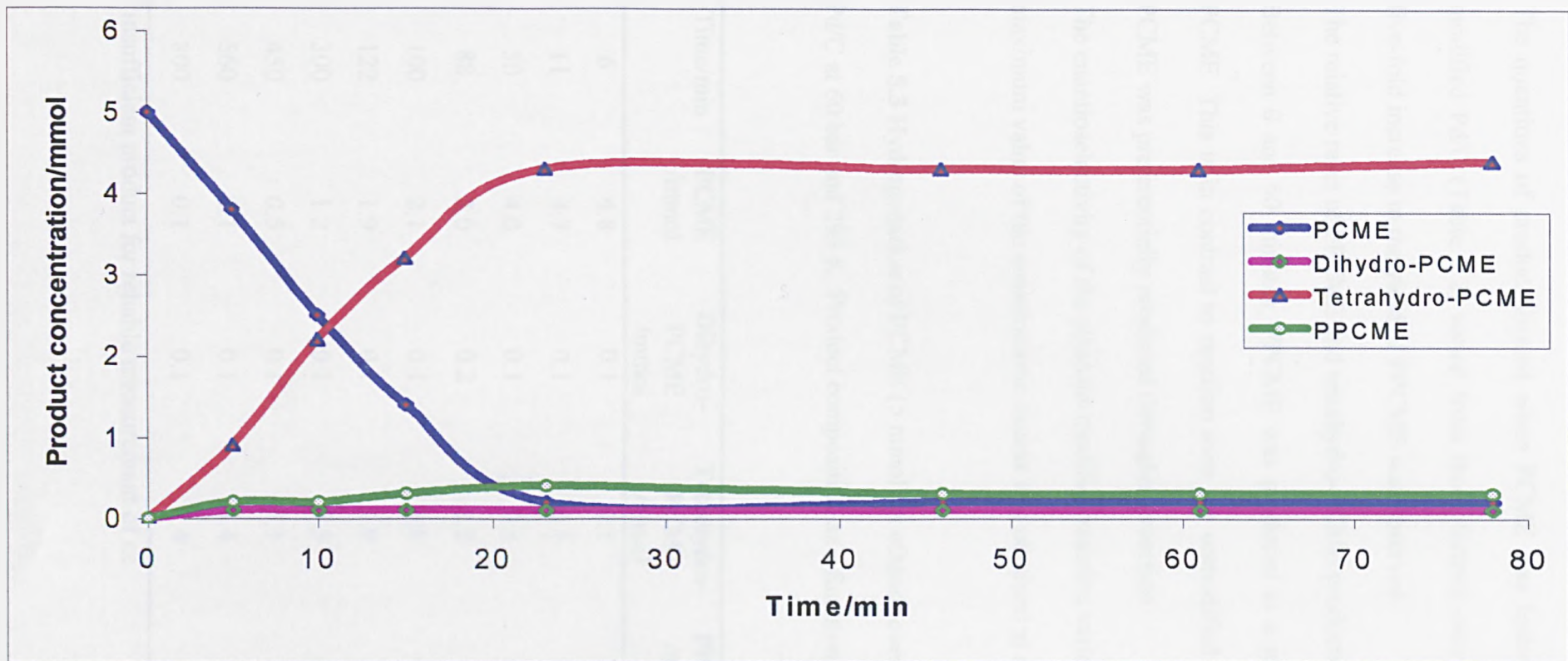


Figure 5.7 PCME hydrogenation over unmodified Pd/C. Product composition against reaction time.

The quantities of product formed when PCME was hydrogenated over cinchonidine modified Pd/C (Table 5.2) varied from those formed over an unmodified catalyst. A five-fold increase in the yield of PPCME was observed.

The relative rates of PPCME and tetrahydro-PCME production are shown in Figure 5.8. Between 0 and 50 minutes, PPCME was produced at a greater rate than tetrahydro-PCME. This is in contrast to reaction over the unmodified catalyst, where tetrahydro-PCME was preferentially produced throughout reaction

The enantioselectivity of the alkaloid-modified reaction varied with time (Figure 5.9). A maximum value of the enantiomeric excess was obtained at about 60% conversion.

Table 5.3 Hydrogenation of PCME (5 mmol) in ethanol over cinchonidine modified 5% Pd/C at 60 bar and 293 K. Product composition as a function of time.

Time/min	PCME /mmol	Dihydro-PCME /mmol	Tetrahydro-PCME /mmol	PPCME /mmol	ee /%
6	4.8	0.1	0.1	0.1	- ^a
11	4.7	0.1	0.1	0.2	5 (S)
50	4.0	0.1	0.3	0.6	10 (S)
88	3.0	0.2	1.2	0.6	14 (S)
100	2.1	0.1	1.8	1.1	22 (S)
122	1.9	0.1	1.9	1.1	23 (S)
300	1.2	0.1	2.5	1.2	16 (S)
450	0.5	0.1	3.1	1.3	14 (S)
560	0.1	0.1	3.4	1.4	12 (S)
800	0.1	0.1	3.4	1.4	10 (S)

^a insufficient product for reliable measurement of ee

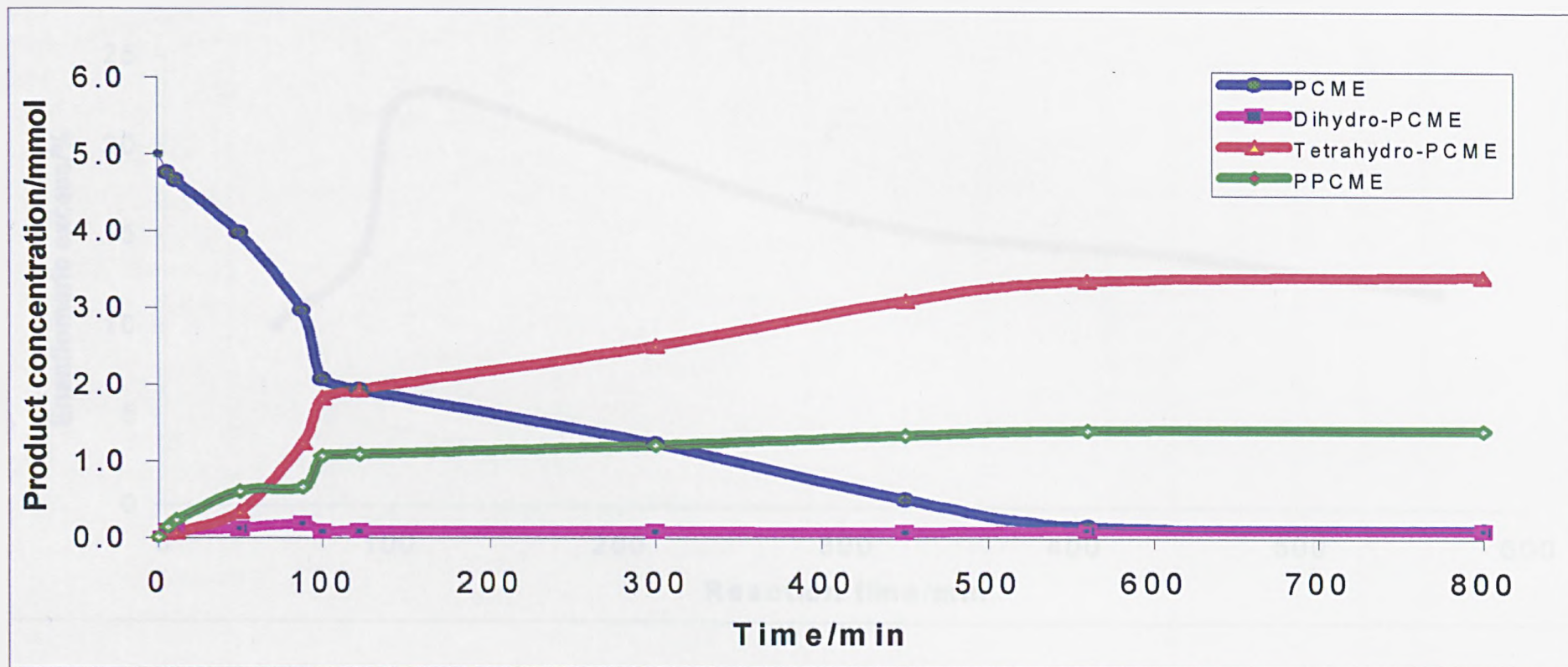


Figure 5.8 PCME hydrogenation over cinchonidine modified Pd/C. Product composition against reaction time

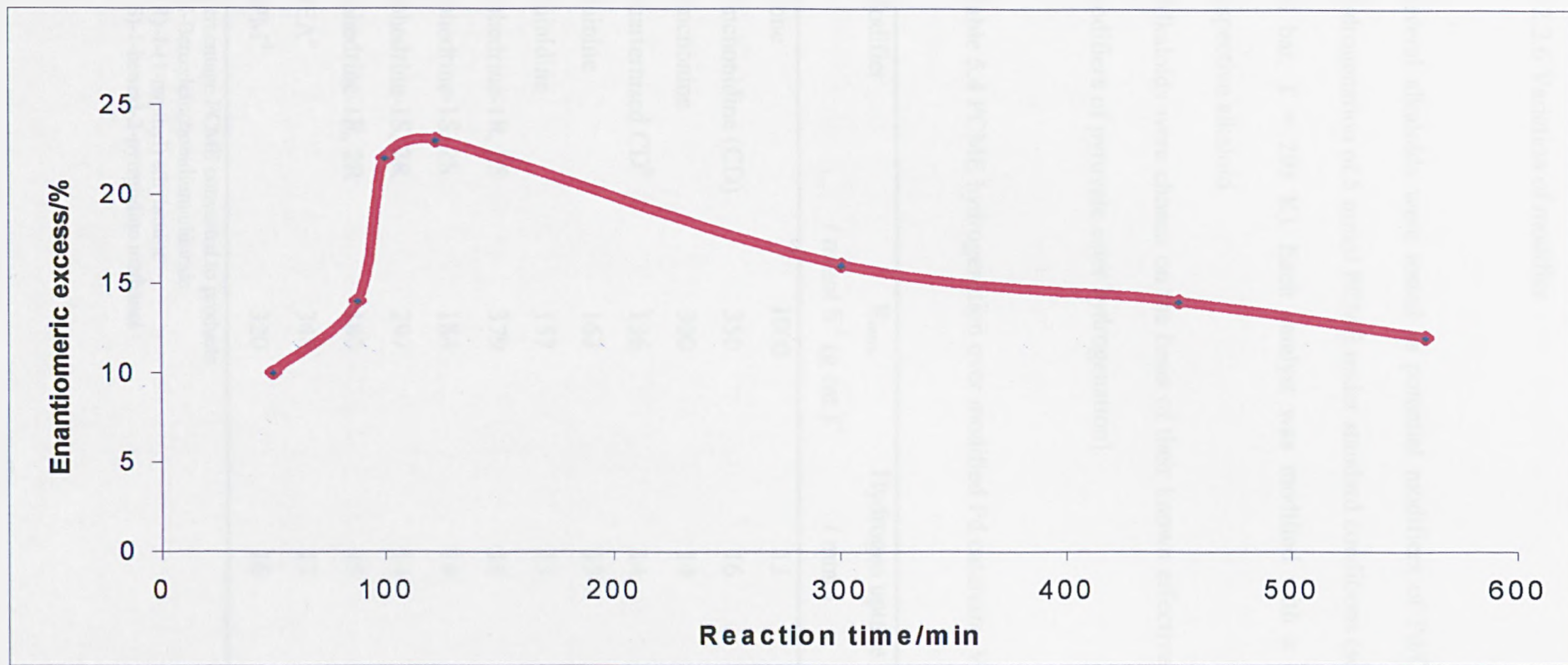


Figure 5.9 PCME hydrogenation over modified Pd/C. Variation of enantiomeric excess with time.

5.2.2.6 Variation of modifier

Several alkaloids were tested as potential modifiers of Pd/C for the enantioselective hydrogenation of 5 mmol PCME under standard conditions (solvent = EtOH, pressure = 60 bar, T = 293 K). Each catalyst was modified with a 0.034 M solution of the respective alkaloid.

[Alkaloids were chosen on the basis of their known effectiveness or ineffectiveness as modifiers of pyruvate ester hydrogenation].

Table 5.4 PCME hydrogenation over modified Pd catalysts. Variation of modifier.

Modifier	R_{\max} / mmol h ⁻¹ (g cat.) ⁻¹	Hydrogen uptake / mmol	Conv. ^a / %	ee / %
None	1000	13	95	0
Cinchonidine (CD)	350	16	98	12 (S)
Cinchonine	300	14	88	11 (R)
Quarternised CD ^b	136	14	90	0
Quinine	163	15	80	2 (S)
Quinidine	157	13	60	2 (R)
Ephedrine-1R, 2S	379	16	98	11 (S)
Ephedrine-1S, 2S	184	14	96	10 (R)
Ephedrine-1S, 2R	297	14	97	12 (R)
Ephedrine-1R, 2R	180	15	99	11 (S)
NEA ^c	348	13	94	0
BPM ^d	320	16	97	0

^a percentage PCME converted to products

^b N-Benzylcinchonidium chloride

^c (R)-1-(1-naphthyl) ethylamine

^d (S)-1-benzyl-2-pyrrolidine methanol

Product compositions for reactions involving variously modified catalysts were analysed at high conversions, as shown in Table 5.5.

Table 5.5 Hydrogenation of PCME (5 mmol) in ethanol over variously modified 5% Pd/C at 60 bar and 293 K. Products at high conversion.

Modifier	Conv. ^a /%	Dihydro- PCME /mmol	Tetrahydro- PCME /mmol	PPCME /mmol	ee /%
None	95	0.1	4.6	0.3	0
Cinchonidine (CD)	97	0.1	3.5	1.4	12 (S)
Cinchonine	88	0.1	3.7	1.2	11 (R)
Quarternised CD ^b	90	0.2	4.5	0.3	0
Quinine	98	0.1	4.4	0.5	2 (S)
Quinidine	98	0.1	4.3	0.6	2 (R)
Ephedrine-1R, 2S	98	0.1	4.3	0.6	11 (S)
Ephedrine-1S, 2S	96	0.1	4.3	0.6	10 (R)
Ephedrine-1S, 2R	97	0.1	4.3	0.6	12 (R)
Ephedrine-1R, 2R	99	0.1	4.0	0.9	11 (S)
NEA ^c	94	0.3	3.8	0.9	0
BPM ^d	97	0.2	4.3	0.5	0

^a percentage PCME converted to products

^b N-Benzylcinchonidium chloride

^c (R)-1-(1-naphthyl) ethylamine

^d (S)-1-benzyl-2-pyrrolidine methanol

When PCME was hydrogenated to high conversion over either a modified or unmodified catalyst, the major product was tetrahydropyrazine.

The product compositions and values of the enantiomeric excess obtained for reactions involving CD and CN were similar at high conversion.

Pd/C modified by quarternised CD produced a racemic PPCME as expected by comparison with pyruvate ester hydrogenation.

When Pd/C was modified by quinine or quinidine, reactions were generally slower and weakly enantioselective than those for which the catalyst was modified by cinchonidine or cinchonine.

The four stereoisomers of ephedrine all gave product compositions at high conversion that were similar to those shown by quinine and quinidine. The failure of NEA and BPM to induce enantioselectivity in PCME hydrogenation is significant, as they are effective in pyruvate hydrogenations (see discussion below).

5.2.2.7 Variation of catalyst support

The effect of varying the catalyst support was investigated as shown in Table 5.6. Hydrogenation of 5 mmol PCME were carried out under standard conditions (solvent = EtOH, pressure = 60 bar, T = 293 K). Each catalyst was modified by 0.034 M cinchonidine. The quoted values of the enantiomeric excess are an average for a number of reactions.

Table 5.6 PCME hydrogenation over modified Pd catalysts under standard conditions. Variation of catalyst support.

Support	R_{\max} / mmol h ⁻¹ (g cat.) ⁻¹	Hydrogen uptake / mmol	Conv. / %	ee (S) / %
Carbon	350	16	98	24 (S)
Alumina	10	2	10	*
Silica	12	3	8	*
Titania	174	16	98	4

* insufficient product for reliable measurement of ee

The table shows Pd/C to be the best catalyst in terms of efficiency, conversion and enantioselectivity. Pd/TiO₂ was active but provided poor enantioselectivity. When alumina or silica-supported catalysts were tested, little reaction occurred; GCMS analysis of these reactions showed that a variety of products were formed, but none was identified.

5.2 Results: Catalysis by Ni

The enantioselective hydrogenation of β -keto esters over NaBr promoted Raney Ni modified by R, R-tartaric acid has a well-documented history (2, 3). The most recent advance has involved the modification of Raney Ni using tartaric acid and pivalic acid (trimethylacetic acid) as synergic modifiers (4).

Work undertaken at the University of Hull by Wilkinson, diversified the application of this doubly modified catalyst and achieved the enantioselective hydrogenation of pyridine-2-carboxylic acid methyl ester (5). In the present work, this catalyst has been reproduced (Section 2.3.2.2) and its efficacy for the enantioselective hydrogenation of PCME tested. A selection of results is shown in Table 5.6.

The hydrogenation of PCME in toluene and methanol over this modified Raney Ni afforded the corresponding piperazine with low but detectable enantioselectivity. Reaction in THF or butan-1-ol gave slower reactions (lower conversions) and no enantiomeric excess.

The margin of error with chiral GC has been calculated to be $\pm 1\%$, therefore reaction in methanol may have been racemic. However, the results obtained from hydrogenation in toluene were considered positive and outside experimental error. This was tested by

modifying Raney Ni with S, S-tartaric acid and pivalic acid whereupon an inversion in the sense of enantioselectivity was observed (entry 3, Table 5.7).

Table 5.6 Hydrogenation of PCME (5 mmol) at 60 bar and 323 K over Raney Ni modified by R, R-tartaric acid and pivalic acid.

Solvent	R_{\max} / mmol h ⁻¹ (g cat.) ⁻¹	Uptake /mmol	Conversion /%	ee /%
Toluene	134	11	54	2 (S)
Toluene	152	20	92	2 (S)
Toluene ^a	147	20	94	2 (R)
Tetrahydrofuran	103	20	72	0
Tetrahydrofuran	127	21	76	0
Butan-1-ol	94	26	63	0
Butan-1-ol	81	25	61	0
Methanol	131	20	89	1 (S)
Methanol	143	21	93	1 (S)

^a Modified with S, S-tartaric acid

5.3 Discussion: Catalysis by Pd

5.3.1 Pyrazine-2-carboxylic acid (PCA)

Racemic piperazine-2-carboxylic acid was formed when PCA (as its potassium salt) was hydrogenated over cinchonidine modified Pd/C. The rate was lower than that for unmodified hydrogenation.

The absence of any enantioselectivity may be attributable to a lack of a reactant-modifier interaction because the potassium salt of the acid was being used. Free acid-modifier interaction has proved to be critical for enantioselective hydrogenation of prochiral α,β -unsaturated acids, such as tiglic acid over cinchonidine modified palladium (6) ref. This reaction was discussed in Chapter 1, and the main features of the mechanism are as follows.

- 1 Cinchonidine is adsorbed to the catalyst via its quinoline moiety, which effectively acts as a surface-anchoring group.
- 2 Tiglic acid forms a H-bonded precursor state with adsorbed cinchonidine, the H-bond being between the -COOH group of the acid and the quinuclidine -N of the alkaloid.
- 3 The energetics of the rotation of tiglic acid about this H-bond are such as to lead to selective enantioface adsorption of the acid in the vicinity of adsorbed cinchonidine.
- 4 Hydrogenation of tiglic acid adsorbed by the favoured enantioface produces 2-methyl butanoic acid showing an enantiomeric excess.

In the $K^+ PCA^-$ system, the decrease in r_{max} implies that cinchonidine is adsorbed onto the catalyst, but the lack of an enantiomeric excess clearly indicates no reactant-

modifier interaction. Since the PCA^- anion cannot form a H-bonded precursor state, the failure to achieve enantioselectivity is not unexpected.

The importance of this interaction was further tested by attempting enantioselective hydrogenation of the potassium salt of tiglic acid over cinchonidine modified palladium under conditions where the free acid is enantioselectivity hydrogenated.

After reaction, the free acid was regenerated and analysis indicated that racemic 2-methyl butanoic acid was the sole product formed; the importance of the $-\text{COOH}$ function in the reactant was thereby confirmed.

The effect on r_{max} of increasing the mass of cinchonidine is shown in Table 5.1. When the surface concentration of cinchonidine was increased r_{max} decreased indicating a reduction in catalyst surface area available for racemic hydrogenation.

5.3.2 Pyrazine-2-carboxylic acid methyl ester (PCME)

The hydrogenation of PCME was investigated because the reactant is soluble in a variety of common solvents. Being an ester, the reactant was not suitable for the formation of a pre-cursor state with adsorbed alkaloid, and indeed cinchona-modified Pd is not enantioselective for the hydrogenation of tiglic acid methyl ester (7). It was therefore contrary to expectation that PCME hydrogenation to PPCME occurred enantioselectively.

The difference in activity for modified and unmodified hydrogenation is shown in Figure 5.2. The lower rate for the modified reaction is simply attributed to a reduction in the catalyst surface available for reactant adsorption when this occurs in competition with alkaloid adsorption.

5.3.2.1 Proposed mechanism for enantioselective hydrogenation of PCME over cinchonidine modified Pd/C

A mechanism for the enantioselective hydrogenation of PCME is presented to interpret to discuss the results reported in section 5.2.2. Certain assumptions have been made and mechanistic parallels with the enantioselective hydrogenation of α -ketoesters and of α , β -unsaturated acids have been drawn. Visualisation of the surface processes are presented for the Pd (111) surface which is the configuration expected to dominate for Pd metal particles present in these catalysts.

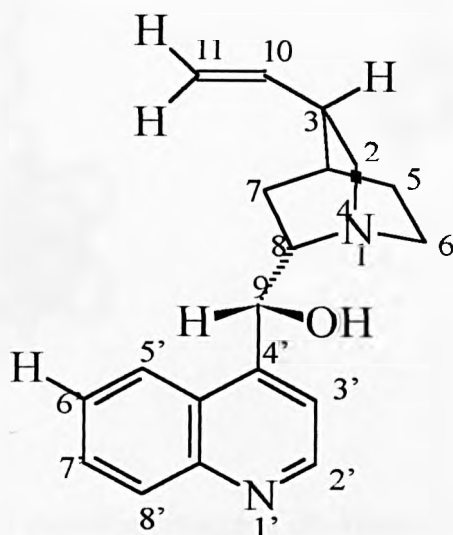
5.3.2.1.1 Adsorption of cinchonidine on palladium

Cinchonidine possesses three major structural characteristics that play a critical role not only in surface adsorption but also in enantiodifferentiation (Figure 5.10). First, the quinoline ring serves to provide strong adsorption to the metal surface (effectively acting as a surface anchoring group); second, the stereogenic centre at the 9-position plays an important role in determining the conformation of alkaloid molecule and finally the quinuclidine-N atom provides a point of interaction between adsorbed modifier and adsorbed reactant.

Work reported independently by Simons and Slipszenko identified three possible minimum energy conformations for CD (8, 9). The results from their work was confirmed by the author using different molecular modelling software (Cerius2, see Section 2.2.14).

The three minimum energy conformations were determined by rotation of the molecule about the $C_4'-C_9$, C_8-C_9 , C_3-C_{10} and C_9-O bonds, the first two being the most important; the torsion angles and their relative energies are given in Figure 5.10. The computer software calculated the energies for the isolated molecule (as it would be in a vacuum) at 0 K, making the relevance of the values to the experimental study limited.

The molecular modelling images relating to conformations A, B and C are given in Figures 5.11 (a to c). [For the purpose of this study it is assumed the quinuclidine nitrogen is protonated (see later)]



Conformation	$C_3'-C_4'-C_9-C_8$ /°	$C_7-C_8-C_9-C_4'$ /°	C_4-C_9-OH /°	$C_2-C_3-C_{10}-C_{11}$ /°	Energy /kcal mol ⁻¹
A	97	286	306	141	28.9
B	63	176	310	144	27.8
C	255	177	310	145	27.5

Figure 5.10 Structure of cinchonidine and principle torsion angles for its three minimum energy conformations

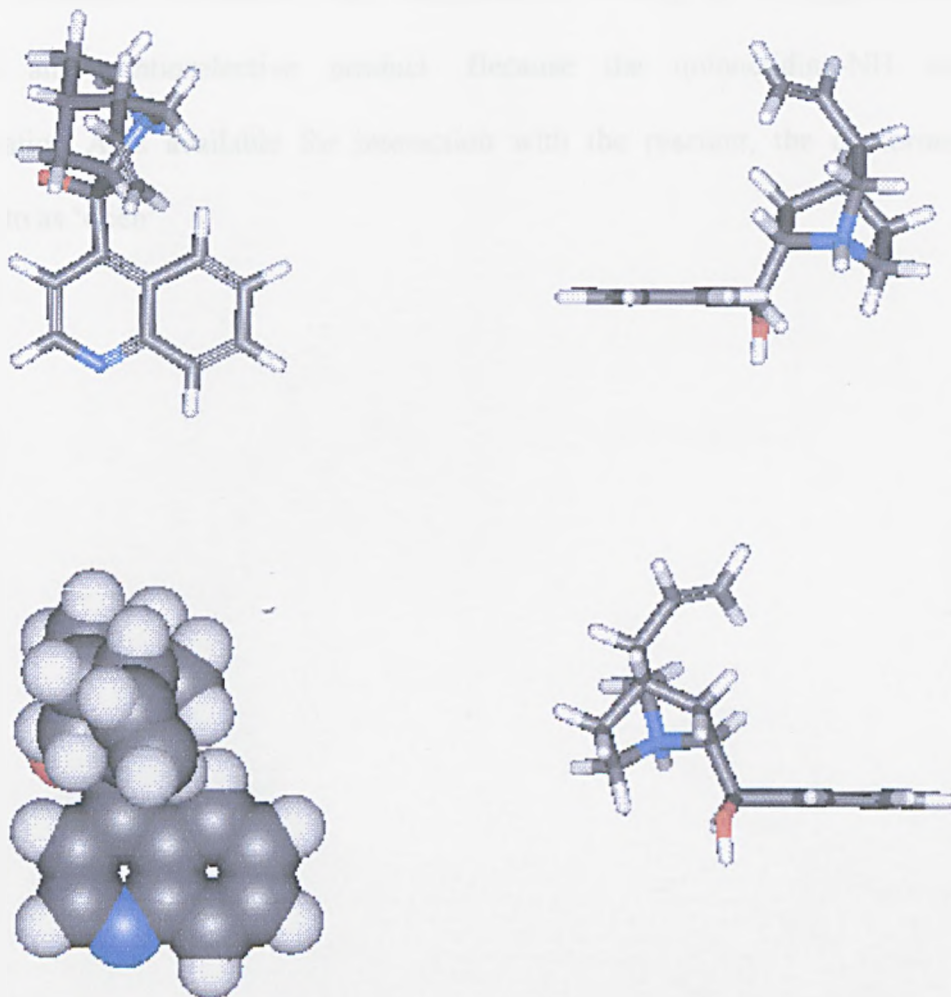


Figure 5.11(a) Molecular modelling image of conformation A of protonated cinchonidine

Although the energy differences between the three conformations are small, conformation A has been shown (by nmr) to predominate in solvents such as ethanol, and it is generally agreed this conformation of cinchonidine is of most relevance to enantioselective catalysis (10). If cinchonidine was adsorbed in this conformation at a flat surface, a ‘pocket’ would be formed bounded by the quinoline ring and the protonated quinuclidine-N; PCME adsorbed in this pocket might undergo selective enantioface adsorption. It is shown below that this positioning would permit PCME to

form a H-bonded interaction with cinchonidine, which, on hydrogenation would produce an enantioselective product. Because the quinuclidine-NH atom in conformation A is available for interaction with the reactant, the conformation is referred to as 'open'.

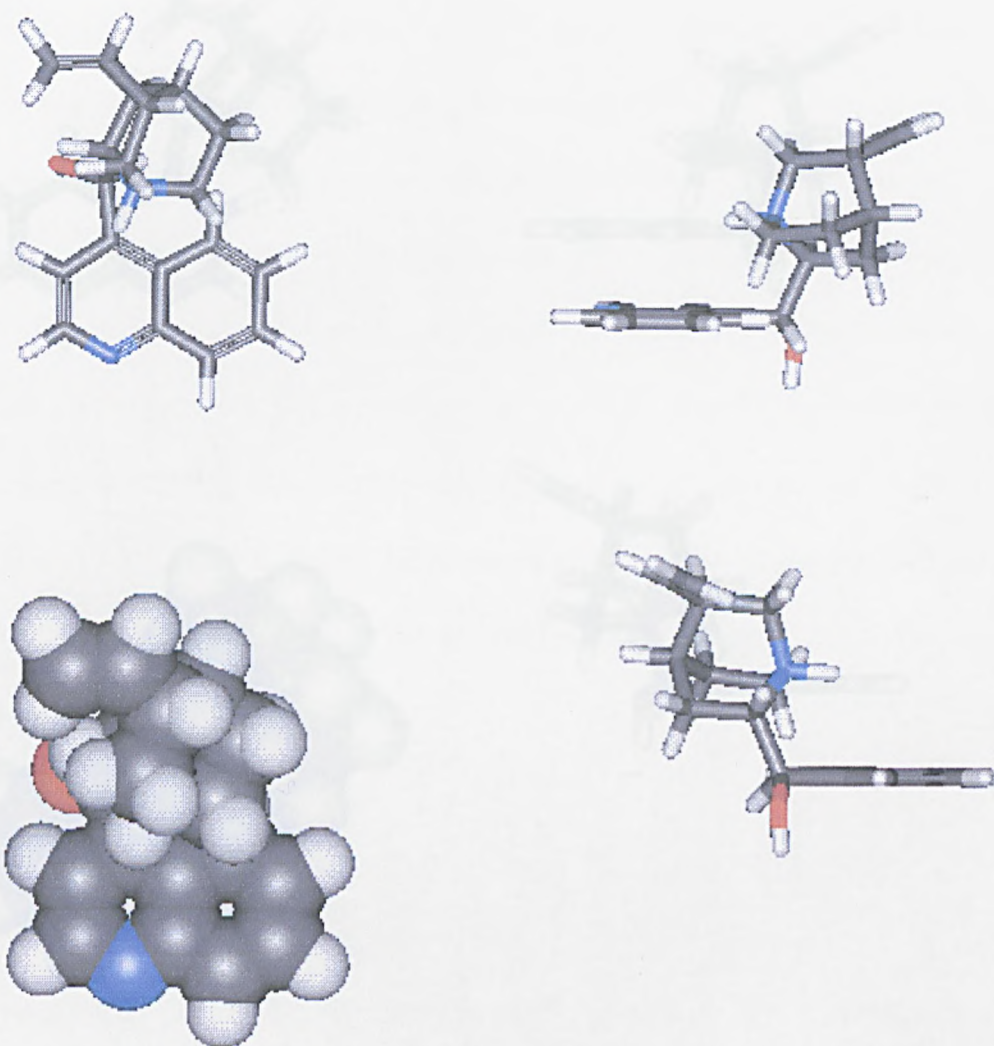


Figure 5.11(b) Molecular modelling image of conformation B of protonated cinchonidine

In conformation B the protonated quinuclidine-N is positioned over the quinoline ring and the arrangement is referred to as 'closed' because interaction with adjacently adsorbed reactant is not possible. Thus if the modifier was adsorbed onto the catalyst surface in this conformation, a racemic product would be obtained from the hydrogenation of any pro-chiral compound adsorbing at adjacent sites.

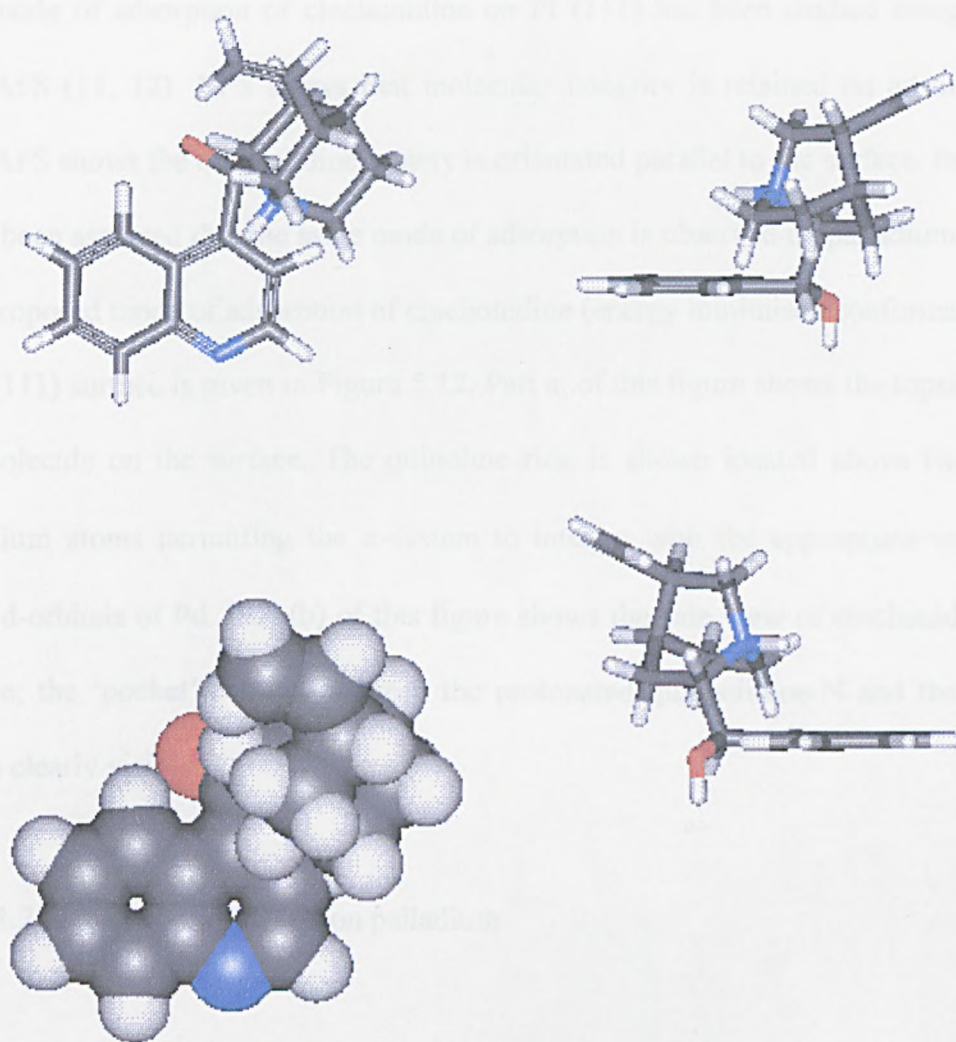


Figure 5.11(c) Molecular modelling image of conformation C of protonated cinchonidine

Similarly, conformation C is also a 'closed' formation, since the quinuclidine-N is located over the quinoline ring preventing any possible interaction with adjacently adsorbed reactant. This conformation of the modifier would not be expected to confer product enantioselectivity upon hydrogenation.

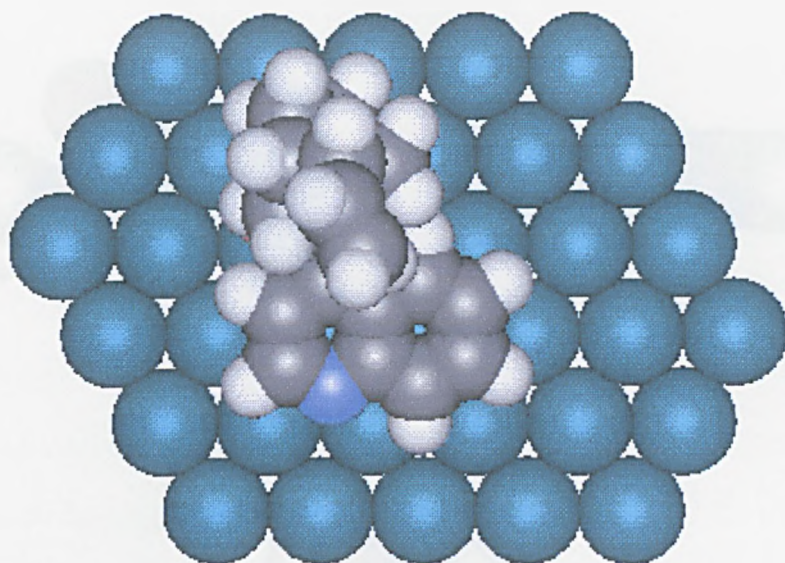
The mode of adsorption of cinchonidine on Pt (111) has been studied using XPS and NEXAFS (11, 12). XPS shows that molecular integrity is retained on adsorption, and NEXAFS shows the quinuclidine moiety is orientated parallel to the surface. In this study it has been assumed that the same mode of adsorption is observed on palladium.

The proposed mode of adsorption of cinchonidine (energy minimised conformation A) on a Pd (111) surface is given in Figure 5.12. Part a, of this figure shows the topside view of the molecule on the surface. The quinoline ring is shown located above two adjacent palladium atoms permitting the π -system to interact with the appropriate unfilled and filled d-orbitals of Pd. Part (b) of this figure shows the side view of cinchonidine on the surface; the 'pocket' formed between the protonated quinuclidine-N and the quinoline ring is clearly visible.

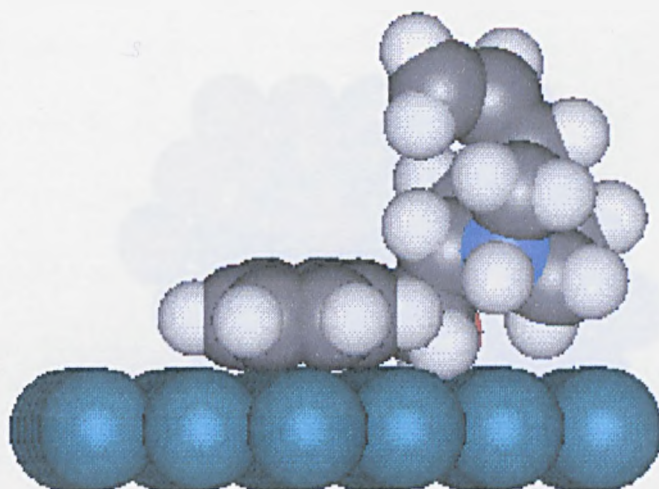
5.3.2.1.2 Adsorption of PCME on palladium

Next, we must consider how PCME interacts with the catalyst. The minimum energy conformation of PCME has been determined using molecular modelling (Figure 5.13 (a)). It is a fairly 'flat' structure.

The deuterium exchange investigation of unsubstituted pyrazine on Pd/C (Chapter 3) showed H/D exchange occurred in all ring positions. Therefore, it is assumed PCME adsorbs in a co-planar fashion to the palladium surface. (Figure 5.13 (b, c)).

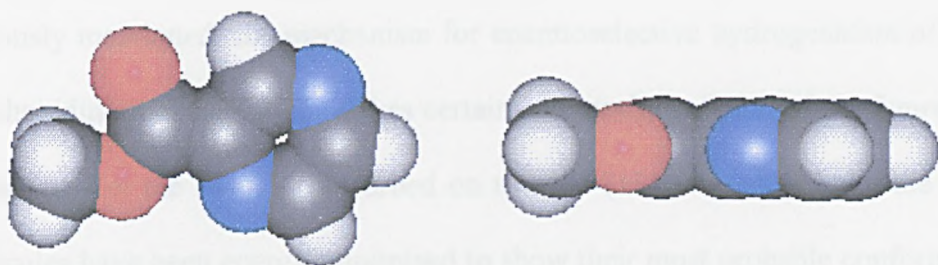


(a)

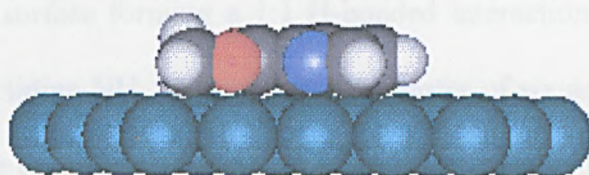


(b)

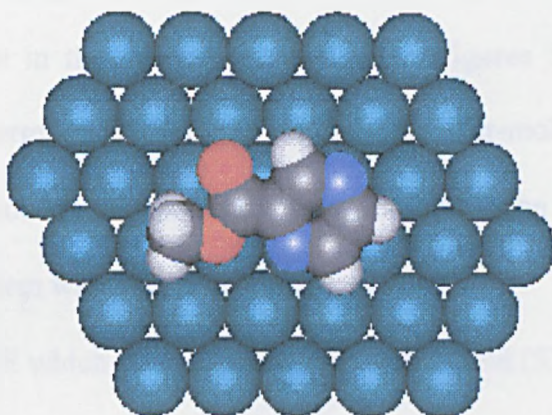
Figure 5.12 Proposed mode of protonated cinchonidine adsorption onto Pd (111)



(a)



(b)



(c)

Figure 5.13 The energy-minimised structure of PCME and its proposed adsorption onto a Pd (111) surface

5.3.2.1.3 Proposed mechanism of reaction

As previously mentioned, the mechanism for enantioselective hydrogenation of PCME over cinchonidine-modified Pd/C makes certain assumptions. Some of the figures show the reactant and/or the modifier adsorbed on to a Pd (111) surface. While the surface and molecules have been energy-minimised to show their most probable conformations, the computer calculates the structures for vacuum conditions and zero degrees Kelvin.

It is proposed that the more energetically favoured enantioface adsorbs adjacent to cinchonidine on the surface forming a 1:1 H-bonded interaction between its carbonyl group and the quinuclidine-NH. The subsequent transfer of six adsorbed H-atoms from the palladium surface to adsorbed PCME, from below the plane of the ring (the normal mode of H-addition to π -adsorbed aromatic ring systems in metal-catalysed hydrogenations) would provide (S)-PPCME.

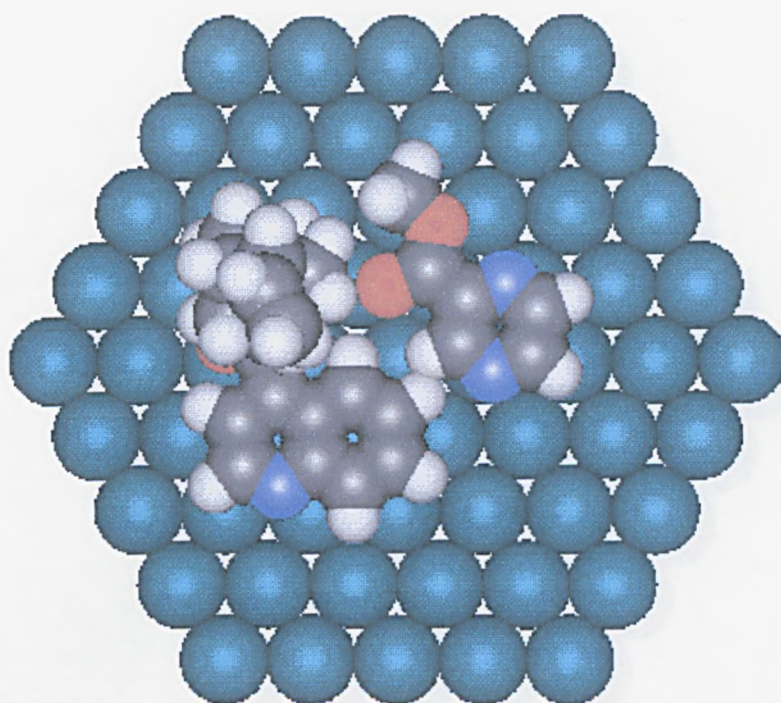
This hypothesis was investigated using molecular modelling. PCME was 'docked' with protonated cinchonidine in the orientations shown in Figures 5.14 and 5.15. These arrangements were energy-optimised, the intra- and inter-molecular distances and angles recalculated to produce the minimum energy conformation for the molecules; the total energy of each system was then calculated.

The orientation of PCME which on hydrogenation would yield (S)-PPCME had a lower total energy than the enantioface giving (R)-PPCME (105 kcal mol⁻¹ as compared to 281 kcal mol⁻¹). This suggests the enantioselective site should favour an S-directing process in PCME hydrogenation and this agrees with the observed sense of enantioselectivity.

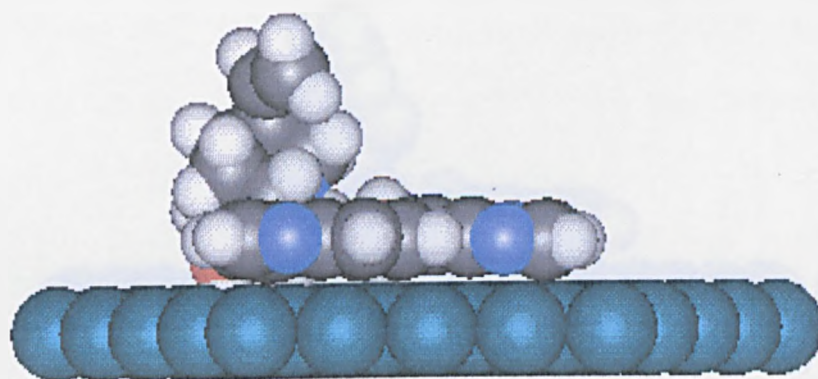
It should be emphasised that these calculations take no account of the presence of the metal surface since the computer packages are incapable of the highly complicated calculations required to derive the true band structure of the metal surface. These calculations effectively refer to molecules in the gas phase at zero degrees Kelvin. However, it is assumed that the relative values give a strong indication of actual inter-molecular effects.

The role of the quinuclidine-NH appears to be critical as hydrogenation over N-Benzylcinchonidium chloride (quarternised cinchonidine) modified Pd/C yielded racemic PPCME. This prevents the carbonyl group of PCME interacting with cinchonidine, thereby impeding selective enantioface adsorption.

The preferential formation of (R)-PPCME over *cinchonine* modified Pd/C can be interpreted by use of the same mechanism.

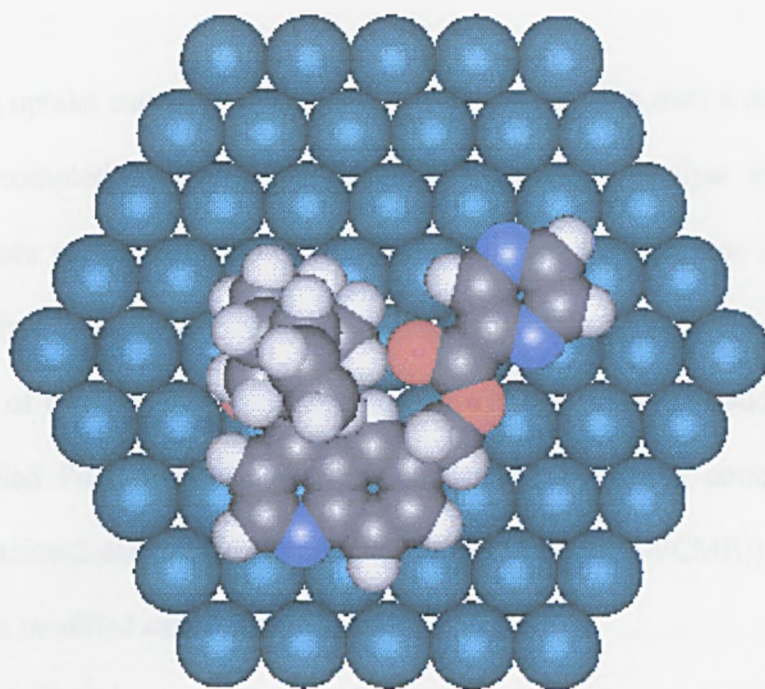


Top view

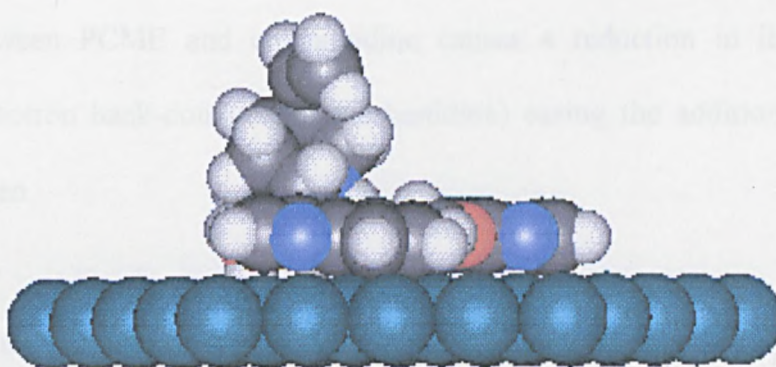


Side view

Figure 5.14 Interaction of PCME with protonated cinchonidine on Pd (111) to produce (S)-PPCME



Top view



Bottom view

Figure 5.15 Interaction of PCME with protonated cinchonidine on Pd (111) to produce

(R)- PPCME

5.3.2.2 Comparison between modified and unmodified reaction

The hydrogen uptake curves (Figure 5.2) showed that reaction over a modified catalyst continued to completion whereas reaction over unmodified catalyst stopped after the uptake of where only 2 moles of hydrogen. Therefore the presence of cinchonidine activates the final double bond in the ring towards hydrogenation.

The structure of the compound formed after a two-mole hydrogen addition to PCME over unmodified Pd/C was discussed in Chapter 4. The same compound (1,4,5,6-tetrahydropyrazine-2-carboxylic acid methyl ester (Tetrahydro-PCME)) was formed by reaction over a modified catalyst.

As tetrahydro-PCME has a 'carbamate-like' structure (carbamates are also known as urethanes and are formed by the reaction of an alcohol with isocyanate, they are generally unreactive due to the degree of conjugated stability in their structure), reduction by hydrogen may be expected to be difficult. However, the H-bonded interaction between PCME and cinchonidine causes a reduction in its conjugated stability (by electron back-donation to cinchonidine) easing the addition of the final mole of hydrogen.

5.3.2.3 Variation of reaction variables

Orders of reaction for enantioselective hydrogenation were +0.6 in hydrogen and -0.2 in PCME. This is indicative of weak adsorption of hydrogen and strong adsorption of PCME.

The rate of reaction (r_{\max}) increased with increasing temperature, in a manner that does not conform with the Arrhenius equation, and hence a value for the apparent activation energy could not be obtained.

When temperature reached 340 K the observed r_{\max} was approximately the same as that for reaction over an unmodified catalyst. It is therefore possible a change in the mode of cinchonidine adsorption had occurred, which in turn could increase the available area for racemic hydrogenation. This would appear to be the case as increasing temperature caused a reduction in product enantioselectivity, a collapse occurring at about 310 K. Similar behaviour has been observed for pyruvate ester hydrogenation over Pt which is attributable to a change in the adsorbed state of cinchonidine to a tilted state at ~ 320 K (1). Such a change in the mode of modifier adsorption could reduce the effectiveness of the previously proposed modifier interaction, and the resulting hydrogenation would produce an increased yield of racemic product.

The value of r_{\max} and enantioselectivity in the final product varied with increasing concentration of cinchonidine in solution as reported in section 5.2.2.4.

An increase in cinchonidine concentration caused a rapid reduction in the observed r_{\max} . This was not unexpected, as an increase in surface concentration of modifier would have reduced the available area for racemic PCME hydrogenation. The value of the enantiomeric excess would therefore be expected to *increase* with increasing cinchonidine concentration.

This was observed up to approximately 0.034 M whereafter the enantiomeric excess remained constant at a value of 24 % (as did r_{\max}). This shows that surface coverage of cinchonidine increased with increasing coverage up to approximately 0.034 M at which concentration maximum surface coverage was achieved. It is therefore to be expected that the number of enantioselective sites also increased with increasing modifier

concentration up to 0.034 M, as did the enantiomeric excess over this range. Above 0.034 M a stable surface situation existed with the enantiomeric excess independent of modifier concentration. For this reason, a modifier concentration of 0.034 M was used as the standard.

The observation that enantiomeric excess (and r_{\max}) does not change with increasing modifier coverage after the 0.034 M threshold does not preclude the possibility that further cinchonidine adsorption could be occurring on the carbon support.

5.3.2.4 Analysis of Product compositions

5.3.2.4.1 Unmodified hydrogenation

PCME was hydrogenated over unmodified Pd/C at a reproducible r_{\max} of approximately $1000 \text{ mmol h}^{-1} (\text{g cat.})^{-1}$ to yield a small quantity of racemic PPCME. The product distribution given in Figure 5.7 indicates that the product formed in excess, irrespective of reaction time, was tetrahydro-PCME. As the reactant (PCME) was consumed, the concentration of tetrahydro-PCME immediately increased, reaction rate falling to zero after 25 minutes. The amount of the desired PPCME remained low throughout the reaction, possibly due to the inherent stability of the carbamate-like conjugated tetrahydro-PCME, and its inability to convert to piperazine under our reaction conditions.

The product formed by addition of one mole hydrogen, dihydro-PCME, was present also in trace quantities throughout the reaction. Curiously, it also showed no further reactivity, indicating that it could not compete with tetrahydro-PCME for the surface.

5.3.2.4.2 Hydrogenation over cinchonidine modified Pd/C

The products formed as PCME was hydrogenated over cinchonidine modified Pd/C (Figure 5.8) differed significantly from those over an unmodified catalyst.

The amount of PPCME produced was much higher than that formed in the unmodified reaction. Indeed, it appeared that the addition of cinchonidine facilitated PPCME production. However, after 100 min of reaction time, the concentration of PPCME rose only very slowly and the enantiomeric excess decreased. This high initial yield is attributed to PPCME being produced predominantly at the enantioselective site, i.e. in the vicinity of adsorbed alkaloid. The marginal increase after 100 min is attributable to racemic PPCME being formed from tetrahydro-PCME.

During a reaction, cinchonidine may desorb from the catalyst surface, or enantioselective sites may be irreversibly destroyed. In turn, this would reduce further enantioselective PPCME production, allowing PPCME produced at racemic sites to dilute the overall enantioselectivity of the system.

Further evidence for the desorption of cinchonidine or the destruction of enantioselective sites is given by the time dependence of the quantity of tetrahydro-PCME formed. At the point where the enantiomeric excess starts to drop, the amount of tetrahydro-PCME rapidly increased. This may indicate that, from this point, no enantioselective sites are available to facilitate the conversion to PPCME.

When the catalyst was modified by N-benzylcinchonidium chloride (quarternised cinchonidine), the quantity of *racemic* PPCME produced was similar to that observed when PCME is hydrogenated over an unmodified catalyst. This again indicates the presence of cinchonidine helps facilitate PPCME production.

The hydrogenation of PCME over *cinchonine* modified Pd/C gave the expected inverse in the sense of enantioselectivity. (R)-PPCME was produced at a similar rate to that observed by reaction over cinchonidine modified Pd/C, but a lower value of the enantiomeric excess was obtained (14 %).

5.3.2.5 Other catalyst modifiers

5.3.2.5.1 Modification by quinine

The hydrogenation of PCME over quinine modified Pd/C was investigated. Values of Γ_{\max} were lower than those over cinchonidine modified catalyst and reaction was only mildly enantioselective.

Structurally the only difference between quinine and cinchonidine, is the presence of a methoxy group at the 6' position of the quinoline ring. It is clear from Figure 5.14 that such a substituent would grossly hinder the desired alkaloid-PCME interaction, and hence the observed substantial reduction in enantiomeric excess is entirely to be expected. The product distribution from this reaction is given in Table 5.5. The concentration of PPCME was low compared to that formed in the cinchonidine modified reaction. This strengthens the argument that the presence of the methoxy group on the quinoline ring is preventing PCME adsorption at the enantioselective site adjacent to the modifier, and therefore there is no route available to reduce the resonance stability of tetrahydro-PCME (see earlier).

The hydrogenation of PCME over quinidine modified Pd/C gave the expected preferential formation of (R)-PPCME, but again the disadvantageous effect of the 6-methoxy group in the modifier is evident.

5.3.2.5.2 Modification by ephedrine

Ephedrine, $\text{PhCH(OH)CH(Me)NHMe}$, has been shown to be a mildly effective Pt modifier for enantioselective pyruvate ester hydrogenation (13). On that basis, the four stereoisomers of ephedrine were investigated as potential Pd modifiers for enantioselective PCME hydrogenation. The values of r_{max} for reaction over catalysts modified by each stereoisomer varied, but all gave a similar value of the enantiomeric excess at about 11%.

Ephedrine-1S, 2S and -1S, 2R each induced enantioselectivity favouring the (R)-product, whereas ephedrine-1R, 2R and -1R, 2S each facilitated preferential (S)-product formation. The sense of enantioselectivity was therefore determined by the configuration of the carbon atom immediately adjacent to the aromatic ring.

The product distribution is given in Table 5.5. Again tetrahydro-PCME was produced in excess with PPCME being produced in small quantities. Unlike hydrogenation over cinchonidine modified Pd/C, no enhanced PPCME yield was observed.

A systematic investigation of possible modifier-reactant interactions was undertaken to help formulate a mechanism for PCME hydrogenation over ephedrine modified Pd/C.

Proton NMR spectroscopy on solutions of ephedrine-1R, 2S (E) and PCME (P) in toluene- d_6 (at 313 K) indicated that some form of associative interaction was taking place. Using a range of solutions with different [E]/[P] ratios, the change in chemical shift ($\Delta\delta$) was measured for all proton types in both ephedrine and PCME (excluding the exchangeable -OH and -NH types).

As [E]/[P] changed from 1.0 to 0.2 there was an almost identical high frequency shift for each of the four CH proton types in the side chain of ephedrine ($\Delta\delta$ in the range +0.026 to +0.031). In contrast, the aromatic protons in ephedrine showed virtually no

change ($\Delta\delta < +0.005$). This suggests (i) a significant association of PCME with the side chain of ephedrine and (ii) no π -stacking association between ephedrine and the pyrazine ester occurs. A bis (H-bonding) interaction that brings ephedrine into the aromatic deshielding cone of pyrazine is the most likely interaction (Figure 5.16). In the range $[E]/[P] = 1.0$ to 5.0 , the pyrazine proton adjacent to the carboxylate group was shifted to low frequency ($\Delta\delta = -0.015$), this is in sharp contrast to the shift of $+0.015$ for the other two pyrazine ring protons; the OMe protons show a small shift of $+0.005$. These results are again best interpreted in terms of a bis (H-bonded) interaction between the pyrazine ester group and ephedrine side chain (Figure 5.16).

Selective enantioface adsorption of a reactant is the prerequisite for its enantioselective hydrogenation. Such adsorption would be achieved if the complex shown in Figure 5.16 was adsorbed directly onto the Pd surface by both aromatic moieties or if PCME was able to adsorb adjacent to pre-adsorbed ephedrine utilising the same H-bond interactions (Figure 5.17). In either case, the transfer of six adsorbed H-atoms from the Pd surface to adsorbed PCME from below the plane or the ring would yield (S)-PPCME. The sense of the observed enantioselectivity is therefore interpreted.

The same mechanism applies to PCME hydrogenation over catalysts modified by the other ephedrines, and interprets the regulatory effect of enantioselectivity on the configuration of the carbon atom α - to the phenyl ring. The β -carbon atom is important only insofar as it acts as a spacer between the α -carbon atom and the basic-N atom; its configuration is of no significance in determining the steric course of the reaction.

Thus this proposed mechanism requires the presence of (i) an aromatic moiety to allow adsorption onto the surface and (ii) the $-C_{\alpha}(OH)-C_{\beta}(NH)-$ function to facilitate H-bonding interactions.

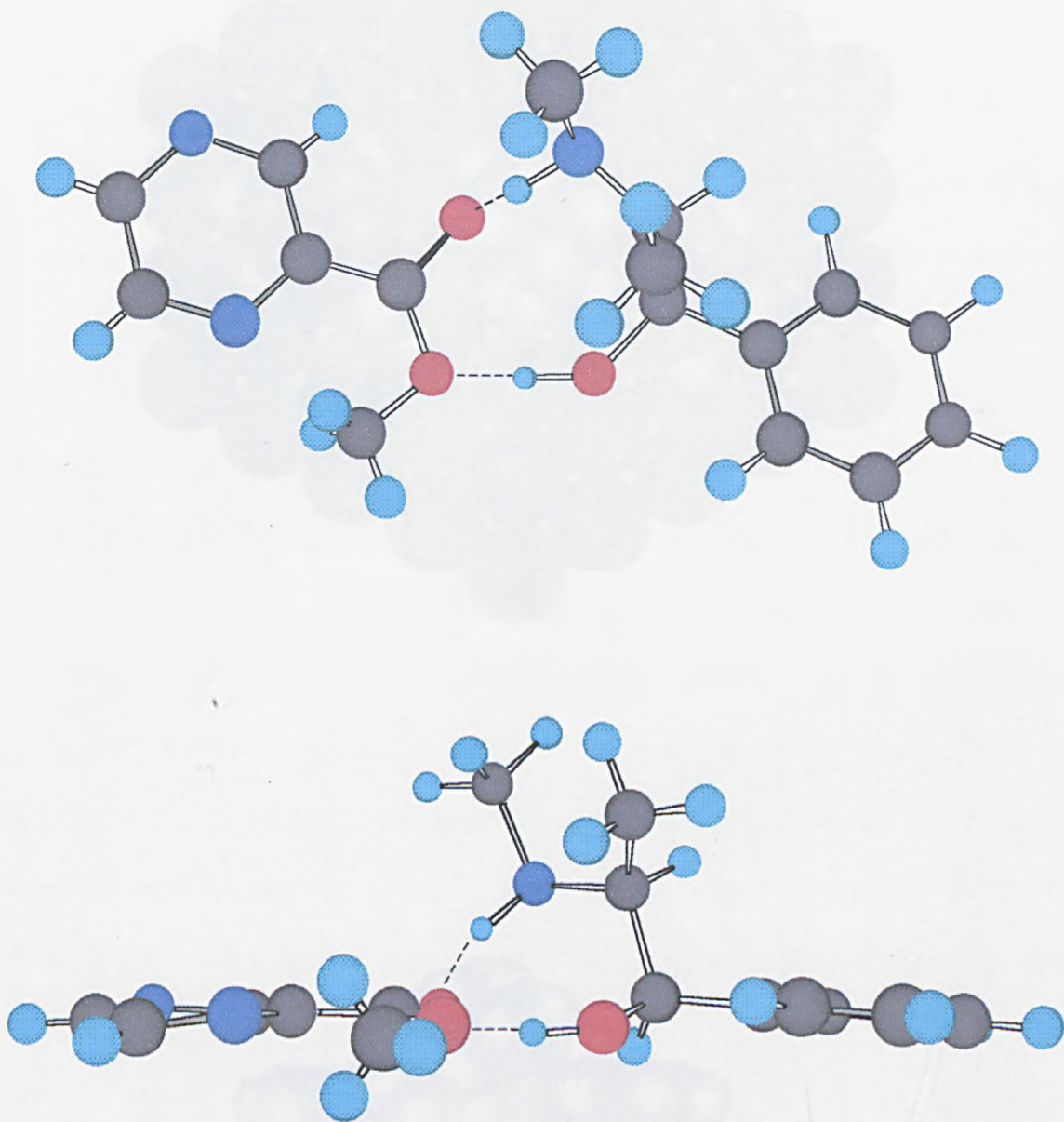


Figure 5.16 Proposed bis (H-bonded) adduct between PCME (left) and ephedrine-1R, 2S (right)

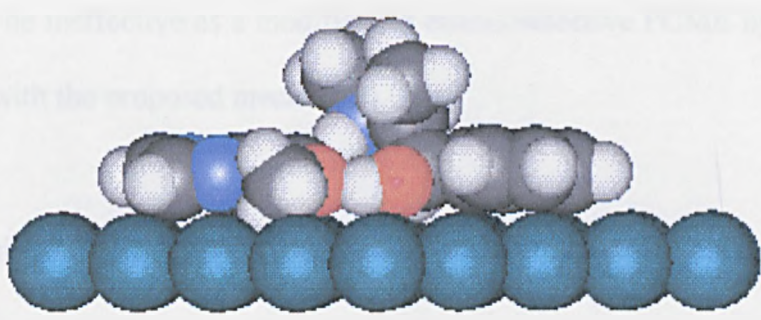
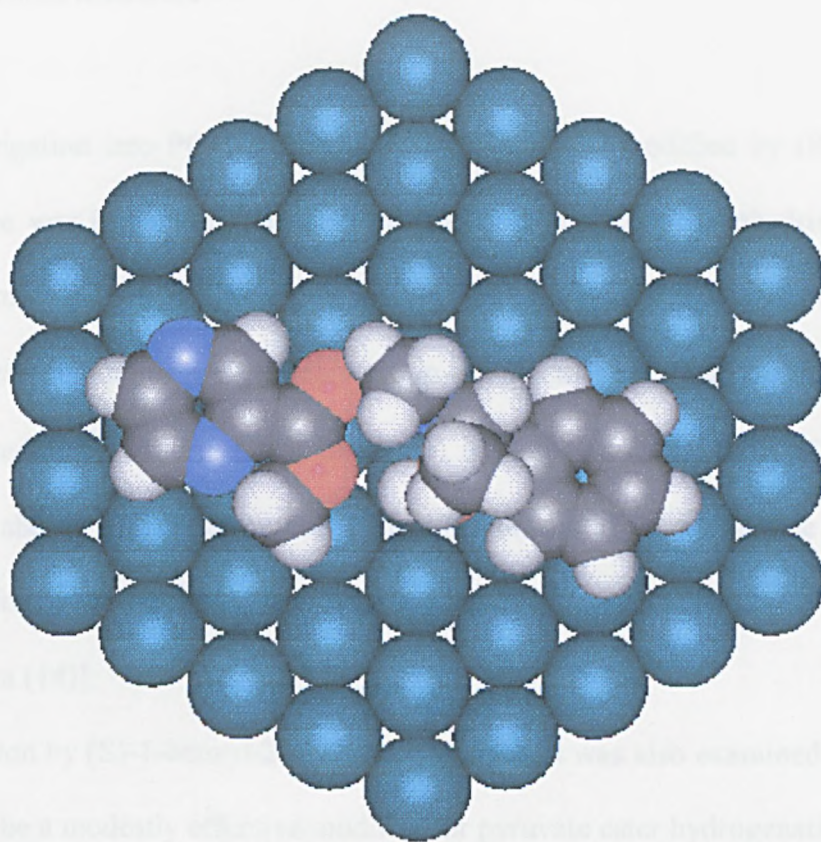


Figure 5.17 Proposed interaction of PCME and ephedrine-1R, 2S on Pd (111)

5.3.2.5.3 Other modifiers

An investigation into PCME hydrogenation over Pd/C modified by (R)-1-(1-naphthyl) ethylamine was undertaken because its structure, like that of ephedrine, contains an aromatic moiety separated from the basic N-function by two carbon atoms *but it has no* $C_{\alpha}(OH)$ *group*. The absence of this group proved to be critical; no enantioselectivity was induced in the hydrogenation of PCME, as expected on the basis of the mechanism proposed above. [It should be noted that (R)-1-(1-naphthyl) ethylamine is an effective modifier for enantioselective pyruvate ester hydrogenation, which occurs by a different mechanism (14)].

Modification by (S)-1-benzyl-2-pyrrolidine methanol was also examined [again this has proven to be a modestly effective modifier for pyruvate ester hydrogenation (15)].

Its structure contains both an aromatic moiety and a $-C(OH)-C-N=$ function but the geometric relationship is different to that of cinchonidine and ephedrine in that the hydroxyl C-atom *is not adjacent to the aromatic moiety*. Additionally, the N-atom is separated from the aromatic group by only one carbon atom. Entry 12 of Table 5.4 shows it to be ineffective as a modifier for enantioselective PCME hydrogenation, as is consistent with the proposed mechanism.

5.4 Discussion: Catalysis by Ni

The enantioselective hydrogenation of PCME over R,R-tartaric acid/pivalic acid modified Raney Ni in toluene, afforded PPCME in low enantioselectivity (2% (S)). As previously mentioned, the obtained enantiomeric excess was verified by use S,S-tartaric acid; this produced an inverse in the sense of enantioselectivity (2% (R)).

A range of reaction solvents other than toluene was investigated, such as methanol and butan-1-ol (the latter has been the most successful reaction solvent used by Webb for enantioselective β -keto esters hydrogenation over tartaric acid modified Raney Ni (16)) but none was more effective than toluene for enantioselective PCME hydrogenation.

As the value of the enantiomeric excess was low and the potential for the further development of the system was limited, an in-depth mechanistic investigation of reaction was not warranted.

5.4.1 Mode of enantioselection

The mode of enantioselection in the hydrogenation of PCME can be visualised, based on Sugimura's model for the interaction between R,R-tartaric acid, pivalic acid and the substrate (see Figure 5.18, (17)). The conformation of tartaric acid on the surface is based upon previous X-ray and neutron diffraction analyses of the metal salts of tartaric acid (18, 19). It is considered that one hydroxyl group of the adsorbed tartaric acid is close to the catalyst surface (site 1) and the second is less so (site 2). Tartaric acid then forms an associative H-bonded complex with pivalic acid at site 2 and this leaves site 1 free to interact with the carbonyl group of PCME via another hydrogen bond, there being a steric interaction between the alkyl part of the ester group and the *t*-butyl group of pivalic acid.

PCME adsorbed by the enantioface shown in Figure 5.18 would undergo hydrogenation by the addition of 6 H-atoms from the surface to below the plane of the adsorbed pyrazine ring. Such addition would yield (S)-PPCME, and the observed sense of enantioselectivity is therefore interpreted.

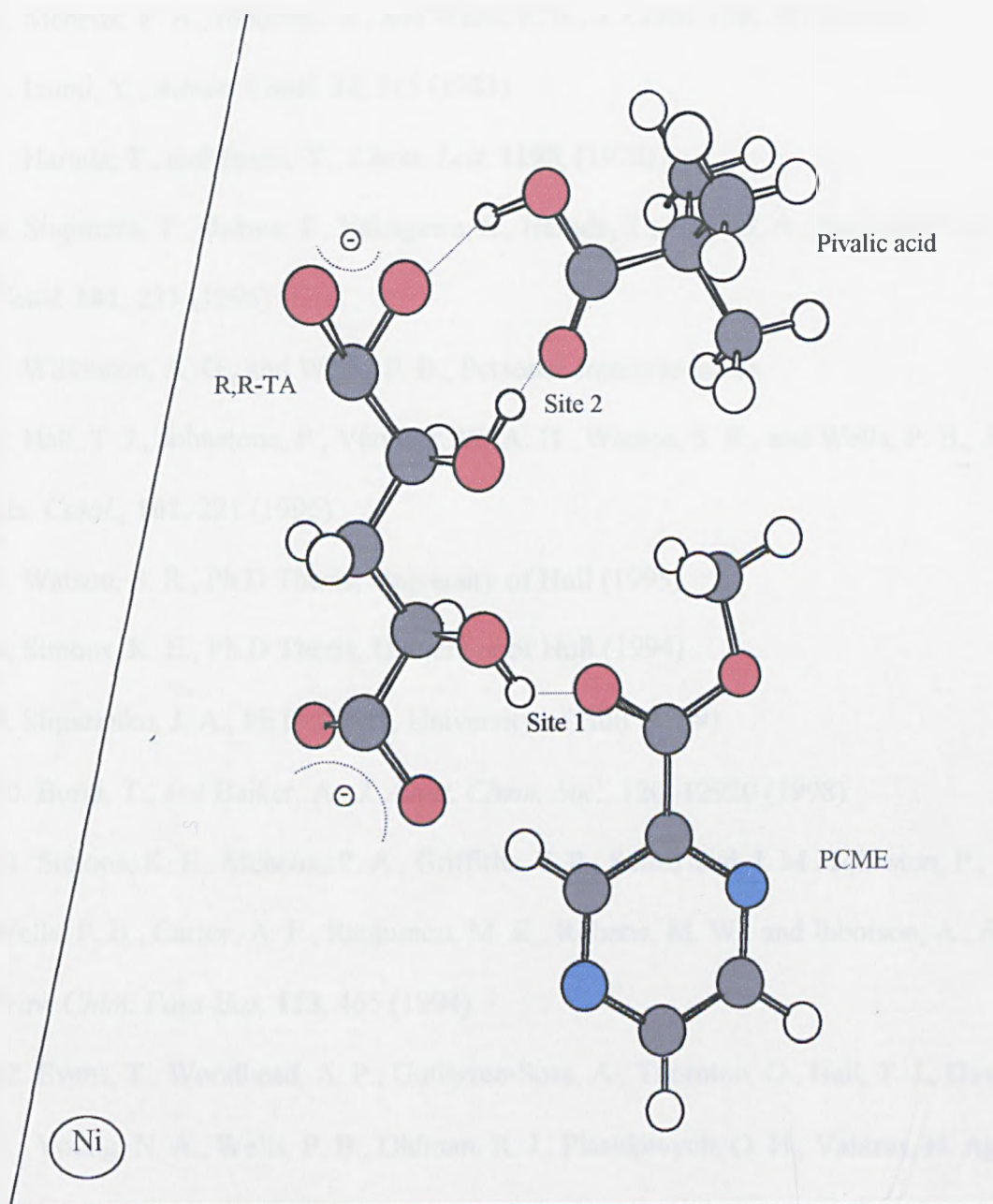


Figure 5.18 Hydrogenation of PCME over R,R-tartaric acid/Pivalic acid modified Raney Ni. Proposed mode of reactant-modifier interaction

References

1. Meheux, P. A., Ibbotson, A., and Wells, P. B., *J. Catal.* **128**, 387 (1991)
2. Izumi, Y., *Advan. Catal.* **32**, 215 (1983)
3. Harada, T., and Izumi, Y., *Chem. Lett.* **1195**, (1978)
4. Sugimura, T., Osawa, T., Nakagawa, S., Harada, T., and Tai, A., *Stud. Surf. Sci. Catal.* **101**, 231 (1996)
5. Wilkinson, A. G., and Wells, P. B., Personal communication
6. Hall, T. J., Johnstone, P., Vermeer, W. A. H., Watson, S. R., and Wells, P. B., *Surf. Sci. Catal.*, **101**, 221 (1996)
7. Watson, S. R., Ph.D Thesis, University of Hull (1995)
8. Simons, K. E., Ph.D Thesis, University of Hull (1994)
9. Slipszenko, J. A., Ph.D Thesis, University of Hull (1999)
10. Burgi, T., and Baiker, A., *J. Amer. Chem. Soc.*, **120**, 12920 (1998)
11. Simons, K. E., Meheux, P. A., Griffiths, S. P., Sutherland, I. M., Johnston, P., Wells, P. B., Carley, A. F., Rajumon, M. K., Roberts, M. W., and Ibbotson, A., *Recl. Trav. Chim. Pays-Bas*, **113**, 465 (1994)
12. Evans, T., Woodhead, A. P., Gutierrez-Sosa, A., Thornton, G., Hall, T. J., Davis, A. A., Young, N. A., Wells, P. B., Oldman, R. J., Plashkevych, O. H., Vahtras, H. Agren., and Carravata, V., *Surf. Sci.*, **436**, L691 (1999)
13. Blaser, H. U., Jalett, H. P., Monti, D. M., Rebert, J. F., and Wehrli, J. T., *Stud. Surf. Sci. Catal.*, **41**, 153 (1988)
14. Simons, K. E., Wang, G., Heinz, T., Giger, T., Mallat, T., Pfaltz, A., and Baiker, A., *Tetrahedron Asymm.*, **6**, 505 (1995)
15. Meheux, P. A., Ph.D Thesis, University of Hull (1991)

16. Webb, G., and Wells, P. B., *Catal. Today*, **12**, 319 (1992)
17. Sugimura, T., Osawa, T., Nakagawa, S., Harada, T., and Tai, A., *Stud. Surf. Sci. Catal.* **101**, 231 (1996)
18. Bostelaar, L. J., Graaf, R. A. G., Holsbergen, F. B., Reedijk, J., and Sachtler, W. M. H., *Inorg. Chem.* **23**, 2294 (1984)
19. Newton, M. D., and Jeffrey, G. A., *J. Amer. Chem. Soc.*, **99**, 2413 (1976)

Chapter 6

Conclusions

The challenging aims of this project have been achieved. These can be categorised into three areas.

1. The hydrogenation of pyrazine over Pd and other PGM's has been investigated and an insight into its reactivity and selectivity has been observed. Fundamentally, many similarities between the hydrogenation of benzene and pyrazine are apparent, but with pyrazine having a greater strength of adsorption to Pd, and therefore more likely to be a catalytic poison.

Most reported work in the area of N-heterocycle hydrogenation over PGM's has been undertaken using pyridine. In this study the rates of hydrogenation between pyrazine and pyridine were investigated. Pyrazine hydrogenates at a faster rate than pyridine, which was explained using deuterium-exchange reactions. Pyridine has been shown to adsorb onto a surface at a tilted angle, showing exchange at the 2- and 6- positions only. Complete exchange was observed in pyrazine, indicating co-planar adsorption and therefore facile H-atom addition.

2. The investigation into unmodified hydrogenation of some monosubstituted pyrazines demonstrated how aromatic ring reactivity is affected by attached substituents.

The initial concerns with the insolubility of 2-PCA were soon dispelled when the soluble ester was used in its place. This allowed a comprehensive study of substituted pyrazine reactivity to be undertaken.

The unusual chemistry observed for 2-PCN hydrogenation was intriguing. The rate and degree of hydrogenation was shown to be affected by the pH of the system.

3. The enantioselective hydrogenation of PCME had not previously been achieved. In fact, this thesis reports the first example of direct enantioselective hydrogenation of an aromatic N-heterocycle. As enantioselectivity in the final product was achieved over several differently modified catalysts, explanations and mechanisms are described. The greatest enantiomeric excess of around 25% was achieved over CD modified Pd/C. While this figure does not represent the 95% + enantiomer yield observed in some homogeneously catalysed reactions, the fundamental groundwork has been achieved and provides foundation for further work and growth. Many questions remained unanswered, in fact the surface of this fascinating area of work has barely been scratched, but it is hoped this system can be developed to answer many of the remaining questions.